

**Functional Characterization of Enolase from *Mycobacterium tuberculosis***

**Thesis submitted to the Jawaharlal Nehru University**

**in partial fulfillment of the requirement for the award of the degree of**

**DOCTOR OF PHILOSOPHY**

**IN**

**BIOTECHNOLOGY**

**BY**

**AMIT RAHI**



**SCHOOL OF BIOTECHNOLOGY  
JAWAHARLAL NEHRU UNIVERSITY  
NEW DELHI-110067  
INDIA**

**2017**



School of Biotechnology  
Jawaharlal Nehru University  
New Delhi-110067, India

## CERTIFICATE

This is to certify that the work entitled "Functional Characterization of Enolase from *Mycobacterium tuberculosis*" submitted to the School of Biotechnology, Jawaharlal Nehru University, New Delhi in partial fulfillment of the requirements for the award of the degree of Doctor of Philosophy, embodies faithful record of original research work carried out by **Amit Rahi**. This work is original and has not been submitted so far in part or full for any other degree or diploma of any other university.

Prof. Rakesh Bhatnagar  
(Supervisor)  
School of Biotechnology  
Jawaharlal Nehru university  
New Delhi-110067

Amit Rahi  
(Ph.D. candidate)

Prof. Andrew M. Lynn  
(Co-supervisor)  
School of Computational  
& Integrative Sciences,  
Jawaharlal Nehru University,  
New Delhi-110067

Dr. Rupesh Chaturvedi  
(Co-supervisor)  
School of Biotechnology,  
Jawaharlal Nehru University,  
New Delhi-110067

Prof. Pawan. K. Dhar  
(Dean, SBT)  
School of Biotechnology,  
Jawaharlal Nehru University,  
New Delhi-110067

August, 2017  
School of Biotechnology,  
Jawaharlal Nehru University,  
New Delhi-110067

*Dedicated to Almighty*

*“Imagination Is More  
Important Than Knowledge”*

*~Albert Einstein*



## *Acknowledgements*

*First of all, would like to thank the almighty for making me capable of persuing and completing this work with all his blessings inspite of innumerable odds and hardships.*

*I sincerely acknowledge Prof. Rakesh Bhatnagar, my supervisor for all his guidance and courage that sailed me through. He was the one who constantly helped me and stood by my side. He made me realize my zeal to do better and has made me a better human being, both academically as well as personally. I would like to express my gratitude to Dr. Nirupama Banerjee.*

*I would like extend my sincere thanks to my co-supervisors, Prof. Andrew M. Lynn and Dr. Rupesh Chaturvedi. Besides being my ideal, Prof. Andrew M. Lynn has always motivated me and has always helped me and my friends in several bioinformatics related studies.*

*I am really thankful to Dr. Rupesh Chaturvedi and Dr. Deepak Gaur for their scientific inputs and suggestions.*

*Prof. Abhinav Grover is a great devotee of Lord and has supported me personally as well as professionally.*

*I would like to thank Prof. Uttam K. Pati, dean School of Biotechnology who inspired me to take admission in PhD as well as its completion. He urged me not to waste time and focus on finishing my research.*

*I would like to be grateful to all my professors (all faculty members) at the SBT for their support and encouragement.*

*I am thankful to the SBT office staff, especially Tiwari sir for extending his timely help to me ever since my MSc days till my PhD tenure.*

*I would like to thank my all the BSL-3 lab staff Ghanshyam jee, Naveen bhai, Rajiv Bhaiya (computer), Bahadur jee, Alexander sir, Govind and Vikas for supplying me with several essential lab necessities on time.*

*I have stayed in this lab for a long duration therefore I would like to thank all my past as well as present lab mates for being a part of my journey here. I am grateful to the almighty that I received full support of all my friends whoever stayed with me as my friend and colleague during this whole duration.*

*I would like to thank Vikas who has always helped me unconditionally as a junior as well as friend. He has been helping me physically, mentally as well as financially. This was not possible without Somya who has also helped me and supported me. They have been very nice to me althrough. Alongwith them, Damini has always been a friend and a well wisher to me. As a junior she has been always helpful and has always been willing to help and support me in my time of need.*

*Jaishree has been like a sister to me and she has always supported me with her involvement in my work with complete willingness to take care of each and every detail. Surinder is a nice junior we have received in our lab and is a person with good vibes.*

*I am greatful to Shivangi and Shivani, who have been my seniors during my initial days in this lab and Shivangi being a really good friend now. She is a huge devotee to Lord Krishna.*

*Sumit and Rehan bhai have been an integral part of all my research. Besides being my friends, they have always worked towards the fulfilment of all my scientific endeavours. Sumit being an expert in the wet lab practices while Rehan bhai is an expert in Bioinformatics.*

*I really delight the company of my junior cum friend Deepak and I like having a stroll with him around the campus.*

*I have spent my leisure times with Cycle wale bhaiya cum friend at Godavari and I realize that he is a great human being and been an emotional support indeed.*

*Last but not the least, i would like to mention my four best friends of all the times: Shehzad bhai, Shashi kumar Suman, Miraz bhai and Alisha. They are all different but unique is their place in my life as well as heart.*

*Getting short of words to thank my parents and Vicky, Parul and Dimple my siblings. It is impossible to explain the contribution of my mom and dad in this whole endeavour and the immense support that I have continuously received inspite of number of unprecedented failures and disappointments coming in my way while being here. My cousin Deshbandhu shares an equally important place in my life along with Atiya who is my bhabhi and supports me hugely.*

*Amit*

## List of Publications

1. **Rahi A**, Dhiman A, Singh D, Lynn A.M, Rehan M, Bhatnagar R: **Exploring the interaction between *Mycobacterium tuberculosis* Enolase and human plasminogen using computational methods and experimental techniques.** (*Journal of Cellular Biochemistry*, *accepted for publication*, **2017**)
2. **Rahi A**, Matta SK, Dhiman A, Garhyan J, Gopalani M, Chandra S, Bhatnagar R: **Enolase of *Mycobacterium tuberculosis* is a surface exposed plasminogen binding protein.** *Bba-Gen Subjects* **2017**, **1861**(1):3355-3364.
3. Dhiman A, **Rahi A**, Gopalani M, Bajpai S, Bhatnagar S, Bhatnagar R: **Role of the recognition helix of response regulator WalR from *Bacillus anthracis* in DNA binding and specificity.** *Int J Biol Macromol* **2017**, **96**:257-264.
4. Joon S, Gopalani M, **Rahi A**, Kulshreshtha P, Gogoi H, Bhatnagar S, Bhatnagar R: **Biochemical characterization of the GTP-sensing protein, CodY of *Bacillus anthracis*.** *Pathog Dis* **2017**, **75**(4).
5. Gopalani M, Dhiman A, **Rahi A**, Kandari D, Bhatnagar R: **Identification, Functional Characterization and Regulon Prediction of a Novel Two Component System Comprising BAS0540-BAS0541 of *Bacillus anthracis*.** *Plos One* **2016**, **11**(7).
6. Gopalani M, Dhiman A, **Rahi A**, Bhatnagar R: **Overexpression of the pleiotropic regulator CodY decreases sporulation, attachment and pellicle formation in *Bacillus anthracis*.** *Biochem Bioph Res Co* **2016**, **469**(3):672-678.
7. Gorantala J, Grover S, **Rahi A**, Chaudhary P, Rajwanshi R, Sarin NB, Bhatnagar R: **Generation of protective immune response against anthrax by oral immunization with protective antigen plant-based vaccine.** *J Biotechnol* **2014**, **176**:1-10.
8. Manish M, **Rahi A**, Kaur M, Bhatnagar R, Singh S: **A Single-Dose PLGA Encapsulated Protective Antigen Domain 4 Nanoformulation Protects Mice against *Bacillus anthracis* Spore Challenge.** *Plos One* **2013**, **8**(4).
9. **Rahi A**, Rehan M, Garg R, Tripathi D, Lynn AM, Bhatnagar R: **Enzymatic characterization of Catalase from *Bacillus anthracis* and prediction of critical residues using information theoretic measure of Relative Entropy.** *Biochem Bioph Res Co* **2011**, **411**(1):88-95.
10. Gorantala J, Grover S, Goel D, **Rahi A**, Magani SKJ, Chandra S, Bhatnagar R: **A plant based protective antigen [PA(dIV)] vaccine expressed in chloroplasts demonstrates protective immunity in mice against anthrax.** *Vaccine* **2011**, **29**(27):4521-4533.

*TO BE PUBLISHED:*

- ✚ Generation and characterization of monoclonal antibody (MAbs) against *Mtb* enolase
- ✚ Enzymatic characterization of TatD-like nuclease of *Bacillus anthracis*
- ✚ Role of the Transmembrane Domains of *Mycobacterium tuberculosis* ABC Transporters in Drug Efflux.

*CONFERENCES, WORKSHOPS / EVENTS:*

- ✚ Attended **The International Conference on *Bacillus anthracis*, *Bacillus cereus*, and *Bacillus thuringiensis* - held September 1-5, 2013**, in Victoria, Canada.
- ✚ Attended **Bioepoch 2013** organized by School of Biotechnology, JNU.
- ✚ Attended The International Conference on ***Bacillus ACT, 2015*** held in October 27-31, 2015, in New Delhi, India.
- ✚ Completed ASM-SBS Workshop on Biorisk Management for *Bacillus anthracis* (**26 Oct, 2015**) organized by **The American Society of Microbiology and Society for Bio-Safety India**.
- ✚ Participated in “**Brucellosis 2016 International Research Conference**”, held at National Agricultural Science Complex (NASC), New Delhi, India during November 17-19, 2016.
- ✚ Participated in **BioEpoch, 2017** held at the School of Biotechnology, JNU, New Delhi, India on March 23-24, 2017.



# Table of Contents

<b>LIST OF ABBREVIATIONS .....</b>	<b>1-3</b>
<b>1. INTRODUCTION.....</b>	<b>4-7</b>
<b>2. REVIEW OF LITERATURE.....</b>	<b>8-27</b>
2.1. TUBERCULOSIS (TB)	
2.1.1 Global scenario	
2.2. TYPES OF TB	
2.2.1. Pulmonary v/s extrapulmonary TB	
2.2.2. Active v/s latent TB	
2.2.3. Miliary TB	
2.3. CAUSES OF TB	
2.3.1. Transmission	
2.3.2. <i>Symptoms</i>	
2.4. PATHOGENESIS OF TUBERCULOSIS	
2.4.1. Granuloma	
2.5. DIAGNOSIS	
2.5.1 Evidence of TB bacteria	
2.5.2. TB diagnostic tests	
2.5.3. Chest x-ray as TB test	
2.5.4. The TB skin test	
2.5.5. Interferon gamma release assay (IGRAs)	
2.5.6. Serological tests	
2.5.7. Sputum smear microscopy	
2.5.8. Fluorescent microscopy	
2.5.9. Culturing bacteria for TB test	
2.5.10. TB drug susceptibility tests	
2.6. TREATMENT	
2.6.1. New drugs and their resistance mechanisms	
2.7. NEW VACCINES TO PREVENT TB	
2.8. TB+HIV-A DUAL EPIDEMIC	
2.9. PLASMINOGEN AND PLASMIN SYSTEM	
2.10. ENOLASE	
2.10.1. Reaction mechanism	

## 2.11 IMPLICATIONS OF ENOLASE

2.11.1 Enolase in bacteria

2.11.2 Enolase in fungi

2.11.3 Enolase in protozoan parasites

## 3. MATERIALS AND METHODS ..... 28-45

### 3.1. MATERIALS

3.1.1 Reagents and biochemicals

3.1.2 Bacterial strains

3.1.3 Kits

3.1.4 Oligonucleotides

3.1.5 Cell lines and mice strains

### 3.2 MOLECULAR BIOLOGY METHODS

3.2.1 Isolation of genomic DNA from *Mtb*

3.2.2 PCR amplification of genes

3.2.3 DNA extraction from agarose gels

3.2.4 Restriction digestion

3.2.5 Construction of recombinant clones

3.2.6 Site directed mutagenesis

3.2.7 Preparation of competent cells of *E. coli*

3.2.8 Acid fast staining of *Mtb*

3.2.9 Preparation of electrocompetent cells of *Mtb* H37Rv

3.2.10. Transformation of competent cells of *E. coli*

3.2.11 Electroporation of *M. tuberculosis* cells

3.2.12 Screening of the clones

3.2.13 Over-expression of recombinant proteins

3.2.14 Western blot analysis

3.2.15 Affinity purification

3.2.16 Protein estimation and dialysis

3.2.17 Enzyme kinetics of *rMtb* Enolases

3.2.18 Plasminogen binding analysis for WT Enolase and its variants by end-point ELISA

3.2.19 *In vitro* Plasminogen activation /Plasmin formation assays

- a. With rEno (recombinant Enolase)
- b. With *Mtb* whole cells

3.2.20 Immunofluorescence (Confocal) microscopy

3.2.21 Transmission electron microscopy (TEM)

3.2.22 Flow cytometry

3.2.23 Surface Plasmon Resonance (SPR)

### 3.3 IMMUNOLOGICAL METHODS

3.3.1 Mice immunization & CFU estimation

3.3.2 Histopathology of the lungs

3.3.3 Hybridoma generation & screening of clones

### 3.4 BIOINFORMATICS

3.4.1. Data retrieval

3.4.2. Molecular modeling

3.4.3. Protein-protein docking

3.4.4 Analyses of protein-protein docking results

3.4.5. Sequence alignment

## **4. SURFACE EXPOSED ENOLASE OF *MTB* IS A PLASMINOGEN BINDING PROTEIN.....46-59**

Results

Discussion

## **5. EXPLORING THE INTERACTION OF *MTB* ENOLASE WITH HUMAN PLASMINOGEN.....60-70**

Results

Discussion

## **6. MONOCLONAL ANTIBODY (MABS) GENERATION AGAINST *Mtb* ENOLASE.....71-80**

Results

Discussion

## **7. KEY POINTS ..... 81-83**

## **8. REFERENCES..... 84-89**

## **9. APPENDIX..... 90-94**

## **10. PUBLICATIONS..... I-IX**



## *List of Abbreviations*

%	Percentage
βME	Beta mercaptoethanol
μg	Microgram
μl	Microlitre
μM	Micromolar
~	Approximately
°C	Degree celsius
ASA	Accessible Surface area
A <sub>260</sub>	Absorbance at 260 nm
A <sub>280</sub>	Absorbance at 280 nm
A <sub>600</sub>	Absorbance at 600 nm
Ab	Antibody
AFB	Acid fast bacillus
ATP	Adenosine triphosphate
BCG	Bacille de Calmetteet Guérin
BM	Basement membrane
bp	Base pair
cDNA	Complementary DNA
CD	Cluster of differentiation
CFU	Colony forming units
CFU-F	Colony-forming unit-fibroblasts
Ctf	Centrifuged
DMSO	Dimethyl sulfoxide
DNA	Deoxyribonucleic acid
DOTS	Directly observed treatment short-course
ELISA	Enzyme-linked immunosorbent assay
ESAT-6	Early secreted antigen-6



FACS	Fluorescence-activated cell sorting
FBS/FCS	Fetal bovine/calf serum
g	Gravitational force
GFP	Green fluorescent protein
gm	Grams
H&E	Haematoxylin and Eosin
h/hrs	Hour/hours
IFN- $\gamma$	Interferon-gamma
Ig	Immunoglobulin
IL	Interleukin
i.p	Intraperitoneal
i.v	Intravenous
IL-10	Interleukin-10
INH	Isoniazid
LB	Luria-Bertani
LPS	Lipopolysaccharide
LTBI	Latent tuberculosis infection
Ln	Laminin
M	Molarity
mg	Milligram
MAbs	Monoclonal antibody
min/mins	Minute/Minutes
ml	Millilitres
mM	Milli Molar
MDR	Multi-drug resistant
MOI	Multiplicity of infection
<i>Mtb</i>	Mycobacterium tuberculosis
MTBC	Mycobacterium tuberculosis complex
N	Normality

OADC	Oleic Albumin Dextrose Catalase
OD	Optical density
PBS	Phosphate-buffered saline
PBST	Phosphate-buffered saline tween
PCR	Polymerase Chain Reaction
PEG	Poly-ethylene glycol
PPD	Purified protein derivative
PTB	Pulmonary tuberculosis
PZA	Pyrazinamide
Plg	Plasminogen
RNA	Ribonucleic acid
ROS	Reactive oxygen species
SOPs	Standard Operating Procedures
sd	Standard deviation
SE	Standard error
SDS	Sodium dodecyl sulfate
TB/Tb	Tuberculosis
TDR	Total drug resistant
THP-1	Human leukemic macrophage cell line
TST	Tuberculin skin test
t-PA	Tissue-type plasminogen activator
u-PA	Urokinase type plasminogen activator
UV	Ultra violet
VBNC	Viable but non culturable
WHO	World Health Organisation
WT	Wild type
XDR	Extensively-drug resistant

# CHAPTER 1

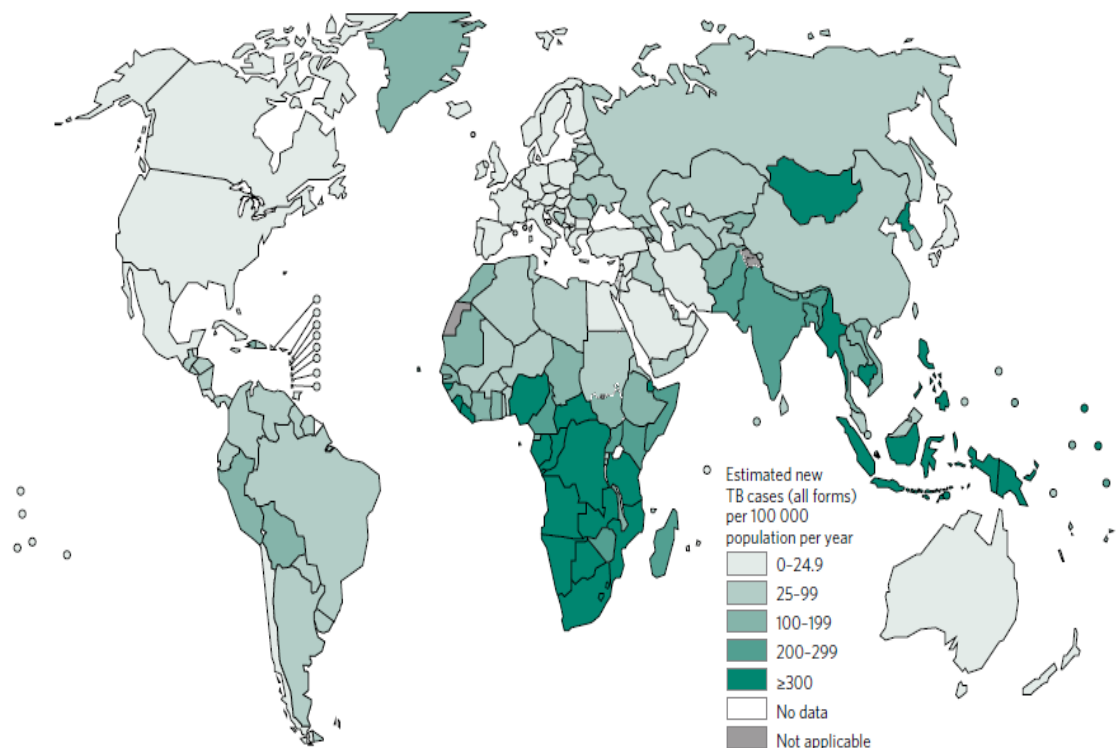
## **INTRODUCTION**

Being the biggest killer amongst the bacterial infections, TB remains a curse to the humanity. Every year, the WHO's statistics on the toll of this dreadful disease takes remains consistently high [1]. It records more than a million deaths annually and majority of the victims remain latently affected by this infection. *Mycobacterium tuberculosis* aka *Mtb* is the causative agent for this infection [2]. Microscopically, these bacilli are 0.2-0.5 $\mu$  in diameter and 2-4 $\mu$  in length. Obligate aerobes, these bacilli are able to contagiously spread from one person to another. While lungs are the major site of infection, the bacilli are actually able to get disseminated systemically from the proximal lymph nodes to the distal parts like bones and the bone-marrow. The disease is mostly associated with latency and thus absence of apparent symptoms of infection in most of the individuals. In case of immunocompromised or old aged victims, the disease can quickly erupt leading to bloody sputum/ phlegm and death. This is why, the disease is the leading killer amongst the HIV patients [1].

Though preventable, the disease has become uncontrolled majorly due to the failure of the BCG vaccine which is clearly unable to protect the adults from this disease and has remained a shield against TB in children only. Moreover, the treatment of TB is difficult and prolonged. There is a whole list of drugs that are used combinatorially for treatment of TB which means that no single drug is able to cure the ailment completely. This situation gets worsened by the fact that often the infective *Mtb* strain is found to be resistant to several drugs/ antibiotics making it a tough choice for the clinicians and health workers [3]. Due to this, of late there have been very few drugs reaching the market while still being queued up awaiting to be used in therapy as there is a huge apprehension of an accompanied drug resistance. For the underdeveloped and the developing countries of the world, it still remains an unmanaged health problem as there exists a communication gap between the chief health bodies and the health professionals at the regional health centres thereby keeping the majority of people's health at risk to TB and its forms called as the extra-pulmonary TB [4].

Major part of the research has been focused to discover newer and more efficacious vaccines against TB many of which are chasing or trailing in the clinical trials. Despite being a century old malady, a lot is yet to be discovered in terms of the molecular synergy occurring during infection. We have recently demonstrated the presence of Enolase on the *Mtb* cell surface where it may act as a virulence factor and

found it to be a potential vaccine candidate [2]. Enolase is a highly conserved molecule and works as a glycolytic enzyme. It controls the reversible conversion of 2PGA (2-phospho glycerate) to PEP (phospho-enol-pyruvate) [5]. It's role is therefore quite essential for the cell metabolism. *Mtb* contains a single locus coding for a functional enolase molecule with no existing paralogs. The gene product is found to co-exist in the cytosol along with the cell surface. It has been found to be a plasminogen binder and thereby a prospective invasion tool for the *Mtb* which can be activated to plasmin and cause a massive tissue matrix erosion. In the current work, enzymatic characterization of the recombinant *Mtb* enolase molecule has been performed in detail and its plasminogen binding ability has been deciphered using the site specific mutations. It enables us to identify the residues which can be inhibited by suitable drugs thereby abrogating the interaction of *Mtb* enolase with the host plasminogen. Moreover, the exposed molecule is an effective antigen and a vaccine candidate (protective antigen) for



WHO's report on TB 2016

**Fig 1. Estimated TB incidence rates 2015**



*Mtb*. After confirming the antigen's protective efficiency as a vaccine candidate, we have tried to develop MAbs (monoclonal antibodies) against *Mtb* enolase and test the binding specificities of the same. The binding activity of the anti-enolase MAb has been checked with *Mtb* enolase as well as that with the human alpha-enolase. As a measure to prevent any future cross reactivity of the MAb against this highly conserved antigen present in humans as well as *Mtb*, we have done so. Generation of MAbs is a fast growing industry [6]. Monoclonal antibodies find a preferred use as a therapeutic tool against the bacterial infections owing to their high specificity and chemical stability [7].

## CHAPTER 2

### **Review of literature**

## **2.1. TUBERCULOSIS (TB)**

One of the oldest maladies on this earth, TB still remains a health threat and an emergency for the world. Tuberculosis (TB) is a bacterial disease capable of spreading through the air which makes it a dreadful epidemic. Each year, it causes ill-health and death among millions of people [8].

### **2.1.1 Global scenario**

According to the World Health Organization (WHO), TB is a worldwide pandemic. A fact sheet of WHO dated March 2010 on tuberculosis states that overall, one third of the world's population (~2 billion) is currently infected with TB bacteria. According to it, every second someone in the world is newly infected with bacilli and 1 in every 10 of these newly infected people will become sick or infected later in their life. WHO's 2015 report on TB has listed 15 countries with the highest estimated TB incidence rates along with a co-incidence of HIV infections. This includes India, Indonesia, Ethiopia, Lesotho, Myanmar, South Africa, Uganda, the United Republic of Tanzania and Zimbabwe. China, India and Indonesia alone accounted for 45% of global cases in 2015. There were an estimated 10.4 million new (incident) TB cases worldwide in 2015. While in 2014, 9.6 million people are estimated to have fallen ill worldwide with TB [1]. This prefaces the continuously increasing incidence rates for this infection that plagues the whole world.

## **2.2. TYPES OF TB**

### **2.2.1. Pulmonary v/s extrapulmonary TB**

The TB pathogen mostly and primarily localizes in the lungs when it causes **pulmonary TB** while it can actually be found existing in any organ of the host's body e.g. lymph nodes, bone, bone marrow and meninges thus causing an **extra pulmonary** form of TB [9]. 15-20% of the cases of active TB can get converted to the extrapulmonary TB. This prominently includes HIV infected persons along with children and the immune-compromised or old aged people [10]. The fact, that the upper lobes of the lung are better aerated than the lower ones is probably the reason why the former is more affected during active TB disease.

### 2.2.2. Active v/s latent TB

When the TB bacilli are inducing symptoms of infection in a patient then the state is that of **active TB**, it is now only that a person coughs or sneezes causing disease transmission [4]. However, many people are found to be containing a dormant form of the pathogen known as **Latent TB** and have no apparent clinical signs of a disease thereby remaining asymptomatic. It is evident that even latent individuals maintain the infection stealthily. It has been indicated by various epidemiological studies carried out across developing and non developed countries that 5-10 % of latent individuals tend to develop an active TB disease during their life time.

### 2.2.3. Miliary TB

Miliary tuberculosis is a distinctive form of tuberculosis that is characterized by a wide dissemination into the human body. Its name comes from a specific pattern seen on a chest radiograph showing many tiny spots distributed throughout the lung fields with an appearance similar to millet seeds thus the term "miliary" tuberculosis [11].

## 2.3. CAUSES OF TB

*Mycobacterium tuberculosis (Mtb)* which is the causative agent of Tuberculosis was discovered by Dr. Robert Koch in 1882 as rod-shaped bacteria. These are small, slow-growing bacteria that can live only in people. It is not found in other animals, insects, soil or other non-living things [12]. Mycolic acid present in its cell wall, makes it an acid fast species. It resists decolourisation of acid and alcohol. It multiplies slowly, can remain dormant for decades. Therefore, this is one of the major physical determinants of its safe survival and persistence inside the host [13]. *Mtb* is an obligate aerobe, it needs oxygen to survive. For this reason, during active TB disease, *Mtb* complexes are always found in the upper air sacs of the lungs.

The principle cause of human tuberculosis is *Mycobacterium tuberculosis* [8]. Other members of the *Mtb* complex which can cause tuberculosis include *M. bovis*, *M. microti*, and *M. africanum*. *M. microti* is not known to cause TB in humans; infection with *M. africanum* is very rare, while *M. bovis* has a wider host range and is the main cause of tuberculosis in cattle. More frequently the cause of infection by *M. bovis* in

humans is consumption of either unpasteurized milk or milk product and meat from an infected animal. *M. bovis* BCG (attenuated form of *M. bovis*) and *M. smegmatis* being non-pathogenic act as common surrogates for *Mtb* in research [14].

### **2.3.1. Transmission**

Generally, the infection spreads from one individual to another by the release of infective agents from the airways of an infected person in the form of cough or sputum droplets. Therefore the bacterium exits the active patients in the form of tiny microscopic droplets when the TB patient coughs, sneezes, speaks, sings, or laughs. It is noteworthy that only a person with active TB can spread the disease to others [4, 15].

### **2.3.2. Symptoms**

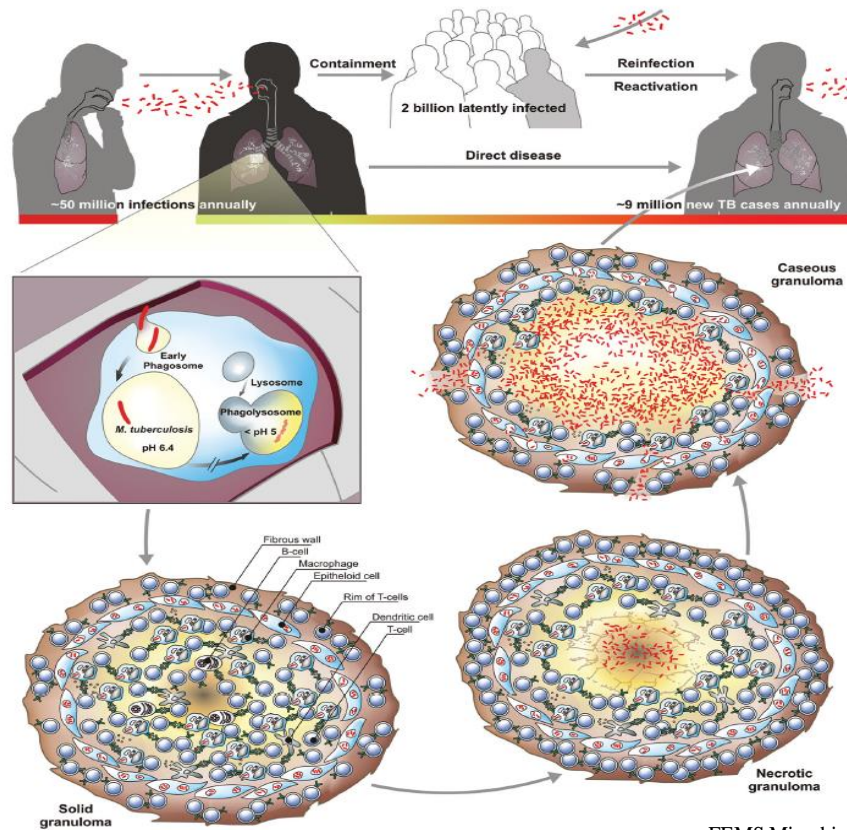
It is chronic, inflammatory infectious disease which may take up to months or even years to culminate into a fulminant disease after the initial infection. Symptoms may be protean and therefore vague to get noticed early enough by the affected person. Tuberculosis can produce atypical sign and symptoms in infants, the elderly and immunocompromised hosts. Although it can affect people of any age, individuals with weakened immune system e.g. with HIV infection, are at an increased risk to TB.. Moreover, in healthy people the active immune system helps wall off the disease. Early symptoms of active TB includes weight loss, fever, night sweats, and loss of appetite reaching up to chronic and highly debilitating stage with cough, chest pain, and bloody sputum/ saliva in some individuals [16].

## **2.4. PATHOGENESIS OF TUBERCULOSIS**

Understanding the pathogenesis of *Mycobacterium tuberculosis* was difficult before the determination of full genome sequences of the various *Mycobacterial* strains. The announcement of the complete DNA sequence of *M. tuberculosis* genome in 1998 marks a preface to the chapter of understanding the pathogenesis of this disease. The sequencing of the virulent laboratory strain H37Rv revealed a genome containing 4,411,529 base pairs encoding approx. 4000 genes. A gene fragment corresponding to the region of difference-1 (RD-1) of the *Mycobacterium tuberculosis* genome, spanning open reading frames Rv3871 to Rv3879c, is missing in all bacillus

Calmette-Guerin (BCG) vaccine strains of *M. bovis*, indicating that this was perhaps the primary deletion event responsible for attenuation of virulent *M. bovis*. The RD-1 locus has, therefore, been considered crucial in the pathogenesis of *M. tuberculosis* [17]. Moreover, very high G-C content remarks another uniqueness of the *Mtb* genome [18].

Being a communicable infection, the bacilli first reach the lungs through the bronchioles where the tubercle bacilli may infect the alveoli within 2 to 3 weeks time. Tubercle bacilli present in the alveoli of the lungs are further ingested by macrophages and due to this a chemotactic response is caused by the continuously multiplying bacilli which brings additional macrophages from the vicinity. Most of these macrophages are not successful in destroying the bacilli, however the enzymes and cytokines that are eventually released by these result in a conclusive lung damage and inflammation [19, 20].



FEMS Microbiology Reviews, 2013

**Fig 1. Transmission and pathology of tuberculosis.** Transmission of TB between individuals occurs via aerosols of infectious bacilli. Upon an inhalation of the infective droplets, the pathogen reaches the lungs and is phagocytosed by the alveolar macrophages. The ingested host cell induces a localized proinflammatory response that attracts the mononuclear cells and T lymphocytes to build up a granuloma, the hallmark of TB. Granuloma maturation (solid, necrotic and caseous) occurs at different velocities and typically culminates in coexistence of all the lesions at the same time during an active TB disease.

### 2.4.1. Granuloma

Macrophages infected with *Mtb* along with freshly immigrant monocytes (Figure 1) constitute an initial inflammatory focus during TB progression. This primary lesion then matures into a granuloma which is the hallmark of TB. Granulomas are well organised structures composed of the various types of immune cells e.g. mononuclear phagocytes of different developmental stages, DCs (Dendritic cells) as well as T and B lymphocytes. Some infected cells move out of these foci to create secondary lesions in the lung. In the majority of individuals the pathogen is controlled at this stage by the immune system and does not spread further thus called as LTBI (Latent TB infection) [21]. At this stage, the bacteria become dormant but may remain alive for decades. This enclosed infection being referred to as latent tuberculosis may therefore even persist through out a person's life without causing any symptoms. However, the

bacteria can get activated anytime later to replicate and escape from the granuloma and spread to the other parts of the lungs causing active pulmonary tuberculosis. This reactivation may occur months or even years after the initial infection. Granulomas are present in a multitude of forms in an infected person. Three major types of granuloma are distinguished as (1) solid granulomas which contain *Mtb*; (2) necrotic granulomas typical for early stages of active TB; (3) caseous granulomas during end-stage or severe TB. The solid granuloma acts as a site for *Mtb* containment during latency (LTBI) and also as the source of tissue damage at the early stage of disease. Here the bacilli are in a stage of dormancy, characterized by low metabolic activity with non- to low-replicating persistence. Often, such bacteria are difficult to grow under normal culture conditions and therefore named as viable but not culturable (VBNC). By doing so the bacteria are able to adapt to the low oxygen stress present around their niche. A lot of research has been done to understand the effects and implications of hypoxia in the context of TB infection [22].

## **2.5. DIAGNOSIS**

TB diagnosis remains in the root of uncontrolled existence of the disease among the human populations. The transmission process is very efficient due to the fact that the droplets can persist in the atmosphere for several hours. Also, infectious doses as low as less than 10 bacilli are enough to start the infection. Once in the lungs, the bacteria meet with the body's first line defence i.e. the macrophages. There are several tests available to diagnose TB as well as to find out if a person is sensitive or resistant to certain drugs used in the treatment of tuberculosis. There are several tests which can be used to determine if someone has latent TB i.e. infected with the TB bacteria without showing any apparent signs or symptoms of illness.

### **2.5.1. Evidence of TB bacteria**

The development of TB disease is a two stage process. In first stage, known as latent TB, a person is infected with bacteria. While in the second stage, known as active TB or TB disease, the bacteria have reproduced sufficiently and therefore cause the person to become sick. A diagnosis of active TB can only be confirmed when there is definite evidence for the presence of TB bacteria in the person's body.



### **2.5.2. TB diagnostic tests**

Some current TB tests take a long time to obtain result while others are not very accurate. The TB tests often have low sensitivity or low specificity. If a TB test has low sensitivity, it means that there will be a significant number of false negatives meaning that the test result is suggesting that a person has not caught TB however this actually may not be true. Similarly, a low specificity means that there will be a significant number of false positives suggesting that a person has TB when he/ she may actually not have TB.

### **2.5.3. Chest x-ray as TB test**

If a person has TB bacteria and resulting inflammation in the lungs then an abnormal shadow may be visible on a chest x-ray. Also, acute pulmonary TB can be easily seen on an x-ray.

### **2.5.4. The TB skin test**

Skin test/ tuberculin test/ mantoux TB test is a very widely used test. It is often used to detect latent TB infections. This involves injecting a small amount of cell-free fluid containing purified protein derivative (PPD) obtained from a human strain of *Mtb* called as tuberculin; into the skin in the lower part of arm. 48 to 72 hours after this injection, the area of skin at the site of injection is monitored to check if there is a hard area or swelling or inflammation, and if there is one then its size is measured. The larger the size of the affected area the greater the likelihood that person has undergone an infection with TB bacteria in the past. It is however, worth keeping in mind that this does not mean that the person is currently suffering from TB disease at the very time of test.

### **2.5.5. Interferon gamma release assay (IGRAs)**

The interferon Gamma Release Assay (IGRAs) is a newly introduced but highly accurate test for TB. This in particular estimates the levels of the interferon gamma (IFN- $\gamma$ ), an inflammatory cytokine/ immune signalling molecule in blood of the suspected TB patients. Also, this cytokine is involved in the formation of the inflamed zone due to the occurrence of delayed type hypersensitivity (DTH) that we observe after tuberculin injection/ mantoux test.

### **2.5.6. Serological tests**

Serological tests for TB are based on detecting the mycobacteria-specific antibodies in the blood sample being tested. However, it is very difficult to accurately assess the infection status of a patient by merely measuring the antibody levels therefore these are highly unreliable. World health organisation (WHO) has prohibited the use of these tests for TB diagnosis.

### **2.5.7. Sputum smear microscopy**

It is a very simple and inexpensive method of directly confirming the presence of TB bacteria in the sputum sample. It is often the first TB tests to be used in the countries with high rate of TB incidence. A thick fluid that is produced in the lungs and the airways i.e. the sputum contains TB bacilli during an active state of infection and is apt to be used as a sample.

Further, the sputum sample is uniformly spread on a glass slide so as to form a thin layer, called as smear. A series of special stains are then applied onto the sample, and the stained slide is viewed under a light microscope to find TB bacteria that might be present therein.

### **2.5.8. Fluorescent microscopy**

Unlike the light microscopy, fluorescent microscopy uses quartz halogen or high pressure mercury vapour lamp as the light source. It aids in a more rapid examination of the specimen covering a large portion of the smear at a single given time point. Mercury vapour lamps however are expensive and take a while to warm up. Moreover they consume a lot of electricity. One way of overcoming these problems is the use of light emitting diodes (LED) as they are illuminated quickly and have a long life. This is why the world health organisation (WHO) has recommended a replacement of the conventional fluorescent microscopy by LED microscopy. LED microscopy has also been recommended to replace the conventional Ziehl-Neelsen light microscopy.

### **2.5.9. Culturing bacteria for TB test**

Growing the test samples in the TB culture media is necessary to identify the TB bacilli. For this, the media can be either solid i.e. culture plates or even liquid media i.e. culture broth. Different media are used to make the process of selection more

accurate for the identification of the disease causative microorganism(s) that might be present in the sample. Agar based solid media is normally used to isolate a single bacterial colony forming unit (CFU) after preparing serial dilutions of the sample provided. Though confirmatory, it is a time taking method of diagnosis. Culture can also take weeks to grow because of slow growth of TB bacilli on the solid media. After an initial confirmation of the TB bacilli, another 4-6 weeks are required to know which TB drugs would be suitable for use in its treatment by doing the drug susceptibility results with the screened/ isolated bacteria.

#### **2.5.10. TB drug susceptibility tests**

Owing to increasing emergence of multi-drug resistant strains of TB bacteria “Drug susceptibility tests” become an essential part of the TB detection process itself. It completely answers the question, “if a person has got drug resistant TB or not”. Some drug susceptibility tests, such as the Gene expert tests can be used to diagnose TB as well as testing for some types of drug resistance.

### **2.6. TREATMENT**

Till 1944, there was no drug for use against TB. It was then that Streptomycin was used for the first time against tuberculosis (**Table 1**). For long, Streptomycin was used as a monotherapy for treating TB. But today we have a whole big range of drugs against TB which can be classified as: First and second line of antibiotics. It shows the scenario of multi drug resistance which is frequently reported by the clinicians and is a growing concern for the health bodies across the globe. Also it hampers the control and eradication of the disease. The drugs are called so because they are the first to be used during TB treatment (**Table 1-2**) [3]. Multidrug resistance or **MDR** is defined as resistance to at least rifampicin and isoniazid which are the two key drugs used in the treatment of the disease. More recently, severe forms of the drug resistance named as **XDR-TB** (extremely drug resistant TB) has been identified. XDR-TB or the infection of an extensively drug resistant strain of *M. tuberculosis* is in addition to being MDR also resistant to any of the

**Table 1. List of anti-TB drugs and their time of discovery**

Antibiotics	Year of discovery
<b>FIRST LINE OF ANTIBIOTICS</b>	
Isoniazid	1952
Rifampin	1966
Pyrazinamide	1952
Ethambutol	1961
Rifabutin	1980
Rifapentine	1965
<b>SECOND-LINE ANTIBIOTICS</b>	
Cycloserine	1952
Ethionamide	1956
P-amino salicylic acid	1946
Streptomycin	1944
Amikacin	1972
Kanamycin	1957
Capreomycin	1963
Levofloxacin	1986
Moxifloxacin (Avelox, BAY 12-8039)	1996
Gatifloxacin	1992

**Nguyen and Thompson *et al*, 2006**

fluoroquinolones and at least one of the three injectable drugs kanamycin , capriomycin and amikacin [23]. Globally in 2015, there were an estimated 4,80,000 new cases of MDR-TB and an additional 100,000 people with rifampicin-resistant TB who were also newly eligible for MDR-TB treatment. India, China and the Russian Federation accounted for 45% of these cases [1]. This makes it imperative for us to understand the mechanisms underlying drug resistance against the various drugs being used. Better knowledge of the mechanism of drug resistance in the TB and the molecular mechanism involved will help us to improve our current therapeutic strategies to cure TB.

Treatment of TB requires a prolonged drug regimen; usually involves simultaneous consumption of several antibiotic drugs for at least 6 months and sometimes even lasts for as

**Table 2. Anti-TB drugs and genes involved in their mechanisms of resistance**

Drug	MIC (mg/L)	Gene	Role of gene product
Isoniazid	0.02-0.2 (7H9/7H10)	<i>katG</i>	catalase/peroxidase
Rifampicin Pyrazinimide Streptomycin	0.05-0.1 (7H9/7H10) 16-50 (LJ) 2-8 (7H9/7H10)	<i>inhA</i>	enoyl reductase
		<i>ahpC</i>	alkyl hydroperoxide reductase
		<i>rpoB</i>	$\beta$ -subunit of RNA polymerase
		<i>pncA</i>	PZase
Ethambutol	1-5 (7H9/7H10)	<i>rpsL</i>	S12 ribosomal protein
		<i>rrs</i>	16S rRNA
Fluoroquinolones	0.5-2.0 (7H9/7H10)	<i>gidB</i>	7-methylguanosine methyltransferase
		<i>embB</i>	arabinosyl transferase
Kanamycin/amikacin	2-4 (7H9/7H10)	<i>gyrA/gyrB</i>	DNA gyrase
Capreomycin/viomycin	2-4	<i>rrs</i>	16S rRNA
Ethionamide	10 (7H11)	<i>tlyA</i>	rRNA methyltransferase
<i>p</i> -amino salicylic acid	0.5 (LJ)	<i>inhA</i>	enoyl reductase
PA-824 and OPC-67683	0.03 (7H9/7H10)	<i>thyA</i>	thymidylate synthase A
TMC207	0.03 (7H9/7H10)	Rv3547	hypothetical 16.4 kDa
		<i>atpE</i>	ATP synthase

Da Silva et al., 2011

long as 12 months. Successful treatment of TB therefore critically depends on the close cooperation between patients and healthcare providers.

However there are other forms of drug resistance namely intrinsic and acquired drug resistance. Intrinsic drug resistance has been attributed to the unusual structure of the mycolic acid component of the *Mtb* cell wall which renders the bacterial cell less permeable to several drugs/ antibiotics. While acquired drug resistance is mainly caused due to spontaneous mutations in chromosomal genes, producing the selection of resistant strains during suboptimal drug therapy. These are different from drug tolerance phenotype exhibited by some strains of *Mtb* which means that the bacteria are able to halt their growth in the presence of antibiotics but continue to survive and resume an active growth kinetics soon after the antibiotic treatment is stopped. It is interesting to note that the bacteria practises drug resistance phenotype at the cost of

their physiological functions which is often expressed as a reduction in its growth, virulence or transmission [3].

### **2.6.1. New drugs and their resistance mechanisms**

New drugs against TB continue to be discovered and tested to increase the effectiveness of MDT (Multi-drug therapy). Moreover it is well known that the different drugs exert their activity by interacting with different molecular targets inside the *Mtb* cell. It is astounding that even before the new drugs get to the clinical use in humans, a resistance mechanism was found to be present in certain *Mtb* strains. Some of the newer drugs against TB are Nitroimidazoles, SQ-109 (diamine analogue of ethambutol), TMC207 (specific inhibitor of micobacterial ATP sythase), NAS-21 AND NAS-91 (inhibits mycolic acid biosynthesis), Benzothiazinones and Phenothiazines [3].

## **2.7. NEW VACCINES TO PREVENT TB**

Prevention remains as the fundamental tool to control TB. A diverse range of adjuvanted vaccines are chasing in the clinical trials towards a final approval while many are still at the stage of research in the labs. This enormous number of vaccines is all aimed to establish a full protection against *Mtb* bacterial exposure in adults apart from being safe. WHO 2015 report enlists many of such promising vaccines currently being scrutinized in the human clinical trial settings. However it remains as a giant challenge to the world till date. The global pipeline of TB vaccine candidates in clinical trials is more robust than at any previous period in history. A TB vaccine either aims to prevent infection (pre-exposure vaccine) or to prevent primary progression to disease or reactivation of latent TB (post-exposure/ therapeutic vaccine).

Currently, there are 15 vaccine candidates in the clinical trials. Results of the phase2 efficacy data will determine whether BCG and/ or H4: IC31 can prevent infection; M72 can prevent disease and the phase 3 data will determine the potential of *M. vaccine* to prevent disease prevalence [24]. Following are brief ups on few of the highly promising vaccines advancing in the clinical trials. H1:IC31R is an adjuvant subunit vaccine combining the *M. tuberculosis* antigen Ag85B and ESAT-6 and

velneva, sIC31 adjuvant. H4:IC31 is being developed as a booster vaccine to *M. bovis* BCG. The vaccine candidate contains a fusion protein of Ag85B and TB10.4 formulated with IC31 adjuvant. It is currently being evaluated in phase 2 of the clinical trials. H56:IC31 is an adjuvant subunit vaccine that combine, three antigens (Ag85B, ESAT-6, and Rv2660c) of *M. tuberculosis* with IC31 adjuvant. VPM 1002 is prepared from the Prague strain BCG by cloning the listerolysin gene from *Listeria monocytogenes* and deleting unease gene. It has been observed to elicit an improved immunogenicity [24].

**RUTIR**-is a non-live vaccine containing fragmented and detoxified *M. tuberculosis* bacteria. The product is a liposomal suspension with a charge excipient. It is a immunotherapeutic vaccine and phase 2 trial of the vaccine has been already completed in South Africa.

**MTBVAC**-It is the first live attenuated *M. tuberculosis* vaccine to enter in phase 1 trials and cleared through recently. The next trial will be in phase 1/2 among adults in South Africa. The vaccine is being developed for use as a potential boost vaccine in adolescents and adults.

**M. Vaccinae**- This vaccine is undergoing a phase 3 trial especially to assess its prophylactic properties against LTBI. It is licensed by China as an immunotherapeutic agent to help in shortening TB treatment regimen mainly for drug susceptible TB [24].

## **2.8. TB+HIV-A DUAL EPIDEMIC**

Prolonged infection of HIV, gradually diminishes the human immune defence mechanisms making their patients susceptible to TB . Therefore people with a co-infection of HIV and TB are frequently encountered by the clinicians and health personnel. Also, TB remains the leading cause of deaths among HIV positive people across the globe. Since, incidence rates of HIV are strikingly high in Africa, HIV is accounted as the key factor contributing to TB in these populations [1, 24].

## **2.9. PLASMINOGEN AND PLASMIN SYSTEM**

The extracellular matrix or ECM is involved in building the structural scaffolds around the tissues and in regulation of several physiological processes. This includes cellular signalling, migration and transport of solutes across the body tissue and cellular barriers. Apart from being the prime acellular component of the tissue matrix, ECM constitutes the anchoring plate for different types of epithelia and is designated as the basement membrane (BM). It also surrounds the blood capillaries and neurons. Evidently, ECM components are attractive targets for adherence and invasion by various human pathogens. The prime ECM components: laminin and collagen are targeted by several microbes for adhesion and

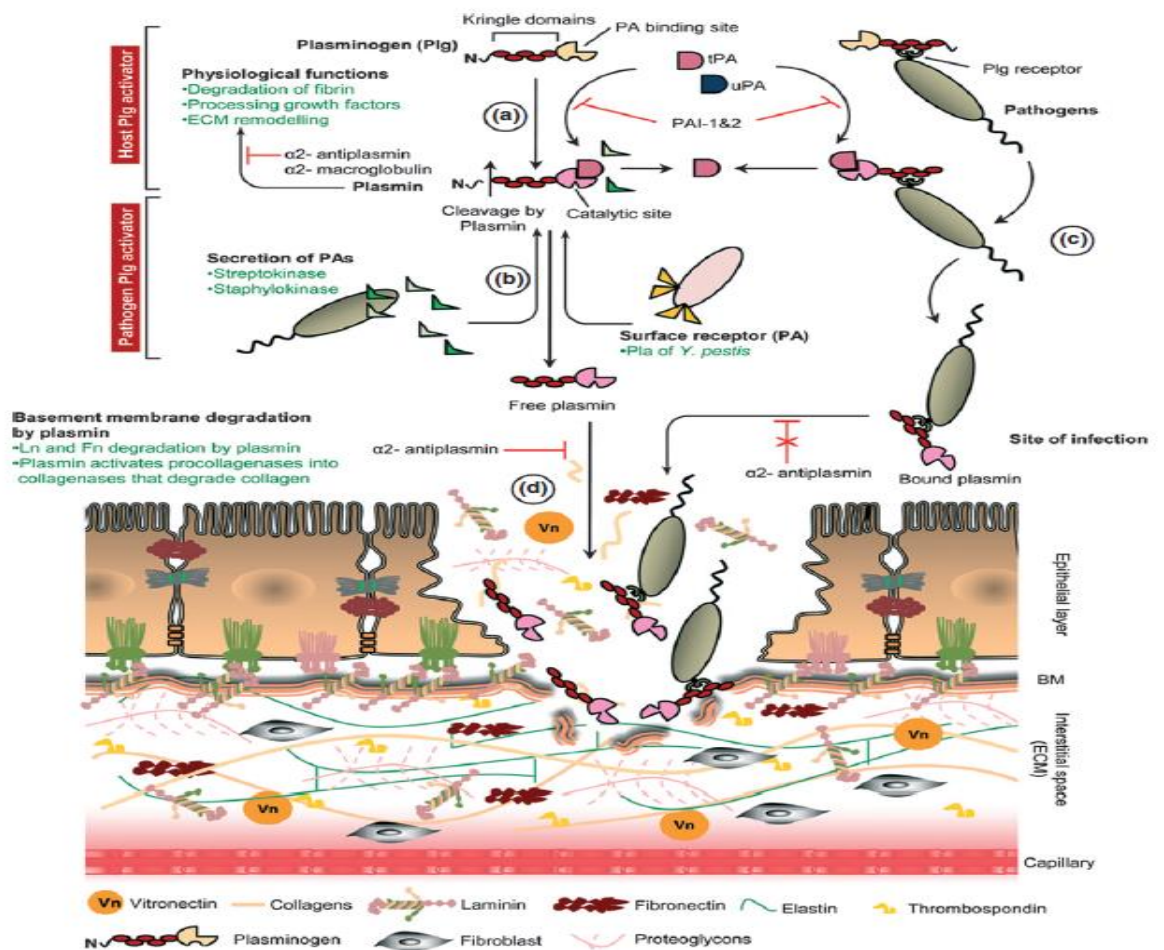




**Fig. 2. Microorganism utilize Plg and host proteases to degrade the host cellular barriers.** **a.** N-terminal (K78) and a C-terminal cleavage (between R 560 – V561) performed by plasmin and tPA/ uPA respectively render the zymogen active. Activation of Plg into plasmin is controlled by the inhibitors PAI-1 and PAI-2 to prevent an excessive response. Additionally, there are plasmin inhibitors such as alpha antiplasmin and alpha2-macroglobulin that inhibit the proteolytic activity of free plasmin. **b.** Streptokinase and staphylokinase are either secreted or cell surface bound activators of Plg. These two proteins have different mechanisms of activating the Plg as compared to tPA and uPA. In contrast the Pla surface protein of *Yersinia pestis* activate Plg in a similar way as tPA/ uPA, that is by cleaving the peptide bond between R560-V561. **c.** Plg is recruited by several bacteria at their surface and subsequently converted into active plasmin, either by host tPA/ uPA or by their own Plg activators. Free plasmin is inhibited by alpha2-antiplasmin, whereas plasmin bound to the bacterial surface cannot be inhibited by alpha2-antiplasmin. Microorganisms, thus use surface bound plasmin as a tool to degrade the BM. **d.** The inflammatory host response causes damage to the epithelial cell layer and the damage is enhanced by, for example neutrophil infiltration and activation of MMPs. Free plasmin and bacterial surface bound plasmin degrade Ln and Fibronectin in the BM. Procollagenase is converted into active collagenase that in turn degrades collagen bound in the BM. The BM is thus destroyed and bacterial pathogens will gain access to the connective tissue and ECM proteins resulting in increased adhesion and invasion of host tissues and capillaries.

induction of host inflammatory responses culminating into their colonization and invasion of host tissues [25] Pathogenic microorganisms deploy their secretory or surface bound proteases or hijacked host proteins e.g. plasminogen (plg) during inflammatory responses, resulting in increased ECM degradation and tissue damage. Moreover, during infection, degraded and exposed ECM components are particularly attractive targets for adherence of pathogens [26].

Plasminogen is a glycoprotein synthesized in the liver and released into the blood circulation as a zymogen. In circulation, plasminogen adopts a closed, activation resistant conformation which upon binding to clots, or to the cell surface adopts an open form that can be converted into active plasmin by a variety of enzymes, including tissue plasminogen activator (tPA), urokinase plasminogen activator (uPA), kallikrein, and factor XII (Hageman factor). It is therefore, proteolytically convertible into the active plasmin protease [27] The main function of plasmin is to degrade fibrin threads (fibrinolysis) which is critically involved in various homeostatic processes including blood coagulation (i.e. hemostasis), cell migration as well as tissue and wound repair. Being a broad specificity protease, plasmin is capable of degrading the other ECM proteins like fibronectin, laminin, and thrombospondin. Plasmin further activates procollagenase into collagenase which can degrade collagen and also activate certain complement mediators leading to enhanced inflammatory reactions [28] . In our body, to strike a balance and prevent the occurrence of excess proteolysis, the activity of plasminogen is stringently controlled, by an array of regulators/inhibitors e.g. plasminogen activator inhibitors PAI 1, 2 (vibronectin serum protein); alpha 2 antiplasmin; alpha2 macroglobulin. Nevertheless, alpha -2

antiplasmin is a major inhibitor of soluble plasmin and thus controls uncontrolled proteolysis during inflammatory responses [29].

Invasive human pathogens are commonly known to recruit host plasminogen onto their cell surface and exploit its protease activity to manifest massive tissue damage. Pathogens use this surface borne proteolytic activity as a mechanism to degrade the surrounding host cell barriers and ECM proteins thereby penetrating the host. Some pathogenic bacteria are also known to secrete their own plasminogen activators like Streptokinase from *Streptococcal* species, and Staphylokinase from *Staphylococcus aureus*.

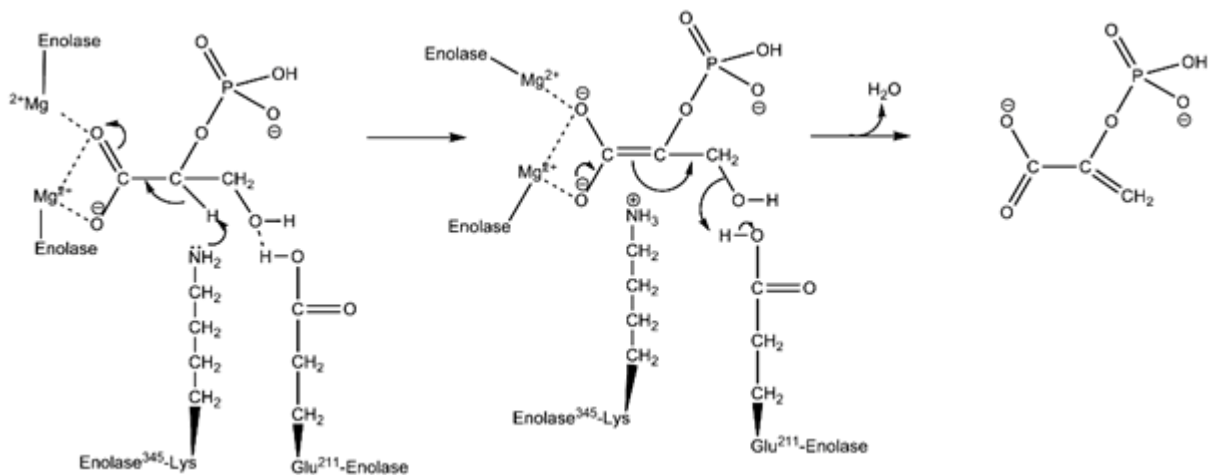
As the field of research regarding plasminogen and microbial pathogenesis is rapidly growing new plasminogen receptors have been unravelled in various pathogens e.g. in *S. pneumonia* [30], *Staphylococcus aureus*, *Brucella abortus*, *B. anthracis*; the respiratory human pathogen *Moraxella catarrhalis* etc [31]. Similarly, pneumococcal endopeptidase (PepO) has recently been reported to be a plasminogen binding molecule in *S. pneumonia* which plays a crucial role in pneumococcal immune evasion of the host cells [32, 33]. Nevertheless, binding of complement component, C4Binding Protein (C4BP) to *Streptococcus pneumoniae* is a known virulence mechanism of this pathogen and it was observed to be increased in the presence of plasminogen [34]. Additionally, many fungal pathogens are also known to utilize the plasminogen based proteolysis for disease progression e.g. *Candida albicans*, *Paracoccidioides* etc [35]. *Borrelia burgdorferi*, a spirochete and causative agent of the famous Lyme's disease lacks endogenous, surface-exposed proteases and therefore to disseminate efficiently through the host tissues it relies on the host proteases e.g. plasmin(ogen) [36]. Similarly, several proteins of *Leptospira interrogans* including a novel Omp-A like protein are known to aid in plasminogen and ECM binding [37]. It is therefore understood that plasminogen binding by surface-anchored pathogen receptors is a ubiquitously implied mechanism of host invasion found to be present from prokaryotic to eukaryotic human pathogens.

## 2.10. ENOLASE

Alpha enolase is a highly conserved glycolytic enzyme that is ubiquitously found in almost all organisms ranging from prokaryotes to eukaryotes. In *Mtb*, enolase is encoded by Rv1023 locus having no existing paralogs. It encodes a 47.2 kDa protein, 429 amino acids in its length. In spite of being a glycolytic enzyme it has been frequently associated with several non-glycolytic functions. This includes its activities as a surface molecule in spite of lacking a signal peptide [5]. Apart from showing diversity in its subcellular localization, enolase shows significant variations in the levels of its expression during the various metabolic growth phases e.g. in a pathogenic bacteria. Though the mechanism of its translocation from the cytosol to the surface remains to be elucidated, it clearly dictates its dominant function during disease progression and pathogenesis. *Mtb* enolase shares significant similarity with the enolase of several pathogenic bacteria and fungi. *Mtb* enolase shares more than 65 % sequence similarity with the enolase of pathogens like *Streptococcus pneumoniae*, *Staphylococcus aureus*, *Corynebacterium diphtheria*, *Brucella abortus*, *Bacillus cereus*, *Plasmodium falciparum*, *Trypanosoma brucei*, *Leshmania mexicana* and *Candida albicans* (Table 1) [33, 38, 39]. The protein is found to be a dimer in most of the higher organisms including fungi but some members of eubacteria e.g. *Bacillus subtilis*, *Streptococcus suis* and *T. maritime* express an octameric form of the protein [40, 41]. In *Mtb*, the protein exists as a dimer indeed.

### 2.10.1. Reaction mechanism

Also known as phosphopyruvate hydratase, enolase catalyzes a reversible conversion of 2-phosphoglycerate (2-PG) to phosphoenol pyruvate (PEP) following a typical “Elimination reaction”. It particularly occurs during basic conditions owing to attack by a nucleophilic species that can aid in the removal of a proton generating a stabilized anionic intermediate. Finally the lone pair on the anion relocates to produce a double bond (enol). Metal ions play an important initial role in stabilizing the negative charge of the substrate, 2-PG at its deprotonated oxygen while increasing the acidity of the  $\alpha$ -hydrogen atom. A positively charged residue mostly lysine, deprotonates this alpha hydrogen atom and the resulting charge is stabilized by resonance to the carboxylate oxygen and metal ion



Reference: Wikipedia

cofactor. Finally, the hydroxide on C3 gets eliminated as water with the help of a negatively charged residue e.g. glutamate and forms the final product which is PEP [42, 43].

## 2.11 IMPLICATIONS OF ENOLASE

### 2.11.1 Enolase in bacteria

A lot of research has been conducted to confirm the role of enolase in mediating a variety of bacterial infections [44]. Being a plasminogen binder, it attains the ability to curtail disease upon host with the use of extracellular and intravascular fibrinolytic system inside the host. This implies the immense potential of enolase molecule to conduct pathogenesis. Studies related to enolase of *S. pneumoniae*, *Aeromonas hydrophila*, *Staphylococcus aureus*, *Brucella abortus* as well as *Mycobacterium tuberculosis* confirm a crucial role played by the pathogen associated enolase during infection [2, 39, 45, 46]. Further it is worth noting that  $\alpha$ -enolase present on the surface of a non pathogenic bacteria like *L. mesenteroides* lacks its plasminogen binding sites [46].

### 2.11.2 Enolase in fungi

Enolase has a remarkable importance in the life cycle of fungal pathogen *Candida albicans* where it has been found to be important for the normal growth and virulence. An enolase deletion mutant of *C. albicans* becomes more sensitive to drugs and less

virulent in nature [47]. Unlike in the gram positive bacteria, *Candida* enolase is a glucan associated protein present in its cell wall [48]. It has been shown that the incorporation of virulence determinants or antigens associated with the glucan component of the fungal cell wall get reduced due to the action of  $\beta$ -1,3 glucan synthase inhibitors e.g. cilofungin. While cell wall associated enolase of *C. albicans* acts as an indirect target of cilofungin, a member of pneumocandins. This coincides with the fact that upon treatment of *C. albicans* with a pneumocandin there was an eventual increase in the cytosolic localization of enolase paralleled with a decrease in its surface distribution [48]. Enolase was detected at *P. brasiliensis* surface and it has been observed that the association of this fungi with epithelial cells and phagocytes was increased in the presence of recombinant enolase [49].

### **2.11.3 Enolase in protozoan parasites**

Malaria is one of the most devastating parasitic diseases. Enolase has been found to be an essential virulence determinant in *P. falciparum*, the causative agent of malaria [50, 51]. *Leishmania spp* are protozoan parasites that are the cause of cutaneous and visceral leishmaniasis. *Leishmania* surface enolase binds plasminogen and this interaction contributes to the virulence of the parasite [38, 52]. An anti-enolase antibody is reported to interfere with plasminogen binding and therefore making this a vaccine candidate antigen.

## CHAPTER-3

# **MATERIALS AND METHODS**

### **3.1-Materials**

#### **3.1.1 Reagents and biochemicals**

Calcium chloride, Agarose, Acrylamide, Magnesium chloride, Phenol-chloroform-isoamylalcohol (PCI), Sodium hydroxide, Ammonium chloride, Sodium bicarbonate, Dimethyl sulfoxide (DMSO), Dulbecco's modified Eagle's medium (DMEM),  $\beta$ -mercaptoethanol, Penicillin, Streptomycin, anti-mouse IgG whole molecule-FITC conjugated, N,N' methylene bis-acrylamide and other chemicals were procured from Sigma-Aldrich, USA. Sodium Chloride, RNase, Potassium chloride, Potassium acetate, Potassium dihydrogen orthophosphate, Di-Potassium hydrogen phosphate, Kanamycin, Glycine, Glycerol, Glucose, Ethidium bromide, EDTA, Coomassie brilliant blue R-250, Bromophenol blue, Bovine Serum Albumin, 5-Bromo 4-chloro 3-Indolyl Phosphate (BCIP), Ammonium per sulphate, SDS, Sucrose, TEMED, Tris-base (Trizma), Triton X-100, Tween-20, Glutamine, HEPES, Sodium acetate, Nickel sulphate and Xylene cyanol were obtained from USB chemicals, USA. Glacial Acetic Acid, HCl, Isopropanol and Methanol were procured from Qualigens, India. All the DNA modifying enzymes were supplied by New England Biolabs. LB agar and LB broth were obtained from Difco laboratories, BD, USA. Ethanol and isopropanol was procured from E. Merck, Germany. Dialysis tubing was procured from Pierce, Thermo Scientific, USA. Bradford's reagent was bought from Biorad. Tissue culture plastic wares e.g. ELISA plates were obtained from Corning, USA. HRP-conjugated anti-mouse IgG1, IgG2a, IgG2b (Santa Cruz), Fetal bovine serum (FBS) (Gibco BRL Invitrogen) were used. Middlebrook 7H9, 7H10, 7H11 and enrichment supplement OADC and ADC were purchased from BD. Electroporation cuvettes (0.2cm) were obtained from Biorad. Plasminogen, FITC-labeled human plasminogen and anti-human plasminogen antibody (monoclonal) was procured from BioMac. HRP-conjugated anti-human IgG secondary antibody was bought from Jackson ImmunoResearch laboratories. polyethylene glycol (PEG), Lysine and D-Val-Leu-Lys-p-nitroanilide dihydrochloride, HAT selection media (50X), complete adjuvant and incomplete adjuvant, anti-mouse IgG gold-conjugated antibody and Urokinase, were obtained from Sigma. Round bottom flasks, beakers and other glasswares were obtained from Borosil Glassworks Limited, India and USA.

### **3.1.2 Bacterial strains**

For propagating and over-expression of the desired clones, DH5 $\alpha$  and BL21- $\lambda$ DE3 strains of *E. coli* were used respectively. *Mycobacterium tuberculosis* H37Rv, *M. bovis* BCG were used. All experiments pertaining to *Mycobacterium tuberculosis* strains were carried out in Biosafety level 3 containment facilities.

### **3.1.3 Kits**

Gel extraction kit and plasmid extraction kit was obtained from Qiagen, USA. BD OptEIA™ ELISA kit was purchased from BD Biosciences Pharmingen, USA. AFB staining kit was obtained from BD, USA. KOD Plus mutagenesis kit for site directed mutagenesis was obtained from Toyobo.

---

### **3.1.4 Oligonucleotides**

All the sequence-specific oligonucleotides were custom synthesized by Sigma Genosys, USA and the complete sequence of all the primers used in the current work has been incorporated in Table 1 and 2.

### **3.1.5 Cell lines and mice strains**

Sp2/0Ag14 Myeloma cell line was from ATCC, Pune. Pathogen-free, 4-6 weeks old, inbred female Balb/c mice and C57bl/6 mice were procured from National Institute of Nutrition (N.I.N.), Hyderabad, India. Swiss albino female mice (4-6 weeks old) were fetched from Animal house facility at Jawaharlal Nehru University (JNU), New Delhi. The regulations of Institutional Animal Ethics Committee (IAEC) of Jawaharlal Nehru University were followed in all mice experiments.

## **3.2 MOLECULAR BIOLOGY METHODS**

### **3.2.1 Isolation of genomic DNA from *Mtb***

For isolation of genomic DNA from *Mtb* H37Rv, a loopful of the fully grown *Mycobacterium* colony was suspended in 1ml of GTE buffer (Glucose, Tris and EDTA) and was mixed thoroughly by vortexing and then centrifuge at 8000g for 15 minutes.



**Table 1:** Details of cloning performed

S No	Clones	Vector backbone	Restriction sites	Approx. Protein size (in KDa)	Forward primer	Reverse primer
1	<i>Mtb</i> Eno (full length)	pET28a	BamHI -HindIII	50	GGCCGGATCCGTGCCGAT TATCGAGCAGGTTAGG	GGCCAAGCTTCTATTT CGTCTCGCACGCGAAC CG
2	<i>Mtb</i> Eno (full length)	pMV261	EcoRI-HindIII	50	GGCCGAATTCGTGCCGATT ATCGAGCAGGTTAGG	GGCCAAGCTTCTATTT CGTCTCGCACGCGAAC CG
3	C terminal <i>Mtb</i> Eno	pET28a	BamHI -HindIII	37	GGCCGGATCCCCAAACGC GCACATTC	GGCCAAGCTTCTATTT CGTCTCGCACGCGAAC CG
4	N terminal <i>Mtb</i> Eno	pET28a	BamHI -HindIII	No expression	GGCCGGATCCGTGCCGAT TATCGAGCAGGTTAGG	GGCCAAGCTTCCCCC GACATAACGGAAC
5	human $\alpha$ -Eno	pET28a	NcoI-XhoI	40	GGCCCCATGGGCATGATC GAGATGGATGGAACAG	GGCCCTCGAGCTTGGC CAAGGGTTTCTGAA G
6	human $\alpha$ -Eno	pGEMT	Not applicable	N.A.	GGCCCCATGGGCATGATC GAGATGGATGGAACAG	GGCCCTCGAGCTTGGC CAAGGGTTTCTGAA G

**Table 2:** Site directed mutagenesis

S. No.	Name of mutants	Template DNA	Forward Primer	Reverse Primer
1.	Enolase (wt)	<i>Mfb</i> Genomic DNA	GGCCGGATCCGTTGCCGATTATCG AGCAGGTTAGG	GGCCAAAGCTTCTATTTCGTCTC GCACGGGAACCG
2.	K429A	pETeno clone	GGCCGGATCCGTTGCCGATTATCG AGCAGGTTAGG	GGCCAAAGCTTCTAGGCCGTCTC GCACGGGAACCG
3	S190A	pETeno clone	GGGGTCCCTGAAAAAGGAGGGG CTGTC	TTGAGCGCGTGGTACACCTCAG
4	K193A	pETeno clone	CGCTCAAGTCGGTCCCTGGCAAAG GAGGGCTGTCCAC	GTGGACAGCCCCCTCTTTGCCA GGACCGACTTGAGCG
5	K194A	pETeno clone	AAGCGGAGGGGCTGTCCACCG	TCAGGACCGACTTGAGCGCGT GG
6	T199A	pETeno clone	CCGCCGGCCTGGGCGACGAAAG	ACAGCCCCCTCCTTTTTCAGGAC CG
7	D250A	pETeno clone	CCGCCGGCACCGGCTACGTC	TGAAGA ACTCGGTGGCCGC
8	K429A+ K193A	pET429Eno clone	CGCTCAAGTCGGTCCCTGGCAAAG GAGGGCTGTCCAC	GTGGACAGCCCCCTCTTTGCCA GGACCGACTTGAGCG
9	K429A+ K194A	pET429Eno clone	AAGCGGAGGGGCTGTCCACCG	TCAGGACCGACTTGAGCGCGT GG
10	K429A+ K193A+ K194A	pET429A+193AEn o clone	CAGCGGAGGGGCTGTCCAC	CCAGGACCGACTTGAGCGCG
11	S190A+ T199A+ K193A	pET190A+199AEn o clone	GGCAAAGGAGGGGCTGTCCGCC	AGGACCGCCTTGAGCGCG

The pellet obtained was resuspended in 450 µl of GTE buffer and was transformed to a 2 ml eppendorf tube. The bacterial culture was killed by boiling the tube at 80°C for 60 minutes. The tube was then cooled and 50 µl of 10 mg/ml lysozyme solution was added. The contents were mixed gently and the tube was incubated for 24 h at 37°C. All these steps were done in a biosafety hood. After the lysozyme treatment, the cells were treated with 100 µl of 10% SDS and 50 µl of 10 mg/ml Proteinase K. The added contents were mixed gently and incubated at 55 for 40 minutes. Thereafter, the cells were treated with 200 µl of 5M NaCl and mixed by vortexing 16 µl preheated cetyltrimethyl ammonium bromide (CTEB) solution at 65 °C was added to the sample, mixed gently and was incubated at 65°C for 30 minutes. Thereafter an equal volume of chloroform, isoamylalcohol (24:1) was added and mixed by gentle shaking. The tube was centrifuged at 8000 g for 15 minutes at the room temperature. The upper 900 µl of aqueous layer was transferred to a fresh microcentrifuge tube and 560 µl (0.7 volumes of chilled isopropanol) was mixed gently by inversion until DNA had precipitated. The tube was incubated at -20°C for 30 minutes. The precipitated DNA was pelleted at 12000 g for 15 minutes. The supernatant was discarded. The DNA pellet was washed with chilled 70 % ethanol. The pellet was recovered by spinning at 12000 g for 15 minutes. The pellet was air dried and finally dissolved in sterile water or TE buffer. The pellet was stored at 4 °C overnight to allow the DNA to dissolve.

### **3.2.2 PCR amplification of genes**

Prior cloning, the ORF corresponding to each gene was amplified from the genomic DNA of *Mtb* H37 Rv using Phusion/ Taq polymerase. The PCR condition was as: initial denaturation at the 95 for 5 minutes, denaturation at 95 for 30 s, annealing at 55 for 1 minute, extension at 72 for required time ranging between 0.5-1.5 minutes for a total of 25 cycles.

### **3.2.3 DNA extraction from agarose gels**

For gel purification, the PCR amplified product was fractionated by agarose gel electrophoresis. DNA fragments of right size were excised from agarose gel and were eluted from the gel slice using gel extraction kit (Qiagen) as per the instruction of manufacturers. In brief,

1. Gel pieces containing the DNA fragment of interest were cut into small pieces and transferred to a 1.5 ml microfuge tube. Weigh the gel slice after subtracting the weight of microfuge tube.
2. For every 100mg of gel slice 100 $\mu$ l of capture buffer was added and then the sample was incubated at 55 °C till the agarose gets dissolved in the buffer. Tubes were vortexed intermittently for complete solubilization of gel particles. Samples were loaded on to the gel extraction spin column and centrifuged at 13,000 rpm for 1 minute.
3. The column was washed by adding 500  $\mu$ l of wash buffer followed by a spin at 13,000 rpm for 1 minute.
4. The column was dried by giving a dry spin at 13,000 rpm for 30 sec.
5. The column was transferred in a fresh microfuge tube and the DNA was eluted in autoclaved MQ water. 30  $\mu$ l of MQ water was added onto the column, incubated for 1 min and spin down the column at 13,000 rpm for 1 minute.
6. Residual DNA was again eluted in 30  $\mu$ l autoclaved MQ water by spinning the column at 13,000 rpm for 1 minute.
7. Concentration of purified product was estimated by taking A260 on spectrophotometer.

### **3.2.4 Restriction digestion**

The purified DNA amplicons for each clone was further digested using the suitably chosen restriction enzymes as mentioned earlier in Table 1 of this chapter for further ligation into the desired vector backbone.

### **3.2.5 Construction of recombinant clones**

The digested fragments were resolved on 0.8 % agarose gel and were extracted from the gel as described earlier. The digested DNA fragment was ligated to expression vector to obtain respective clones. Further, ligation was set in 10 $\mu$ l reaction volume with vector DNA (10 ng), PCR product (30 ng), 1 $\mu$ l of ligation buffer (10X) and 1 unit of T4 ligase. The ligation reaction mixture was incubated for 16 hrs at 16°C. The transformants were further grown and used for the preparation of glycerol stocks.

### 3.2.6 Site directed mutagenesis

Point mutations in the coding sequence of the *Mtb* enolase was generated using the KOD Plus mutagenesis kit (Toyobo). Briefly, the pETEnolase plasmid harbouring the wild type enolase was used as template in an inverse PCR reaction along with the mutagenic primers, followed by an overnight DpnI digestion for the template at 37°C as per the manufacturer's protocol. For some mutants, Pfu turbo based PCR method was also employed for mutagenesis. The PCR condition was as: initial denaturation at 95 for 2 minutes, denaturation at 98 for 10 s, annealing at 55 for 1 minute, extension at 68 for 7 minutes for a total of 10 cycles. The products were then self ligated using the T4 polynucleotide kinase and ligation mix from the kit and transformed into the highly competent *E. coli* DH5 alpha cells. Transformed cells were plated on LB Agar plates containing Kanamycin. The transformants obtained were subjected to the dideoxy sequencing reaction so as to confirm the incorporation of the specific mutations in the clone at the desired positions and the absence of any other random mutations elsewhere. The details of the primers used for the mutagenesis are all mentioned in the Table No 2 of this chapter. All the mutant proteins were purified under native conditions using Ni<sup>2+</sup> NTA affinity chromatography as described later in section 3.2.15.

### 3.2.7 Preparation of competent cells of *E. coli*

*E. coli* DH5 $\alpha$  and *E. coli* BL21 ( $\lambda$ DE3) competent cells were prepared using Calcium chloride method. It is frequently used to prepare competent bacterial cells with an yield of  $5 \times 10^6$  to  $2 \times 10^7$  transformed colonies per  $\mu$ g of supercoiled plasmid.

1. The host cell culture was streaked on a LB agar plate from the frozen glycerol stock stored at -80 °C. A single colony was inoculated into 3 ml LB for overnight growth.
2. One ml of the overnight grown culture was further inoculated into 100 ml LB and allowed to grow until A600 reached 0.4.
3. The culture was chilled on ice, transferred to ice cold 50 ml polypropylene tubes and centrifuged at 4000 rpm for 10 min at 4°C in a Sorvall SS34 rotor.
4. The supernatant was decanted and the pellet was resuspended gently in 10 ml of ice cold 0.1 M CaCl<sub>2</sub> and incubated on ice for 30 minutes with intermittent shaking.

5. The cells were then cold centrifuged at 4000 rpm in Sorvall SS34 rotor. The pellet was resuspended in 4 ml of ice cold 0.1 M CaCl<sub>2</sub> containing 20% glycerol (v/v).
6. About 200 µl aliquots were taken for checking viability, contamination and efficiency of transformation. The rest of the suspension was kept at 4 °C for 12-24 hours to enhance the competency of the cells and then stored in aliquots of 200 µl at -80 °C.

### **3.2.8 Acid fast staining of *Mtb***

Acid fast staining of *Mtb* was done by Acid fast staining kit (Himedia), according to manufacturer's protocol. Briefly, smear of a culture was prepared on a slide. The smear was dried and fixed by gentle heating. The slide was covered by carbol-fuchsin and heated from the lower side of the slide intermittently for 8-10 minutes. The slide was washed with water and destained with the acid fast decolorizer, until film exhibited faint pink colour. It was again washed with water and counterstained with methylene blue for one minute. The excess stain was washed with water and the slide was dried and observed under an oil-immersion lenses.

### **3.2.9 Preparation of electrocompetent cells of *Mtb* H37Rv**

1. After 4 days of inoculation with 1% inoculum, the secondary culture of *Mtb* O.D<sub>600</sub>=0.4, 100 ml culture was obtained by culturing in complete 7H9 medium.
2. The culture was centrifuged at 8000 rpm for 10 mins.
3. Supernatant was discarded and pellet was resuspended in 25 ml 10% glycerol (for 50 ml culture) and again centrifuged at 8000rpm/10 min/4°C. This step was repeated.
4. The pellet was washed with 12.5 ml 10 % sterile glycerol twice (8000rpm, 10 mins).
5. The final washed pellet was resuspended in sterile autoclaved 1 ml 10% glycerol (for 100 ml culture pellet).
6. 100µl per microcentrifuge tubes was aliquoted and frozen in -80°C till 2months.

### **3.2.10. Transformation of competent cells of *E. coli***

Plasmid was transformed in the competent *E. coli* DH5 $\alpha$  cells according to the protocol of Sambrook *et al.*, 1989. In brief,

1. 200  $\mu$ l aliquot of competent cells was thawed over ice; DNA was added, mixed by tapping and kept on ice for 30 minutes.
2. The cells were subjected to heat shock at 42°C for 90 seconds in a water bath and were immediately transferred to an ice bath. The cells were allowed to chill for 1-2 minutes.
3. 800 $\mu$ l of LB was added to cells and incubated at 37°C, 200 rpm for 45 minutes.
4. Cells were then pelleted and resuspended in 100  $\mu$ l of LB. The resuspended cell pellet was plated on Luria-Bertani agar plates containing 50  $\mu$ g/ml of Kanamycin. The plates were incubated at 37°C for 16 hours.

### **3.2.11 Electroporation of *M. tuberculosis* cells**

For electroporation of *Mtb* following procedure was followed. In brief,

1. 5  $\mu$ g of plasmid in a volume of 20  $\mu$ l was mixed with 100  $\mu$ l competent cells. All steps were carried out on ice and inside the hood.
2. Competent cells and plasmid mix was transferred in gene pulsar cuvette and electroporated at volt 2.5kv, 25 $\mu$ F for Biorad gene pulsar II.
3. Noted that the time constant shown was above 10.
4. Revival media that is complete 7H9 was added and incubated for 24hrs followed by plating on to Kanamycin (50 $\mu$ g/ml) plus 7H11 plates.

### **3.2.12 Screening of the clones**

The transformants were screened for presence of insert by colony PCR based on the presence of amplification at desired size. Briefly, a single colony of putative clone was emulsified in 10  $\mu$ l of PCR master mix with toothpick and PCR was run. For positive control, Genomic DNA was taken as template. Mini-preparations of plasmid DNA and their restriction analysis were subsequently followed for probable clones showing amplification.

### **3.2.13 Over-expression of recombinant proteins**

All the recombinant proteins were over-expressed in *E coli* BL21 DE3 cells. For this, the expression hosts were cultured upto an O.D<sub>600</sub> of 0.4-0.6 and then IPTG was added to get a final concentration of 1mM thereby inducing over-expression of the protein. A 12 % resolving and 5 % stacking SDS polyacrylamide gel was utilized for the electrophoretic analysis of proteins. 20 µl of supernatant protein samples were analyzed on gel in a Bio-Rad mini gel apparatus (Bio-Rad Laboratories, Hercules, CA, USA). The resolved proteins were visualized by staining the gels with Coomassie brilliant blue (R250 and G-250) followed by destaining the gels to remove excess of stain.

### **3.2.14 Western blot analysis**

The expression of recombinant *rMtb* Enolase was confirmed in uninduced and induced culture lysates by western blotting. Moreover, the *rMtb* Enolase protein was also confirmed by using recombinant protein sera to detect *rMtb* Enolase cell lysate by western blotting. Briefly,

1. Protein samples were resolved on SDS-polyacrylamide gels and transferred to nitrocellulose membrane at a constant voltage of 50 V for 2 hours at 4 °C.
2. Blocking was carried out using 2 % BSA in 1X PBS for 1 hour.
3. For probing the blot with antibody, the membrane was incubated for 1 hour with anti-6X His mouse IgG, diluted 1:5000 in 1X PBS or 1:100,000 dilution of *rMtb*Enolase protein sera in 1X PBS.
4. Blot was washed thrice with PBST (PBS containing 0.1% Tween 20) and then probed with Alkaline phosphatase conjugated anti-mouse IgG, diluted 1:10,000 in 1X PBS for 1 hour.
5. The membrane was again washed three times with PBST and then developed using the substrate solution of NBT/BCIP in alkaline phosphatase buffer.

### **3.2.15 Affinity purification**

All the recombinant proteins were over expressed in BL21 DE3 strain of *E coli* with Hexa-Histidine tag in them and have been purified using the metal affinity



chromatography. The column bound protein was eluted from the columns using a gradient of imidazole concentrations.

### **3.2.16 Protein estimation and dialysis**

Purified protein contained varying concentrations of imidazole to get rid of this protein eluted from the column was dialysed into suitable buffers depending on its end use. For example, PBS pH-7.4 was buffer of choice in all the mice immunization experiments while for the enzymatic activity assays 20 mM Tris pH 8.0 was used. The protein was dialysed into 20 mM HEPES pH 7.6 for the Surface Plasmon Resonance experiments (SPR). Quantification of the protein of interest was performed using the standards of Bovine serum albumin (BSA, 10mg/ml).

### **3.2.17 Enzyme kinetics of *rMtb* Enolases**

Enzymatic activity of rEno (2 µg) was determined at 25 °C in a total volume of 1 ml of activity buffer (100 mM HEPES [pH 7.5], 10 mM KCl, 10 mM MgSO<sub>4</sub>). Enolase catalyzes the reversible conversion of Phospho- enolpyruvate (PEP) to 2-Phosphoglycerate (PGA). The activity was thus measured by monitoring the decrease in PEP absorbance at 240 nm against time using the Cary 100 UV–Vis spectrophotometer (Agilent technologies). An absorption coefficient ( $\epsilon_{240\text{nm}}$ ) of 1400 M<sup>-1</sup> cm<sup>-1</sup> was used to determine the change in PEP concentration using a substrate concentration of 0.05–1.5 mM. Michealis-Menten enzymatic parameters- Km and Vmax were determined.

### **3.2.18 Plasminogen binding analysis for WT Enolase and its variants by endpoint ELISA**

500 ng/well of WT Enolase or its variants were coated in triplicates in 96-well plates and incubated at 4 °C overnight. 500 ng BSA/well was used as a negative control. The wells were washed and blocked with 2% BSA for 2 h. Different dilutions (0.5-0.0125 µM) of human plasminogen (BioMac) were incubated with the WT or mutant proteins for 2 h at RT, followed by 3 PBST (PBS with 0.1% v/v Triton-X 100) washes for 5 min each. The wells were further incubated with 1:10,000 dilution of anti-human plasminogen antibody-Horsh Raddish Peroxidase-conjugated for 1 h followed by 3 PBST washes of 5 min each. TMB was used as substrate for colour development for 15 min. The absorbance was

measured at 630 nm using the microtiter plate ELISA reader (Tecan).

For determining the effect of free lysine towards the interaction between WT and mutant enolase proteins and human plasminogen, 0.1 M lysine was added to the various plasminogen dilutions. Subsequent steps were the same as above.

### **3.2.19 *In vitro* Plasminogen activation /Plasmin formation assays**

#### **a. With rEno (recombinant Enolase)**

rEno (500 ng/well) was coated in 96 well plates in coating buffer (50 mM sodium carbonate, pH 9.6) at 4 °C overnight. The wells were washed and blocked with 2% BSA for 1 h. This was followed by washes and further incubation with plasminogen (500 ng/well) or plasminogen + anti-rEno (1:100 dilution/well) or plasminogen + lysine (0.1 M lysine/well) for 2 h. The wells were again washed and urokinase (100 milliunits/well) was added to the wells for another 3 h. This was followed by addition of plasmin substrate D-Val-Leu-Lys-p-nitroanilide dihydrochloride (Sigma) and absorbance was measured at 405 nm using the microtiter plate ELISA reader (Bio-rad). All the washes were done with 1X PBS and incubations were done at RT.

#### **b. With *Mtb* whole cells**

Plasmin formation on bacterial surface was determined using ELISA with whole *Mtb* cells.  $5.00E + 06$  *Mtb* H37Rv cells (WT and OvnEno) were coated onto 96 well plates in coating buffer at 4 °C overnight. Following steps were the same as described above and were performed in the BSL-3.

### **3.2.20 Immunofluorescence (Confocal) microscopy**

For probing the surface localization of enolase, cells from *Mtb* culture (WT and OvnEno) corresponding to O.D.600 nm ~ 1 were washed and incubated with 2% BSA for 1 h. Next, the cells were washed and incubated with 1:100 dilution of anti-rEno polyclonal sera for 2 h. The cells were again washed and incubated with 1:100 dilution of anti-mouse FITC-labeled secondary antibody for 2 h. This was followed by washing and fixation with 4% paraformaldehyde +0.4% glutaraldehyde for 1 h. All the washes were done with 1X PBS and incubations were done at RT. Cells were mounted on glass slides and fluorescence was visualized with an Olympus Fluoview FV 1000 Laser

scanning confocal microscope. Pre-immune sera treated cells were used as negative control. Image analysis and quantification of per cell fluorescence was done using ImageJ.

### **3.2.21 Transmission electron microscopy (TEM)**

For probing the surface localization of enolase, cells from *Mtb* culture (WT and OvnEno) corresponding to O.D.600 nm ~ 1 were washed and incubated with 2% BSA for 1 h. Next, the cells were washed and incubated with 1:100 dilution of anti-rEno polyclonal sera for 2 h. The cells were again washed and incubated with 1:100 dilution of anti-mouse IgG gold-conjugated (sized 10 nm) secondary antibody for 2 h. This was followed by washing and fixation with 4% paraformaldehyde +0.4% glutaraldehyde for 1 h. All the washes were done with 1X PBS and incubations were done at room temperature. The cells were then mounted on nickel grids (200 mesh; Electron Microscopy Sciences) and stained with Uranyl acetate before viewing using a Jeol 2100 F transmission electron microscope. Pre-immune sera treated cells were used as negative control.

### **3.2.22 Flow cytometry**

Cells from *Mtb* culture (WT and OvnEno) corresponding to O.D.600 nm ~ 1 were washed and incubated with 2% BSA for 1 h followed by incubation with either pre-immune sera (1:100 dilution) or anti-rEno polyclonal sera (1:100 dilution) for 2 h followed by 3 washes of 5 min each. The cells were then incubated with FITC-labeled anti-mouse secondary antibody for 2 h followed by 3 washes for 5 min each. All the washes were done with 1X PBS and incubations were done at RT. This was followed by washing and fixation with 4% paraformaldehyde +0.4% glutaraldehyde for 1 h. The cells were then analyzed for fluorescence signal using FACS Calibur (Beckton Dickinson, Heidelberg, Germany). Fifty thousand events were analyzed for fluorescence using Cell Quest software (Beckton Dickinson). Log-forward and log-side scatter dot plots were used for the detection of cells and a gating region was set to exclude the cell debris and noise.

For visualizing plasminogen binding to the bacterial surface, cells from *Mtb* culture corresponding to O.D.600 nm ~ 1 were washed and incubated with FITC-labeled human plasminogen (BioMac) at a concentration of 20 µg/ml, followed by washes, fixation and visualization as described above.

### 3.2.23 Surface Plasmon Resonance (SPR)

Autolab SPR at the Advanced Instrumentation Research Facility, Jawaharlal Nehru University, New Delhi was used to assess the real time binding of human plasminogen (hPIg) with rEno at physiologically relevant concentrations. For this, the surface activation followed by immobilization of hPIg at concentration of 100 µg/ml and blocking with 100 mM ethanolamine was done as described previously [31]. Binding of rEno (100–800 nM) with immobilized hPIg was done in HBS BIAcore running buffer (10 mM Hepes, 150 mM NaCl, 1.4 mM EDTA, 0.05% Tween-20, pH 7.4) at 25 °C. The association kinetics was monitored for 300 s followed by dissociation for the next 100 s. The binding surface was then regenerated using 50 mM NaOH. All of the binding kinetics experiments were done using rEno as an analyte and BSA as the negative control (for non-specific binding to the surface or immobilized hPIg). The results were plotted as a differential response of hPIg binding to rEno from BSA.

KD value was calculated using the Integrated Rate Law equation;

$$R(t) = E \cdot (1 - e^{-k_s \cdot t}) + R(0),$$

where, E is the maximal extent of change in response at a certain concentration and is equal to  $k_a \cdot C \cdot R_{max} / (k_a \cdot C + k_d)$ ,  $K_s$  is equal to  $(k_a \cdot C + k_d)$ , and  $R(0)$  is the response at  $t = 0$ . E and  $K_s$  were evaluated at each concentration by minimizing the residual sum of squares between observed data and the model equation using solver in MS Excel. Evaluation of  $K_s$  at four different concentrations was then used to calculate KD according to the following equation;

$$K_s = K_a \cdot C + K_d$$

where  $K_s$  is a concentration dependent parameter which in turn is dependent upon association and dissociation rate constants ( $k_a$ ; slope and  $k_d$ ; intercept). The ratio of the intercept to slope of the above line was ascertained to be the dissociation constant or KD.

### **3.3 IMMUNOLOGICAL METHODS**

#### **3.3.1 Mice immunization & CFU estimation**

C57bl/6 (5 weeks old, 20–24 g) female mice were obtained from the National Institute of Nutrition (Hyderabad, India). All studies were approved by the Institutional Animal Ethics Committee and Institutional Biosafety Committee at Jawaharlal Nehru University (New Delhi, India). Mice were divided into four groups- PBS (with adjuvant, n = 8), BCG (n = 8), Ag85B (n = 4) and rEno (n = 8). The experimental groups were immunized with an optimized dose of either 25 µg rEno or 10 µg Ag85B emulsified with complete Freund's adjuvant, intraperitoneally. Boosters with antigen emulsified with incomplete Freund's adjuvant were given on 14th, 28th and 42nd day. BCG (5.00E + 04 CFU) was given as a single dose at the time of first immunization. Blood was collected before every booster for titer determination. Mice were challenged on the 49th day with 2.00E + 06 CFU of virulent *Mtb* H37Rv via tail vein and observed for 8 weeks. Mice were aseptically sacrificed on the 56th day after challenge and lungs were homogenized in PBS with 0.05% Tween-80, followed by plating on 7H11 agar supplemented with 10% OADC and 0.5% glycerol at multiple serial dilutions for CFU analysis. Colonies were counted after 3–4 weeks of incubation at 37 °C and results are expressed as CFU counts per mouse. Number of CFU in control mice injected with PBS + adjuvant is enumerated as control.

#### **3.3.2 Histopathology of the lungs**

The isolated lungs were also processed by fixing in 10% buffered formalin, paraffin embedding, and subjected to hematoxylin and eosin staining for histopathological detection of granuloma, using an Olympus inverted microscope 1X71 equipped with a DP71 camera (Olympus, Tokyo, Japan).

#### **3.3.3 Hybridoma generation & screening of clones**

Traditional hybridoma technology was used for the fusion of the mice splenocytes containing B cells with the myeloma cells. The fusion partner of hybridoma namely myeloma sp2/0Ag14 cell line was cultured in complete DMEM prior fusion and subsequently washed twice with incomplete medium by centrifugation at 2000rpm. Four days before the fusion experiment, mice were hyper-immunized with 50µg enolase protein without adjuvant in PBS. On the day of the experiment, 100 million

splenocytes were taken from the spleens of the hyperimmunized mice and washed in 1X PBS and macerated in the presence of incomplete DMEM to get a cell suspension. The isolated splenocytes were fused with 40-50 million myeloma cells in presence of PEG 1400 and cultured in HAT medium for further selection of successfully fused hybridoma cells. After 7 to 21 days of fusion, approximately 150 hybridoma clones were scrupulously observed, numerated and screened for specific antibody production by indirect ELISA screening.

### **3.4 BIOINFORMATICS**

#### **3.4.1. Data retrieval**

Complete sequence of Enolase for *Mycobacterium tuberculosis* (strain ATCC25618/H37Rv) was retrieved from Swissprot with id P9WNL1. Whereas, enolase from human source have three isoforms  $\alpha$ ,  $\beta$  and  $\gamma$  which were retrieved from Swissprot with ids: P06733, P13929 and P09104 respectively. The X-ray crystal structure of full-length human plasminogen with PDB Id, 4DUR was retrieved from PDB.

#### **3.4.2. Molecular modeling**

Using Modeller 9v14, a 3D structure was generated for *Mtb* Enolase [53]. Crystal structure of enolase from *Synechococcus elongatus* with PDB Id, 4ROP was used as the template. A total of 100 three-dimensional models were generated and 5 best fit models were picked. The selection of 5 best modelled structures out of 100 was performed on the basis of lower value of the Modeller objective function or the DOPE assessment score and with a higher value of GA341 assessment score. To evaluate and select the single best model, stereochemical properties of the five best models were assessed using Procheck v3.0 [54].

#### **3.4.3. Protein-protein docking**

PatchDock v1.0 [55, 56] with default parameters was used for protein-protein docking. PatchDock is an algorithm for molecular docking which provides output as the potential complexes sorted by shape complementarity criteria. In brief, PatchDock employs a jigsaw puzzle technique whereby two molecules are divided into patches (concave, convex, and flat patches) according to the surface shape. These patches, then, be superimposed for possible match using shape matching algorithms. Finally,

the filtering and the scoring, will provide the docked molecules ranked on geometric shape complementarity score.

### 3.4.4 Analyses of protein-protein docking results

Protein-protein interaction plot were generated by Dimplot option of Ligplot+v.1.4.5 [57, 58]. For checking the involvement of enolase interacting residues obtained from Ligplot+, loss in accessible Surface Area (ASA) was evaluated before and after plasminogen binding. It is known that for a residue to be involved in interaction it should lose more than  $10\text{\AA}^2$  ASA in the direction from unbound residue to the bound state [59]. The ASA calculations of unbound enolase and enolase plasminogen complex were performed by Naccessv.2.1.1. The loss in ASA ( $\Delta\text{ASA}$ ) of the  $i^{\text{th}}$  residue in the direction from unbound to bound state was calculated using the expression:

$$\Delta\text{ASA}_i = \text{ASA}_i^{\text{Enolase}} - \text{ASA}_i^{\text{Enolase-Plasminogen}}$$

Where  $\Delta\text{ASA}_i$  is the loss in ASA of the  $i^{\text{th}}$  residue after binding, and  $\text{ASA}_i^{\text{enolase}}$  and  $\text{ASA}_i^{\text{enolase-Plasminogen}}$  are the ASA of  $i^{\text{th}}$  residue before binding and after binding to plasminogen respectively

### 3.4.5. Sequence alignment

The amino acid sequences of three isoforms of human enolase and *Mtb* enolase were aligned using Muscle v.3.8.31 [60] and further analysis and illustration were prepared by Jalview v.2.8 [61, 62].

## CHAPTER 4

**Surface exposed Enolase of *Mtb* is a plasminogen binding protein**



## RESULTS:

### 4.1. Cloning, expression, purification and enzymatic characterization of *Mtb* Enolase

The ORF corresponding to enolase of *Mtb* H37Rv (Rv1023) was identified and PCR amplified using genomic DNA as template and indicated primers (**Table 1, Chapter 3**). The amplicon was double digested and ligated to pET28a to obtain pETH37RvEnolase. Automated dideoxy DNA sequencing was used to verify the sequence of the cloned gene. Recombinant enolase protein (rEno) was expressed as an N-terminal 6X-His fusion protein in *E. coli* BL21( $\lambda$ DE3) cells, induced with 1 mM IPTG for 5 h at 37 °C at an O.D.<sub>600 nm</sub> ~ 0.4. Purification was done from the soluble fraction using Ni<sup>+2</sup>-NTA affinity chromatography as per the manufacturer's instructions. The protein was eluted using an imidazole gradient and dialyzed against 20 mM Tris-Cl [pH 8] and stored at -80 °C for further use. The identity of the recombinant protein was confirmed by MALDI-TOF MS analysis. To generate the K429A point mutant of rEno, a mutagenic reverse primer bearing the nucleotide substitution (**Table 2, Chapter 3**) was used and the gene was cloned in pET28a as described above. Expression and purification of the mutant protein was done as described for the WT rEno. The rEno was also tested for its enzymatic activity. Protein concentration was determined by Bradford reagent using BSA as a standard. Using PEP as the substrate, rEno from *Mtb* exhibited a  $K_M$  of 416  $\mu$ M and  $V_{max}$  of 323  $\mu$ moles  $\text{min}^{-1} \text{mg}^{-1}$ , qualifying its glycolytic function (**Fig 1-2**).

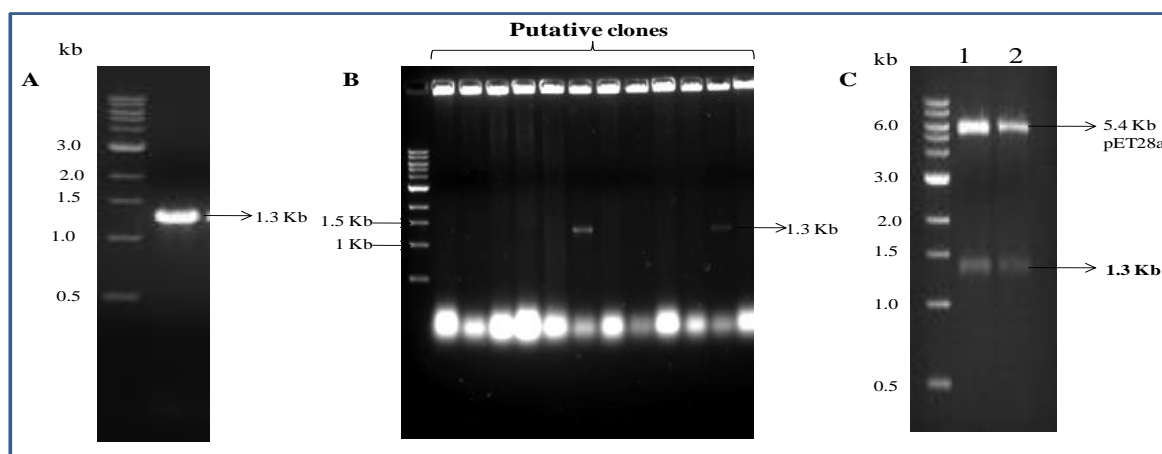


**Fig 1. Cloning of *Mtb* Enolase in pET28a.** A. The ORF corresponding to enolase of *Mtb* H37Rv (Rv1023) was identified and PCR amplified using genomic DNA as template, B. The positive colonies obtained after ligation in pET28a vector were screened by PCR, C. Restriction digestion of the pET28a plasmids isolated from the positive clones using BamHI/HindIII

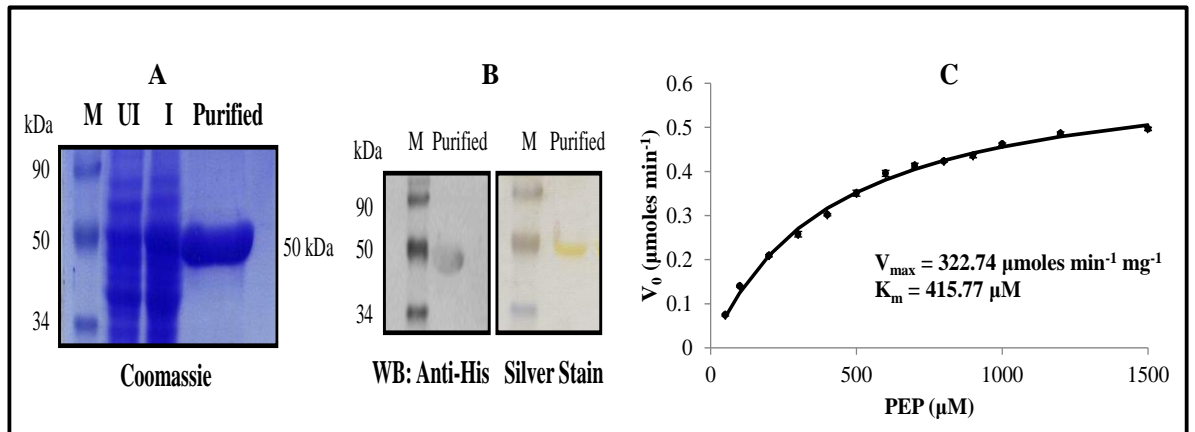


**Fig. 2. Expression, purification and enzymatic characterization of rEno.** **A.** rEno was expressed and purified as an N-terminal his-tagged protein from the soluble extracts of *E. coli* BL21 ( $\lambda$ DE3) using  $\text{Ni}^{+2}$ -NTA affinity chromatography, **B.** The identity and purity of the purified protein was confirmed using anti-histidine western blotting and silver staining, respectively. **C.** rEno catalyzes the conversion of Phosphoenolpyruvate (PEP) to 2-Phosphoglycerate (PGA).

#### 4.2. *Mtb* enolase is immunogenic in humans with active TB disease

Enolase has been shown to be present on the surface of many pathogenic microorganisms, involved in binding to a variety of host proteins [63-66]. In order to

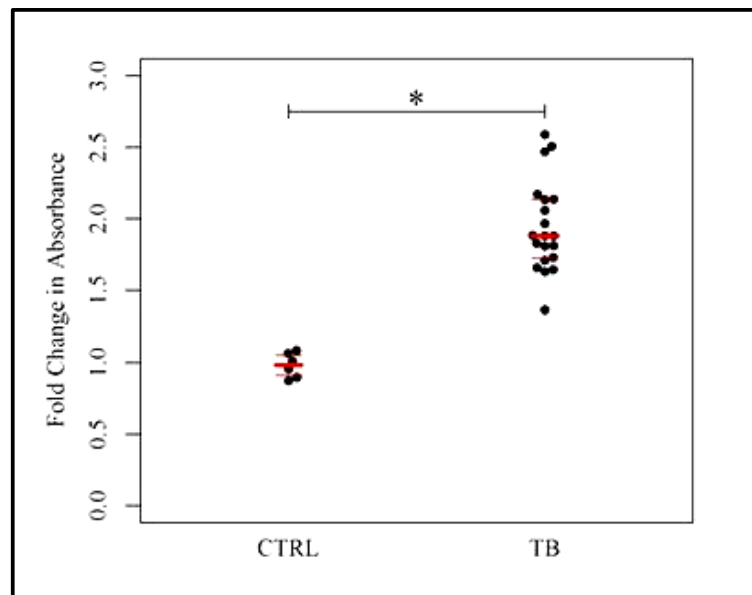


**Fig. 3. Anti-*Mtb* enolase antibodies can be detected in sera from TB patients with active TB disease.** An end-point ELISA was used to measure anti-*Mtb* enolase antibody titer in patient samples with active TB disease (TB,  $n = 20$ ) and healthy individuals (CTRL,  $n = 6$ ). Each dot in black represents an individual with 1st, 2nd and 3rd quartile in red.

elucidate the surface exposure of *Mtb* enolase and its recognition by the human immune system during an active TB infection, anti-*Mtb* enolase IgG levels were evaluated in human serum samples taken from people who were suffering from an

active TB disease. rEno was used as the antigen to measure anti-enolase IgG in the serum samples of control (n = 6) and TB infected individuals (n = 20) using end-point ELISA. Interestingly, a consistent higher antibody response was observed for anti-enolase IgGs in serum samples of TB infected individuals relative to the control group (**Fig. 3**). This result suggested that enolase of *Mtb* was immunogenic in patients suffering from TB and was exposed to the human immune system during the course of infection or as a surface protein of *Mtb*. Antibodies to surface exposed enolase have been reported in natural pneumococcal infection [67] and *B. burgdorferi* infection as well [68].

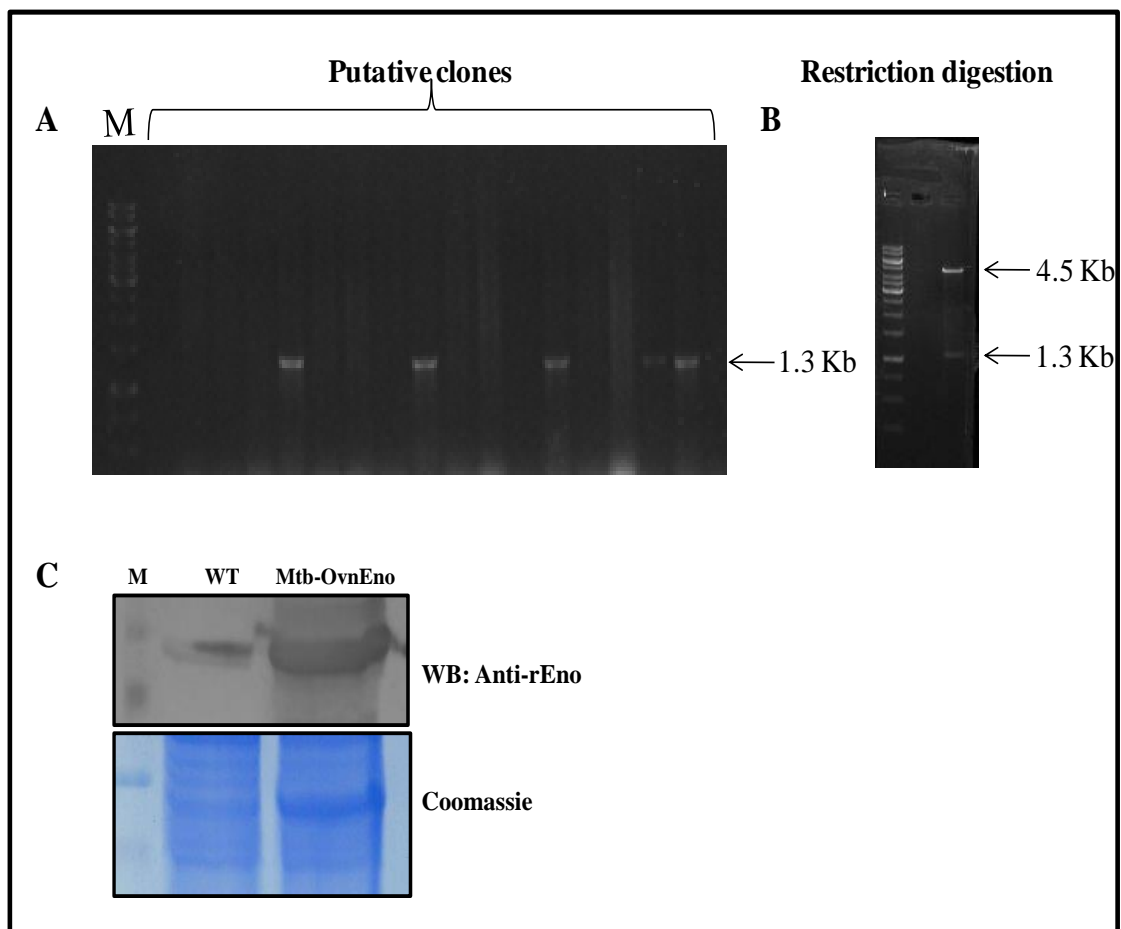


**Fig 4. Cloning in pMV261 and over-expression of rEno in *Mtb*.** A. The positive colonies obtained after ligation in pMV261 vector were screened by PCR, B. Restriction digestion of the pMV261 plasmids isolated from the positive clones using EcoRI/HindIII C. Over-expression of enolase was checked in *Mtb* cell lysates by western blotting using enolase-specific polyclonal sera

#### 4.3. Cloning and electroporation of pMV261:Enolase in *Mtb* H37Rv

The ORF corresponding to enolase of *Mtb* H37Rv was PCR amplified using genomic DNA as template and indicated primers (**Table 1, Chapter 3**). The amplified

fragment was double digested using *EcoRI* and *HindIII* and ligated to pMV261 vector (double digested with the same enzymes) under the HSP60 promoter. Automated dideoxy DNA sequencing was used to verify the sequence of the cloned gene after confirming the presence of insert in the clones using restriction digestion with *EcoRI* and *HindIII*. Further, pMV261:Enolase construct was electroporated in competent cells of H37Rv using Bio-rad Gene. The pellet of both Wt-Eno and Ovn-Eno was resuspended in 1X PBS and subjected to heat inactivation at 100°C for 2 h. The cells were sonicated, centrifuged and the supernatant was subjected to SDS-PAGE and immunoblotting using polyclonal anti-rEno sera (1:5000 dilution). and a single band corresponding to the expected molecular wt of enolase was observed at ~50KDa in SDS-PAGE as well as the western blot (**Fig. 4**).

#### **4.4. Enolase is present on the surface of *Mtb***

Surface localization of *Mtb* enolase was evaluated using antibodies raised in mice against rEno expressed in *E. coli* BL21 strain. The rEno isoform was purified to near homogeneity using Ni<sup>+2</sup>-NTA column chromatography against the 6X-histidine tag. Balb/C female mice (4–6 weeks old) were used for raising polyclonal antisera. The mice were injected with 25 µg of rEno with Freund's complete adjuvant intraperitoneally following a prime-boost regimen. Immunoelectron labeling of intact *Mtb* with anti-rEno polyclonal sera showed localization of enolase on the surface of bacteria. In order to test the concentration dependent export of enolase to the surface of *Mtb*, an enolase overexpressing strain of *Mtb* (*Mtb*-OvnEno) was prepared as described in the methodology. *Mtb*-OvnEno strain expressed more enolase than *Mtb*-WT. Immunoelectron microscopy of intact WT and *Mtb*-OvnEno strains with anti-rEno polyclonal sera showed presence of enolase on the surface. Immunofluorescent staining of both the strains also showed presence of enolase on the surface of *Mtb*. Notably, the *Mtb*-OvnEno strain displayed a higher fluorescence per cell than the WT strain. Furthermore, flow cytometric analysis of both *Mtb*-WT and *Mtb*-OvnEno strains stained with anti-rEno polyclonal sera displayed a considerable shift in their fluorescent labeling. The surface staining with anti-rEno antibodies was

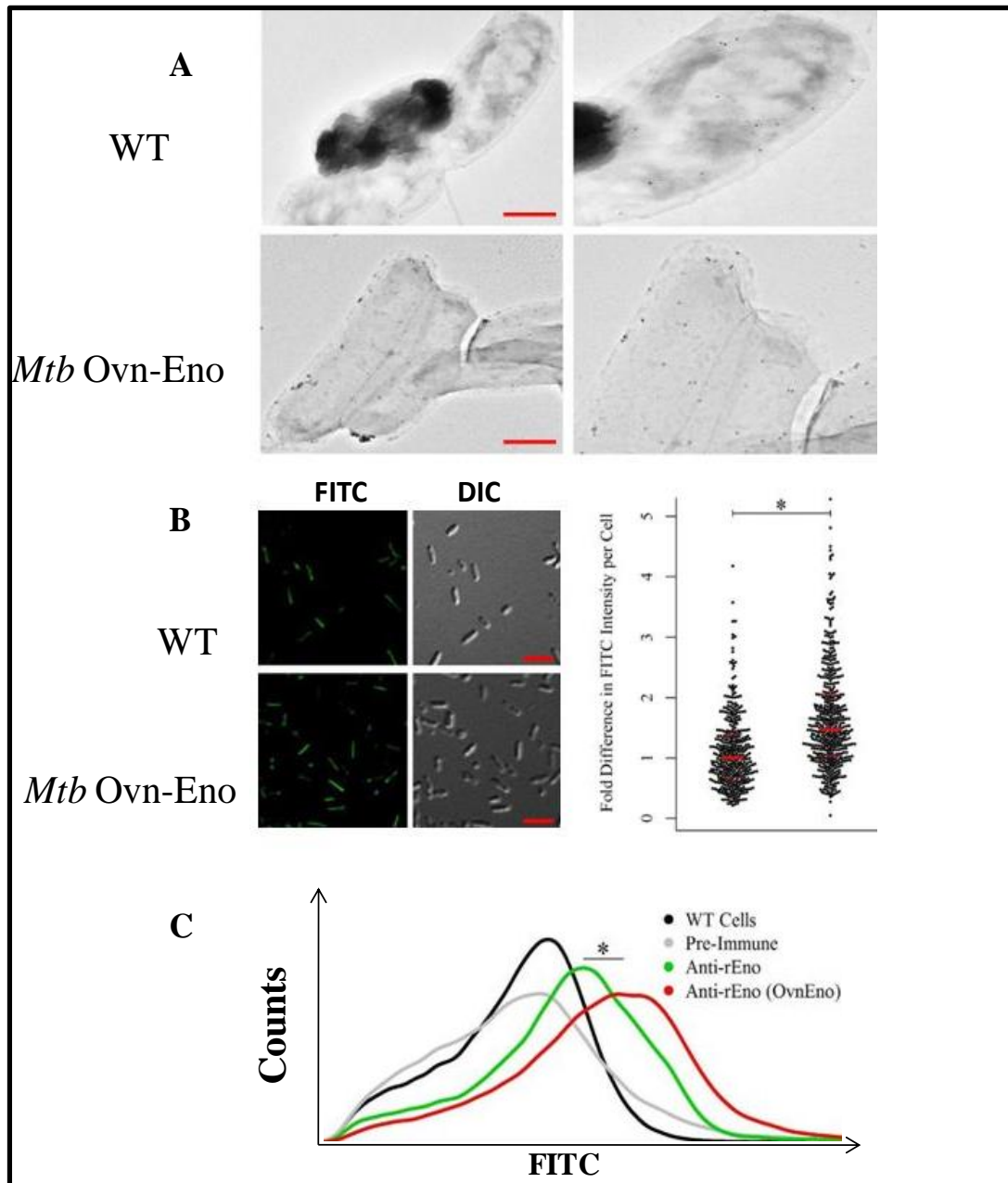


**Fig. 5. Enolase is present on the surface of *Mtb*.** A. WT *Mtb* (panel I and II) and *Mtb* overexpressing enolase (*Mtb*-OvnEno) (panel III and IV) strains stained with anti-rEno polyclonal sera followed by gold conjugated anti-mouse IgG and visualized by TEM. Panel II and IV are magnified views of panel I and III, respectively. Scale bar in red represents length of 1  $\mu$ m. B. WT and *Mtb*-OvnEno strains stained with anti-rEno polyclonal sera followed by FITC conjugated anti-mouse IgG and visualized by confocal microscopy. Fold difference of integrated intensity in the FITC channel of each bacterial cell with respect to WT is shown in the scatter plot. Scale bar in DIC images represents the length of 5  $\mu$ m. Representative images from at least three independent experiments are shown. C. Flow cytometric histograms of pre-immune sera treated, anti-rEno polyclonal sera treated (WT and *Mtb*-OvnEno) and only cells (WT) immunostained with FITC conjugated anti-mouse IgG.

significantly higher in *Mtb*-OvnEno strain than in *Mtb*-WT ( $p$  value < 0.01), suggesting a concentration dependent export and localization of enolase to the

surface (Fig. 5).

#### 4.5. Enolase of *Mtb* binds human plasminogen

Recruitment of plasminogen to the surface of pathogens and its conversion into proteolytic plasmin is studied in relation to their invasive potential to degrade ECM proteins and induce tissue remodeling. The concentration of plasminogen in human serum is in the range of 1.8–2.6  $\mu\text{M}$  [37]. Therefore, binding of rEno to human plasminogen was measured to estimate the significance of this interaction during infection *in vivo*. Real time binding analysis using SPR was employed to calculate the dissociation constant ( $K_D$ ) of this interaction. Association kinetics was used to calculate the  $K_D$  value due to its significantly lower  $\chi^2$  values and lower degree of error than in the dissociation phase. Expectedly, rEno and human plasminogen showed an avid binding with a  $K_D$  of 360 nM, which suggests a possible role of their interaction with respect to the invasive potential of *Mtb* within the host tissue *in vivo*.

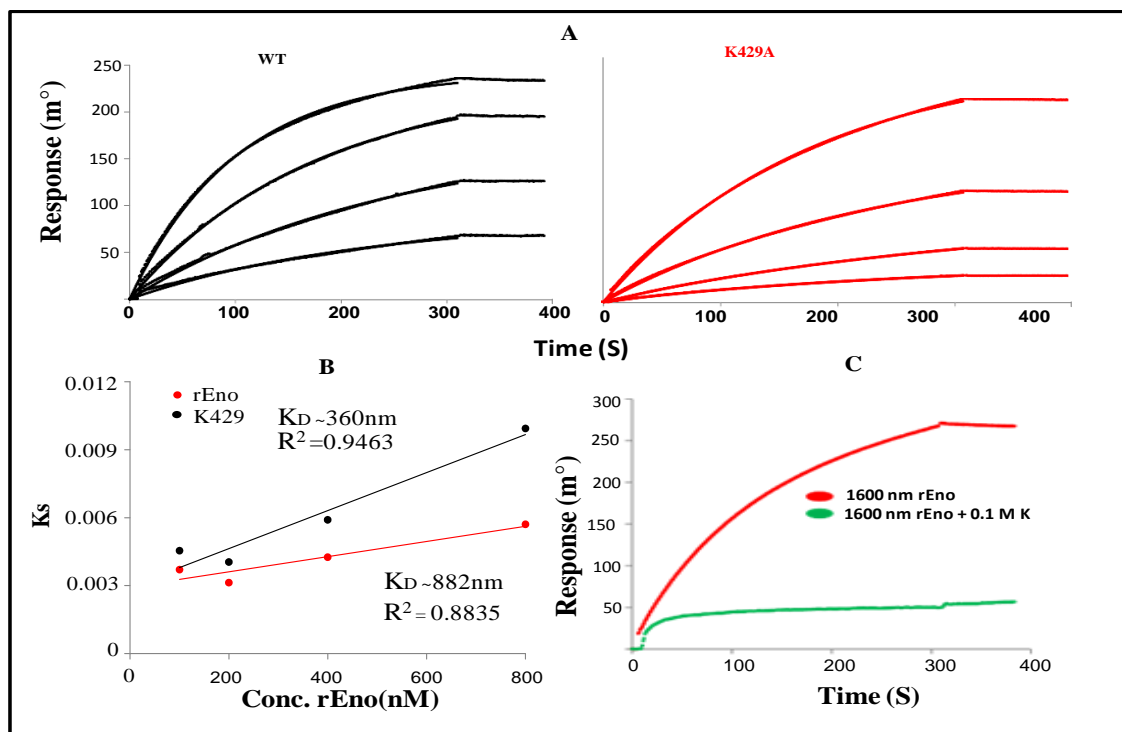


**Fig. 6. rEno binds to plasminogen with high affinity through lysine mediated interactions.** A. SPR sensorgrams for the binding of WT rEno and a point mutant K429A (100–800 nM) to immobilized plasminogen. B. K429A variant of rEno displayed a reduced affinity to plasminogen as compared to WT rEno. The  $K_D$  values obtained are shown using a  $K_s$  vs. Concentration plot. C. Sensorgram showing that lysine can completely abrogate the binding of rEno to plasminogen.

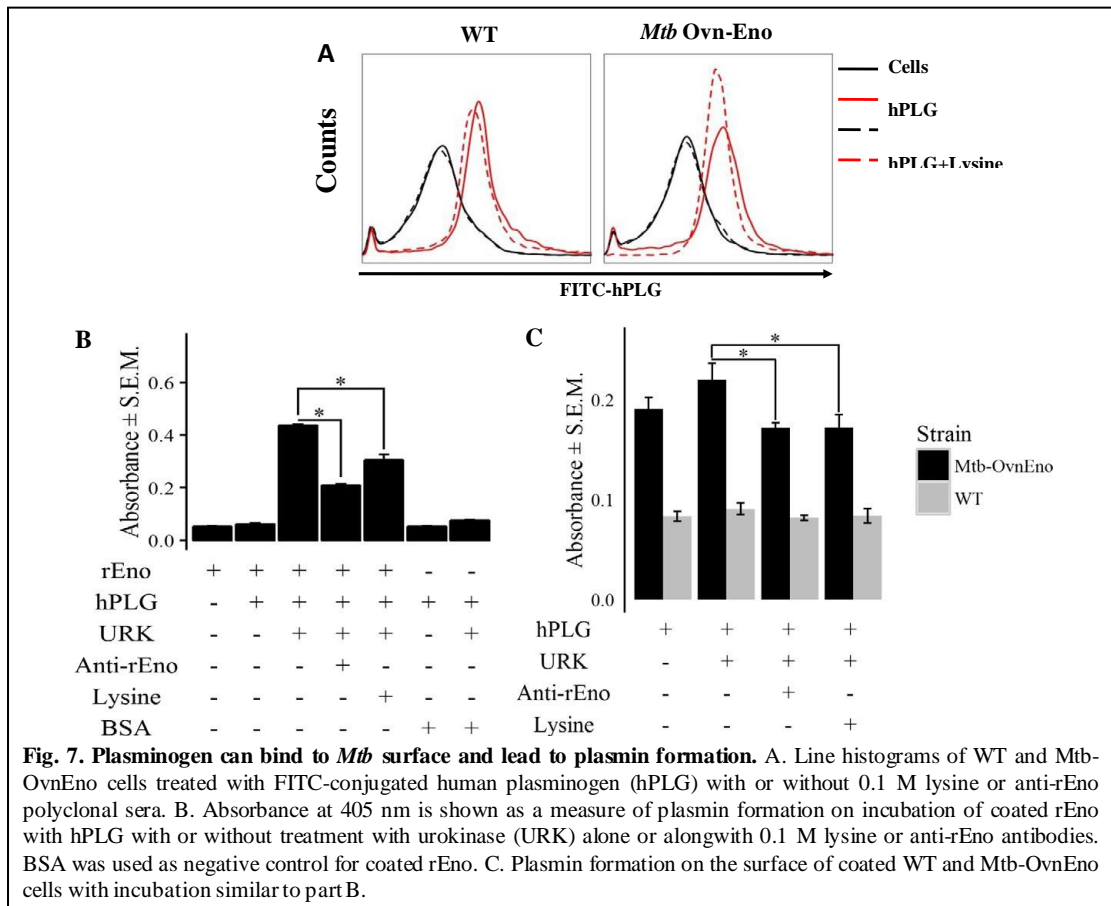
In general, plasminogen binding to moonlighting glycolytic enzymes of pathogens is dependent on their C-terminal lysine residues and their interaction is inhibited in the presence of free lysine in solution [38]. Therefore, the binding of rEno and plasminogen was evaluated in the presence of 0.1 M lysine in order to measure the lysine dependency of this interaction. As expected, 0.1 M lysine was able to completely abrogate the interaction between rEno and plasminogen, suggesting the involvement of C-terminal lysine of *Mtb*-enolase in binding with plasminogen. To further validate this observation, a point mutant of rEno with a lysine to alanine substitution at position 429 was generated and tested for binding to plasminogen using SPR, under conditions similar to WT rEno. A single substitution of the terminal lysine in rEno increased the  $K_D$  of the interaction by ~ 2.5 times to 882 nM. This highlighted and corroborated the importance of C-terminal lysine in the rEno-plasminogen interaction (**Fig. 6**).

#### **4.6. *in vitro* Plasminogen activation (plasmin formation) by rEno**

In order to study the role of high affinity plasminogen binding proteins present on the surface of *Mtb*, conversion of plasminogen into proteolytic plasmin (plasminogen activation) was evaluated upon binding with rEno. As expected, enolase bound plasminogen converted into plasmin upon incubation with urokinase, which is a known plasminogen activator in human plasma. Inhibition of plasminogen binding to enolase by incubation with either 0.1 M lysine or anti-rEno antibodies reduced plasmin formation, indicating that plasmin formation was directly proportional to the levels of enolase bound plasminogen. To further test plasmin formation on *Mtb* surface directly, plasminogen binding to *Mtb* cells was first determined using flow cytometry. Whole *Mtb*-WT cells displayed a high binding to plasminogen which could be abrogated completely in the presence of 0.1 M lysine. Plasminogen binding to whole cells was also reduced by the presence of anti- rEno antibodies, though to a considerably lesser extent than with lysine. *Mtb*-OvnEno strain also displayed binding to plasminogen, and anti-rEno antibodies showed similar reduction in plasminogen binding in this strain, as in *Mtb*-WT strain. Notably, proteins other than enolase on the surface of *Mtb* may also bind to plasminogen in a lysine dependent manner. Plasmin formation on the surface of *Mtb* could be readily detected and it was also found to decrease by incubation with 0.1 M lysine or anti-rEno antibodies. Interestingly,



there was an increased plasmin formation in *Mtb*-OvnEno strain than *Mtb*-WT, suggesting enolase to be one of the major plasminogen binding proteins on the surface of *Mtb*-OvnEno strain (Fig. 7).



#### 4.7. rEno is protective to *Mtb* infection

The results up till now did establish that plasmin formation can occur on *Mtb* surface, in part assisted by the surface localized-h enolase. To test the role of enolase upon *in vivo* infection of *Mtb*, C57BL/6 mice were immunized with purified rEno alongwith adjuvant and given three boosters at an interval of 14 days. The control group was immunized with PBS + adjuvant and for vaccination control, one group was immunized with BCG vaccine strain and another group with a known protective antigen Ag85B as described previously [29,30]. The anti-rEno titer in immunized mice after three boosters during the course of 42 days was 1:512,000. These mice were challenged with  $2 \times 10^6$  CFU of *Mtb* intravenously. Lung tissues of challenged mice were harvested at 56th day post infection and plated for CFUs. Interestingly,



mice immunized with rEno showed significantly less CFU counts in the lung tissue as compared to the PBS immunized control mice. BCG and Ag85B immunized mice also showed a significant reduction in the CFU counts, which was

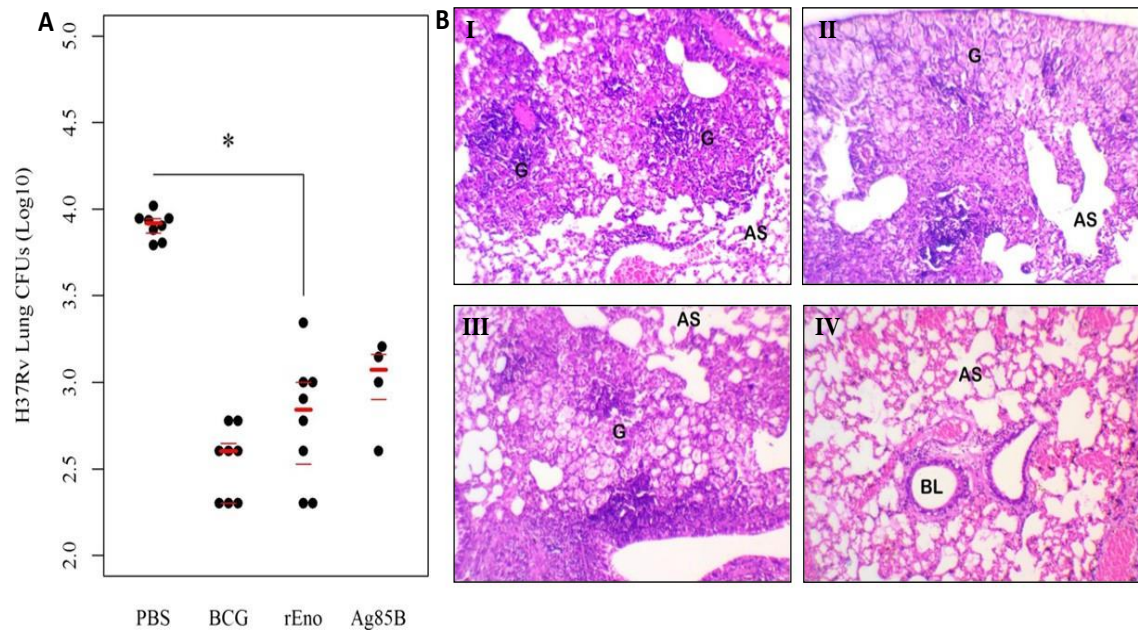


**Fig. 8. Protective efficacy of rEno against *Mtb* H37Rv challenge.** Mice were challenged with virulent *Mtb* H37Rv via tail vein on the 49th day post-immunization, and 8 weeks post-challenge the mice were sacrificed. Lungs were aseptically removed and homogenized in PBS. Appropriate serial dilutions of homogenates were plated for CFU analysis. Colonies were counted after 3–4 weeks of incubation at 37 °C and results are expressed as CFU counts per mouse. Significantly lower CFU counts were observed for the rEno immunized group in comparison to PBS immunized control group. Each point represents CFU load per mouse (n = 8 for PBS, BCG and rEno immunized group and n = 4 for Ag85B immunized group)

B. Photomicrographs (HE x 100x) of lung samples from different groups showing granuloma presence. Panel I- PBS control, Panel II- BCG, Panel III- Enolase, Panel IV- Normal lung. G-Granuloma, AS- Alveolar Spaces, BL- Bronchial Lumen. Representative images are shown.

comparable with the rEno immunized group. This result indicated that a strong antibody mediated

immune response against the surface exposed enolase of *Mtb* significantly inhibited infection load in mice. The lung tissue samples from different groups were also processed for histopathological detection of granuloma formation by hematoxylin and eosin staining. In comparison to the PBS control group, there was a significant reduction in the number of granuloma observed in rEno immunized mice. The PBS group had a total of 20 granulomas, the BCG group had one granuloma while the enolase group had three granulomas in total in the sections shown in the respective figure. This result suggested that plasminogen binding proteins of *Mtb* do play an important role in establishing infection *in vivo* (Fig. 8).

## DISCUSSION

The ability of pathogens to modulate the host fibrinolytic system is a crucial characteristic for tissue invasion. Plasminogen is an abundant protein of the host fibrinolytic system which upon activation into plasmin dissolves fibrin clots [26]. Either using an endogenously expressed plasminogen activator or through subversion of host plasminogen activators, pathogens have evolved a strategy to activate plasminogen and manipulate plasmin activity for their benefit. Recruitment of plasminogen to surface, even without activation, assists in bacterial adhesion. Plasmin activity also leads to degradation of ECM proteins like collagen, fibronectin and laminin, facilitating dissemination and disease spread. Such is the significance of plasmin activity for some pathogens like *Yersinia pestis* and *Salmonella enterica* that they even cause degradation of host plasminogen activator inhibitors (PAIs) to facilitate tissue destruction [69]. Many of such plasminogen receptors in pathogens are surface localized metabolic enzymes [29, 64, 65, 70, 71], with an unknown mechanism of export. There are many proteins across bacterial species which lack any kind of secretory signal peptide and are not characterized in relation to their export into the extracellular environment [72]. The moonlighting glycolytic enzymes are one of the most widely studied regulators in pathogens with respect to their interaction with host plasminogen.

Despite of being one of the major bacterial diseases that have high human mortality, there are very few studies that focus on the moonlighting proteins of *Mtb*, the causative agent of TB. Plasminogen binding capacity of *Mtb* has been confirmed previously by some reports [73, 74]. Although there is no report of the interaction of *Mtb* enolase with plasminogen, there are a few reports which suggest the presence of enolase in the membrane and pellicle fractions of *Mtb* [75, 76]. An earlier study reported the identification of 15 *Mtb* proteins: DnaK, GroES, GlnA1, Ag85 complex, Mpt51, Mpt64, PrcB, MetK, SahH, Lpd, Icl, Fba and EF-Tu as putative plasminogen receptors present in the soluble and culture filtrate extracts of the bacilli [74]. Experimentally, three of them, DnaK, GlnA1 and Ag85B were shown to bind to plasminogen. Interestingly, Ag85B and DnaK, both have been shown to have protective roles against virulent *Mtb* challenge [77]. Another study reported the surface localization and binding of fructose-1,6-bisphosphate aldolase from *Mtb* to plasminogen [78]. We have shown here that enolase is present on the surface of *Mtb* and acts as a host plasminogen binding moonlighting glycolytic enzyme.

Humans express three isoforms of enolase- alpha, beta and gamma. The alpha isoform predominates in most of the body tissues, the beta isoform is mainly present in the muscle and the gamma isoform is mostly localized to neuronal tissue [79]. The amino acid sequence identity between *Mtb* and human enolases is: 51% identity with alpha-enolase, 52% identity with beta-enolase and 54% identity with gamma-enolase.

Next, we elucidated that the *Mtb* enolase binds to host plasminogen with a high affinity. The KD value of 360 nM for this interaction suggested an avid binding between the two proteins *in vivo*. This observation is also in conciliation with the observed KD values for enolase- plasminogen interactions in streptococcal species, however, the affinity was slightly lower for *Mtb* enolase [80-83]. It is well established that plasminogen binding sites in pathogenic plasminogen receptors are lysine-rich motifs. Consequently, the affinity of interaction between rEno and human plasminogen was abrogated in the presence of 0.1 M lysine and reduced to N 2-folds upon point mutating the C-terminal lysine to alanine. Lysine mediated binding of plasminogen to its receptors makes it susceptible to conversion into fibrinolytic plasmin [84]. In streptococcal surface enolase, which is one of the most extensively studied proteins in this class, an internal plasminogen binding site comprising of nine residues mediates binding to plasminogen, in synergy with the terminal lysine residues [80, 85]. Similarly, another study showed that the binding of Group A *Streptococcus* surface enolase to human plasminogen is mediated by two internal lysines (252 and 255) in addition to their C-terminal lysines [86]. Interestingly, *Mtb* enolase lacks these homologous residues important for streptococcal enolases. Further, the C-terminus of *Mtb* harbors a single lysine residue, as opposed to more than one in streptococcus. As a result, mutation of this C-terminal lysine severely reduces plasminogen binding in *Mtb* enolase. Also, absence of the internal plasminogen binding site in *Mtb* enolase might explain its lower affinity towards plasminogen, in comparison to streptococcal enolase.

In the context of TB, plasmin mediated degradation of ECM components could have major consequences for granuloma stability. ECM is a major determinant in the genesis of granuloma formation in terms of migration of immune cells to and from the site of infection and formation of a stable granuloma [87]. MMPs are speculated to play a vital role in the pathology of TB by mediating degradation of collagen in a necrotic

granuloma resulting in the spread of *Mtb* to distant sites [88]. Hence, surface recruited plasmin activity in *Mtb* could be instrumental in mediating bacterial escape from a caseating granuloma. This observation also suggested that enolase can be a potential immunomodulatory agent, as effective antibody mediated recognition of this moonlighting protein can decrease the infectious potential of *Mtb*. As expected, mice immunized with rEno compared to PBS group showed decreased *Mtb* load in lungs. The *Mtb* load post rEno immunization was similar to that of BCG. This result makes enolase a promising candidate to be further tested as a component of vaccine formulations against TB. Major extracellular proteins of *Mtb* like Ag85B, when emulsified with an adjuvant, have been shown before to induce a protective effect against *Mtb* challenge in mice [77]. The response of rEno immunization was comparable to Ag85B, however, BCG imparted the best protection, as has been seen in a number of previous studies also [77, 89]. A successful subunit vaccine against TB must induce immune recognition of a variety of *Mtb* antigens, which are expressed during different stages of infection. This may be achieved by formulation of a cocktail of diverse mycobacterial immunodominant antigens, and enolase could be one of them. However, persistence of protection conferred by enolase immunization needs to be studied in detail in order to investigate the vaccine potential of rEno. Moreover, the protection conferred in an aerosol mode of infection remains to be explored.

Further characterization of other plasmin/plasminogen binding proteins of *Mtb* can delineate the significance of pathophysiology of TB in relation with its tissue invasive potential. Chemical therapeutics against the lysine dependent binding of plasminogen to these surface localized moonlighting proteins can also be exploited. TB is more understood as an intracellular infection of the macrophages, which forms the first line of host innate defense mechanism. However, evasion from antibody mediated recognition and immunity is an important anti-host characteristic for both extracellular and intracellular pathogens. Moreover, anti-mycobacterial antibodies mediated opsonization of *Mtb* enhances the innate and cell-mediated immunity against it [90]. Studies on the effect of plasmin bound to *Mtb* in modulation of uptake by macrophages and phagocytosis can be done on the basis of findings of this report. In summary, this work now establishes the implication of tissue invasive potential of *Mtb* as one of the major regulators of TB and the crucial role of

moonlighting glycolytic enzymes like enolase in it.

## CHAPTER 5

# **Exploring the interaction of *Mtb* Enolase with human plasminogen**

## RESULTS

### 5.1. Molecular model of *Mtb* enolase

The template i.e. Enolase from *Synechococcus elongatus* with PDB Id, 4ROP, showed 63% identity and 76% similarity to *Mtb* enolase sequence (**Fig. 1**). Owing to its high identity with the *Mtb* enolase, *Synechococcus elongates* Enolase acts as a suitable template for modeling. Further, comparison of the model with the template using Ramachandran plot analysis revealed the presence of only one residue in disallowed region similar to that of the template (**Fig. 2**). The number of labeled residues deduced

Template	1	YGTQIAEITAREILDSRGRPTVEAEVHLEDGSVGLAQVPSGASTGTFEAHELRRDDDP	SR	YGG	62
Model	1	MPI-IEQVRAREILDSRGNPTVEVEVALIDGTFARAAVPSGASTGEHEAVELRDGG-D	RY	GG	60
Template	63	KGVQKAVENV-SAIEDALIGLSALDQEGLDKAMIA LDGTPNKKNLGANAILAVSLATAHAAA			123
Model	61	KGVQKAVQAVLDEIGPAVIGLNADDQRLVDQALVDLDGTPDKSR LGGNAILGVSLAVAKAAA			122
Template	124	TSLNLPPLYRYLGGPLANVLPVPMNVINGGAHADNNDVFQEFMIMPV GAPSFK	EA	LRWGA	EV
Model	123	DSAE LPLFRYVGGPNAHILPVPMMNINLGGAHADTAVDIQEFMVAPI GAPS FVEALRWGA	EV		184
Template	186	FHALAKVLKDKGLATGVGDEGGFAPNLG SNKEALELLLT AIEAAGYK	PGEQ	VALAMD	VAS
Model	185	YHALKSVLKKEGLESTGLGDEGGFAPD VAGTTAALDLI SRAIES	AGLR	PGAD	VALALDA
Template	248	FYKNGL-YTCDGVSHEPAGMIGILADLV SQYPIVSI EDGLQEDDWSN	WKT	LT	QQLG
Model	247	FFTDGTGYVFE GTTRTADQMTEFYAGLLGAYPLVSI EDPLS	EDDWDG	WAAL	TASIGDR
Template	309	GDDL FVTNPDRLQS GIEQGVGNVLIKLNQIGTLTETLRTIDLATRS	GYRS	VISHRS	GETED
Model	309	GDDIFVTNPERLEEGERGVANALLVKNVQIGTLTETLDAVT	LAHHG	GYRTM	I SHRSGETED
Template	371	TTIADLAVATRA GQIKTGSLSR SERIAKYNRLLRIEAAALGENALYAGA	IGL	----	GPK
Model	371	TM IADLAVAIGS GQIKTGAPARSERVAKYNQLLRIEALGDAARYAG	DLA	FP	RFACETK

**Fig. 1. Sequence alignment of *Mtb* enolase with the template.** The conserved residues are highlighted in blue with white font color, whereas the rest of the residues and gaps are shown in black font color.

from Ramachandran and Chi1-chi2 plots were also less (**Table 1**). The model thus generated for the *Mtb* enolase protein has been used for all the structure based calculations to predict the amino acid residues involved in its interactions with the human.plasminogen.

**Table 1. Comparative Ramachandran plot analysis of *Mtb* enolase model and the template.** Percentage of residues are given in various regions of plot including most favorable, additional allowed, generously allowed, and disallowed regions. Labeled residues are also listed for all Ramachandran and Chi1-chi2 plots.

Protein	Ramachandran Plot Analysis				Labeled residues	
	Most favorable	Additional Allowed	Generously Allowed	Disallowed	All Ramachandrans	Chi1-Chi2
Template	90.0%	9.2%	0.6%	0.3%	5(outof422)	3(outof223)
Model	91.7%	7.2%	0.6%	0.6%	9(outof427)	6(outof222)

## 5.2. Plasminogen interacting residues of *Mtb* enolase

Protein-protein docking results depict that *Mtb* enolase and plasminogen were having surface complementarity in the interface region and the projections and recesses in the surface were

well interlocked (**Fig. 4**). Ligplot+ provided a long list of interacting residues and the

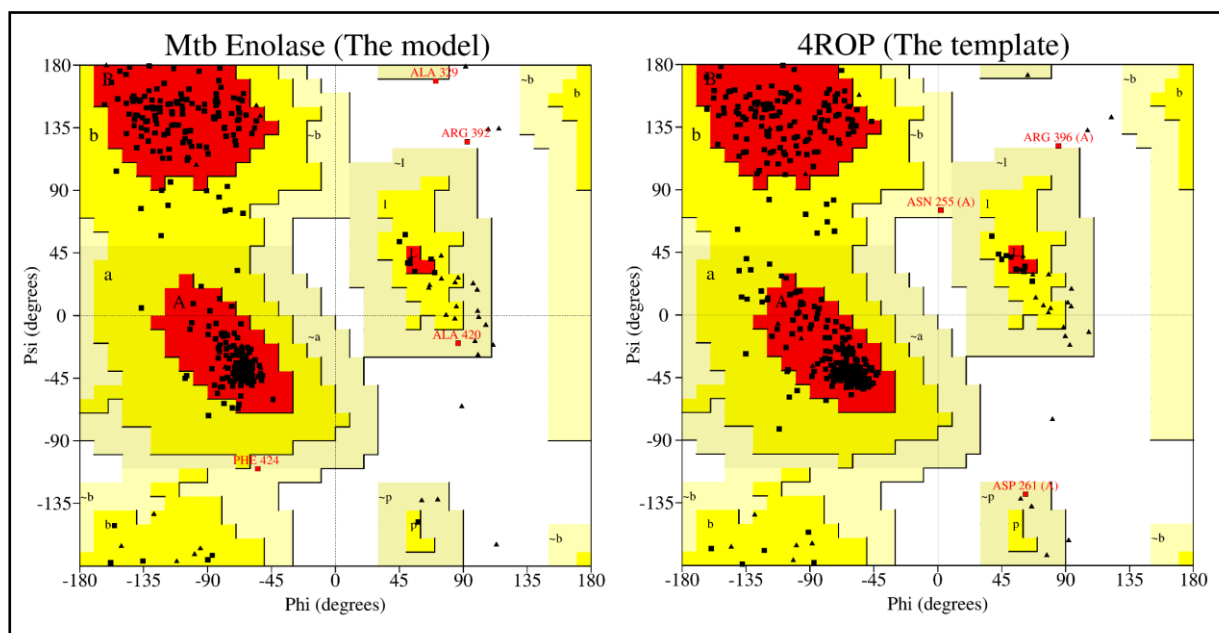


**Fig. 2. Ramachandran plot for *Mtb* enolase model and the template used.** All the residues except Glycine are shown as square dots lying in the four different regions, most favorable, additional allowed, generously allowed, and disallowed regions. Whereas, Glycine residues are shown as triangles as Glycine residues are special in having no side chain (only H-atom), so restriction for being in different regions of the plot does not apply on Glycine residues unlike other residues.

number of non-bonding interactions associated with each residue (**Table 3**). The residues were further filtered on the basis of overall decrease in the ASA by 10 Angstrom or more, thereby shortlisting only 7 residues namely **Lys-193**, **Lys-194**, **Thr-199**, Gly-272, Gly-275, Ala-276, and Pro-278 (**Table 2**). Protein-protein interaction plot for these residues of *Mtb* enolase with



**Table 2. Shortlisted plasminogen interacting residues of *Mtb* enolase.** Each residue is provided with number of non bonding and hydrogen bonding interactions and the loss in accessible surface area (ASA) due to binding.

<b>Residue</b>	<b>Non bonding interactions</b>	<b>Hydrogen bonding interactions</b>	<b>Loss in ASA</b>
Ser-190	5	3	0
Lys-193	47	1	22.7
Lys-194	32	-	69.89
Thr-199	14	-	18.28
Gly-272	6	1	33.93
Gly-275	4	-	27.06
Ala-276	18	-	68.02
Pro-278	12	-	15.89

human plasminogen residues is shown in Fig. 5. One additional residue **Ser-190**, in spite of showing no loss in ASA, was also included as it was involved in 3 hydrogen bonding from 3 different residues (**Table 2**).

### **5.3. Experimental validation of plasminogen binding residues of *Mtb* enolase**

Amino acid residues identified in the preceding section (Section 3.2) were further tested for their binding activity with the human plasminogen. For this, each of the selected residue was substituted by alanine. Secondary structure of all the recombinant proteins expressed and purified in this study was evaluated by CD spectroscopy to estimate the effect of mutation on the protein's structure. Secondary structure determination showed that there was no significant difference between WT and mutant proteins (**Table 4**). Next, the plasminogen binding activity of the WT and mutant enolase proteins was compared using end-point ELISA. A range of plasminogen concentrations were tested for interaction studies with WT and its variants, however, at higher plasminogen concentrations (0.1  $\mu$ M and above) non-specific binding was observed which was comparable to BSA (**Fig 3-6**). At lower plasminogen concentrations (0.05-0.0125  $\mu$ M , loss in

**Table 3. Total plasminogen interacting residues of *Mtb* enolase obtained using Dimplot option of Ligplot+.** Each residue is provided with number of non bonding and hydrogen bonding interactions. Additionally, the loss in accessible surface area (ASA) due to binding is also provided

Residue	Non-bonding interactions	Hydrogen-bonding interactions	Loss in ASA	Residue	Non-bonding interactions	H-bonding interactions	Loss in ASA
Ile-169	9	-	0	Gly-272	6(2)	1	33.93
Pro-172	1	-	0	Leu-273	1	-	6.03
Glu-176	2	-	0	Leu-274	5	-	1.94
Arg-179	5(2)	-	0	Gly-275	4(3)	-	27.06
Trp-180	1	-	0	Ala-276	18(2)	-	68.02
Glu-183	10	-	0	Pro-278	12(2)	-	15.89
Lys-189	3	-	0	Leu-279	3	-	0
Ser-190	5(3)	3(3)	0	Val-280	6(2)	-	0
Val-191	1	-	0	Asp-303	8(3)	-	0
Lys-193	47(3)	1	22.7	Arg-304	19(3)	-	0
Lys-194	32(5)	-	69.89	Val-305	11	-	0
Thr-199	14	-	18.28	Gln-306	3(2)	-	0
Ser-227	2	-	0	His-353	1	-	0
Ala-228	1	-	0	Arg-358	26(3)	-	0
Arg-231	18(3)	-	0	Ser-382	1	-	0
Pro-232	2	-	0	Gly-383	3	-	0
Gly-233	8(2)	-	0	Gln-384	12	-	0
Ala-234	8(3)	-	0	Arg-414	28(3)	-	0
Asp-235	2(2)	1	0	Ala-416	3	-	0
Glu-268	6	-	6.43	Gly-417	3(2)	-	0

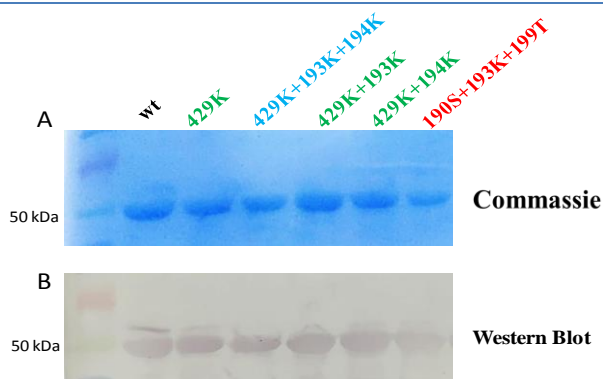


**Fig. 3. Confirming the protein purity and integrity. A.** SDS PAGE profile of WT and mutant enolase of *Mtb* **B.** Anti-Enolase immunostaining

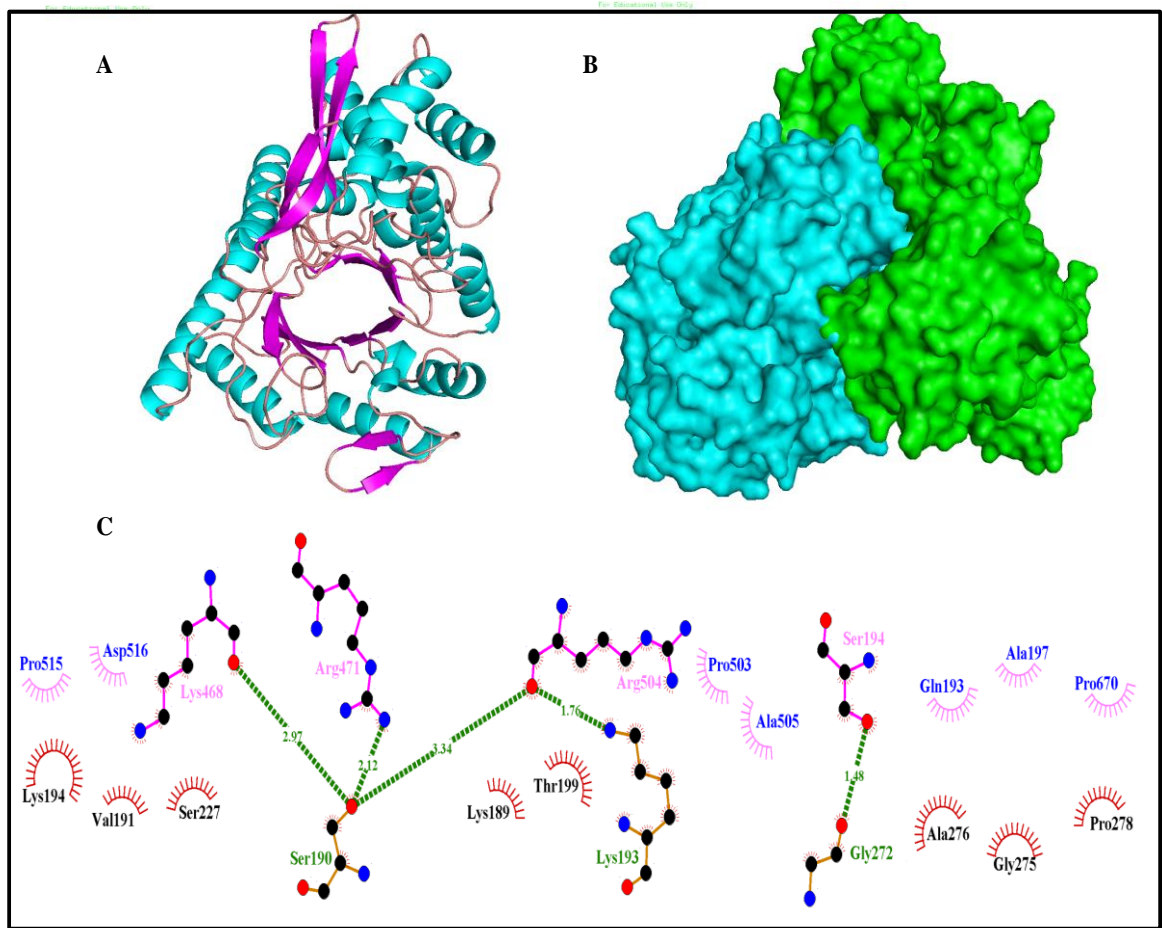


**Fig. 4. Results of protein-protein docking.** **A.** Cartoon representation of protein *Mtb* enolase model. *Mtb* enolase is a beta barrel protein and the beta barrel is shown in the middle as large pore of the protein. **B. Protein-protein docking of *Mtb* enolase and human plasminogen.** *Mtb* enolase is shown in cyan color, whereas human plasminogen in green color. Proteins, shown in surface representation, are binding to each other through complementary shapes at interface region. **C. Protein-protein interaction plot of *Mtb* enolase and human plasminogen.** Plasminogen residues are shown on the top and the *Mtb* enolase residues on the bottom in distinct colors. The hydrogen bonds are shown in green-dashed lines labeled with bond length. The residues forming hydrogen bonds are shown in ball-and-stick models and the other interacting residues are shown as arcs.

plasminogen binding was specifically observed for the mutant enolases. As reported previously by our group, K429A mutant showed nearly 19% decrease in binding with the human enolase. The K194A mutant showed nearly 6% decrease in binding. However, single mutants, S190A and T199A, did not show any significant decrease in binding. The K193A mutant could not be expressed and purified, however, its triple mutant with the aforementioned two inactive residues S190 and T199 showed nearly 9% decrease in binding.

**Table 4. Estimation of protein secondary structure using K2D2 software.** Fractions of the various secondary structure elements present in each of the recombinant protein prepared could be estimated by feeding the CD spectroscopic data into K2D2 software

S. No.	Protein name	% alpha helix	% beta sheets
1.	Wt-Eno	61.33	4.06
2.	S190+T199+K193	61.33	4.06
3.	K194	67.45	3.24
4.	K429	60.44	4.67
5.	K429+K193	60.44	4.67
6.	K429+K193+K194	58.24	6.73
7.	K429+K194	59.98	5.55

As for the mutations of active lysine residues K193 and K194, each of them mutated

Along with most interactive residue K429 resulted into no further decrease in binding. However, interestingly a triple mutant of the 3 lysine residues(**Table 5**)

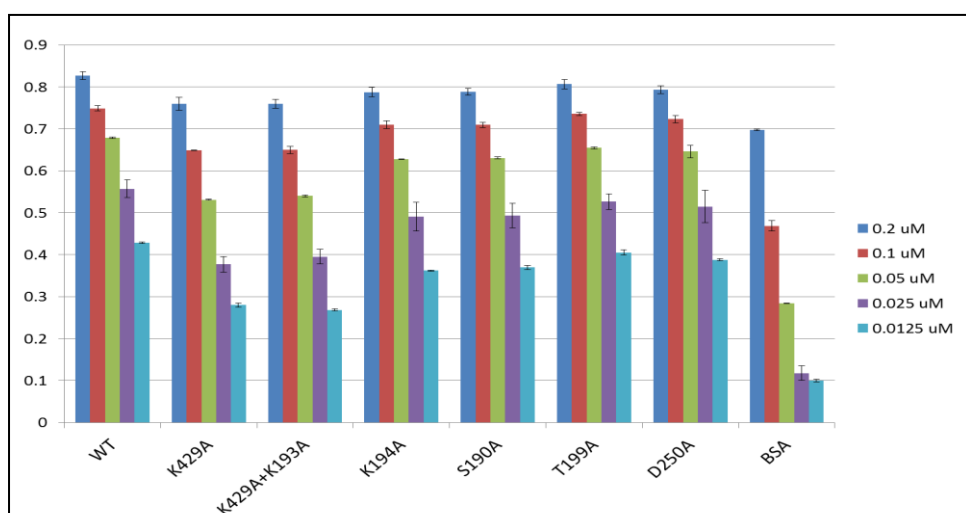


**Fig. 5. Plasminogen-*Mtb* enolase interaction.** A Series of concentrations of plasminogen were tested to estimate its binding with recombinant *Mtb* Enolase and its point mutants in a microtiter based assay

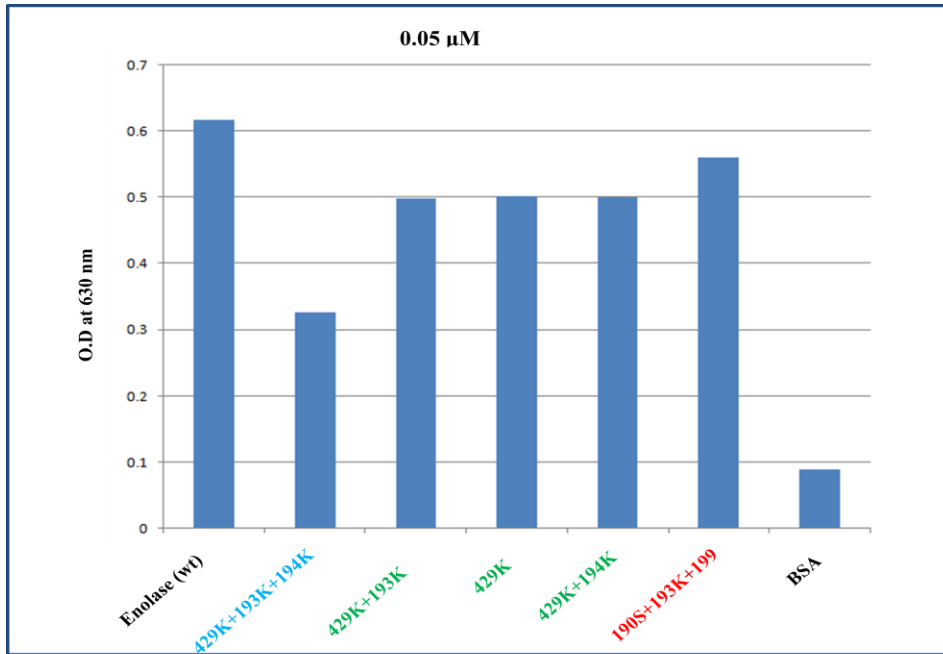


**Fig. 6. Differential plasminogen binding exhibited by the Wt Enolase and its SDMs (at 0.05  $\mu$ M plg).** Enolase or its SDMs (500 ng) was coated onto the ELISA plate and then its binding with the plg was quantified using Indirect ELISA.

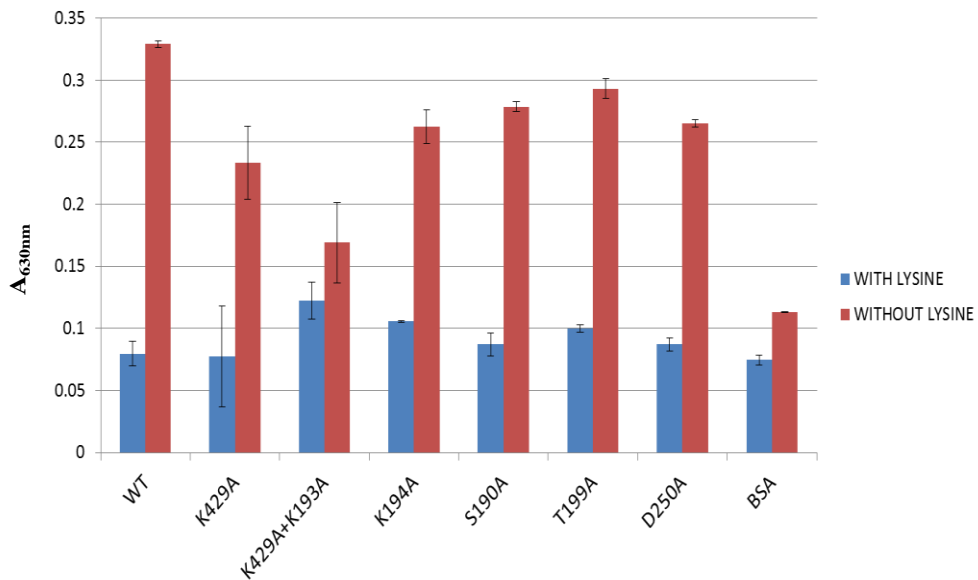


**Fig. 7. Lysine mediated abrogation of the interaction between Plasminogen and *Mtb* enolase. A.** Shows ELISA of all the recombinant mutants of Enolase with human plg in presence and absence of lysine to estimate the abrogation of the plasminogen binding

**Table 5. Tabulation of the percentage decrease in the binding of the proteins with the plg**

S. No.	Protein name	Percentage reduction in binding with plg
1	K429+K194+K193	47.03
2	K429+K193	19.36
3	K429	18.82
4	K429+K194	18.93
5	S190+K193+T199	9.27
6	S190	1.8
7	K194	6.12
8	T199	0

(K193A+K194A+K429A) showed a remarkable loss (approx. 47%) in binding, in comparison to the single mutants. This reduction in binding of the lysine triple mutant (K193A+K194A+K429A) is nearly 1.5 fold greater than that of most effective K429A mutant (**Fig. 8**).

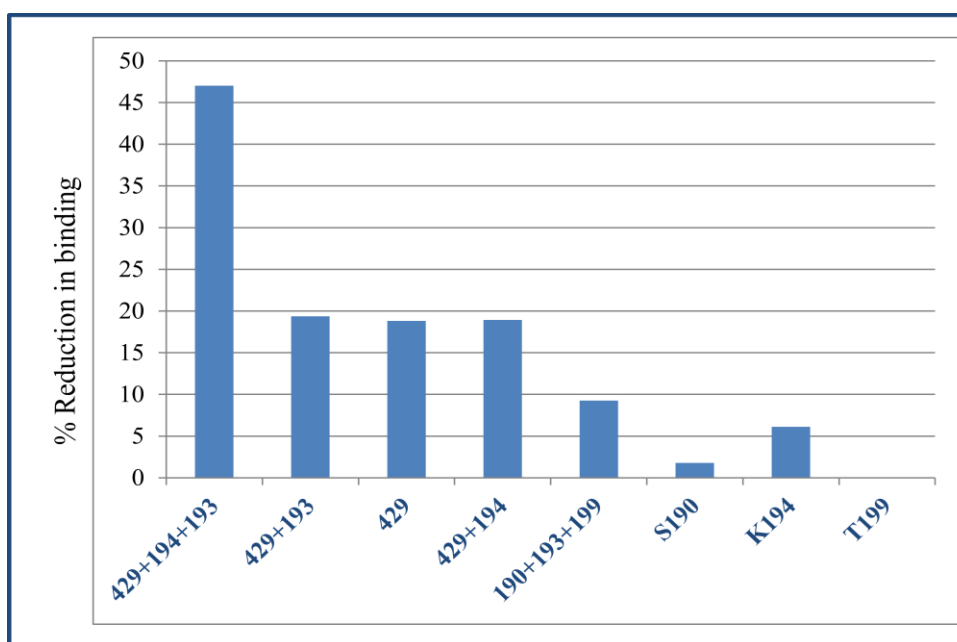


**Fig 8. Percentage reduction in the binding of Mtb enolase and its SDMs with human plg.**

Further, the specificity of this interaction was tested by including lysine in the plasminogen preparations which could abrogate the binding in all the tested WT

and mutant proteins. Notably, the reduction in plasminogen binding is observed upon substitution of lysine residues only (Fig 7).

#### 5.4. Comparison of *Mtb* enolase to human enolase isoforms

The three human enolase isoforms- $\alpha$ ,  $\beta$  and  $\gamma$  are highly identical, showing more than 80% identity with one another (Fig. 9). The *Mtb* enolase distinctly displays an identity of 49.55%, 50%, and 51.80% with  $\alpha$ ,  $\beta$  and  $\gamma$  isoforms of human enolase respectively, while, in general, it has an average identity of 50.45% with human enolase isoforms. Therefore, *Mtb* enolase, not being very close to human enolase, can very well be exploited for designing inhibitors. This fractional difference in the sequences of the *Mtb* v/s human enolase can be appropriately used to our advantage in design of the inhibitors against *Mtb* enolase ensuring a minimal to no cross reactivity with human enolase thereby increasing the safety statistics of the prospective enolase targeted drug (s) against Tuberculosis.

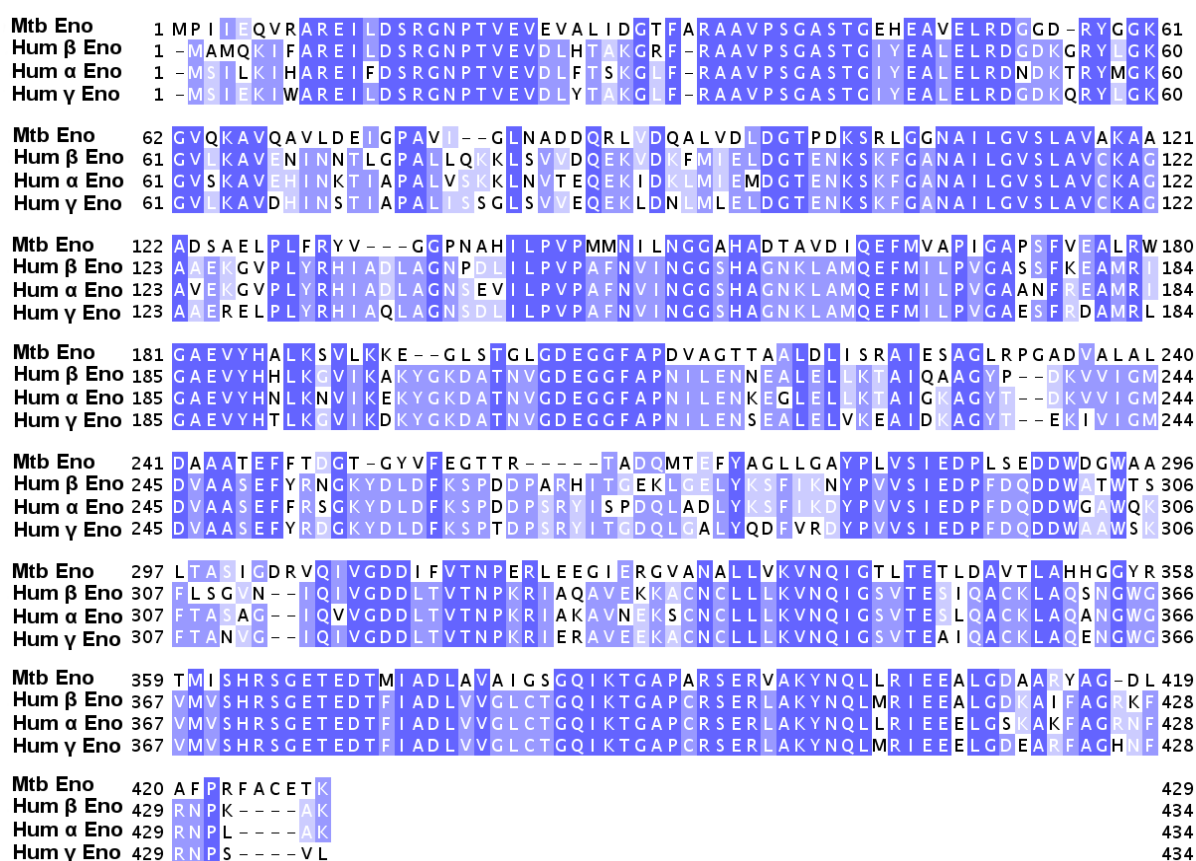


Fig. 9. Multiple sequence alignment of *Mtb* enolase with human enolase isoforms  $\alpha$ ,  $\beta$ , and  $\gamma$ . Conserved positions are highlighted in gradient blue with white font. Dark blue highlighted positions are completely conserved, while light blue highlighted positions are less conserved. The initial and final positions of each protein sequence in the alignment are also provided.

## DISCUSSION

The present study, for the first time explores the interaction of *Mtb* enolase with the human plasminogen using computational methods including protein-protein docking simulations. This has been further validated by introducing site specific mutations in recombinant Enolase followed by performing binding inhibition assays. The protein-protein docking results have revealed the binding pose of *Mtb* enolase and human plasminogen interaction and how the complementary surfaces of *Mtb* enolase and plasminogen were well interlocked indicating towards an optimal binding. This was further reinforced by appreciably high docking scores and number of molecular interactions between the two proteins. Of the proposed eight interacting residues, four residues Ser-190, Lys-193, Lys-194, Thr-199 were selected for subsequent mutation followed by binding inhibition assays. Lys-193 and Lys-194 were found as prime residues playing a role in binding, i.e., mutating these residues into Alanine led to a subsequent loss in the plasminogen binding activity of the resulting mutant proteins. A remarkable decrease, nearly 50 % was observed in the extent of plasminogen binding, upon mutating the above mentioned active lysine residues (Lys-193 and Lys-194) along with the most effective residues Lys-429. The Lys-429 is the C-terminal residue in *Mtb* Enolase, whereas Lys-193 and Lys-194 are the only two consecutively present lysine residues the protein sequence. In addition to exploring the critical residues of *Mtb* involved in its binding with the human plasminogen, *Mtb* enolase has been compared with the three isoforms of the human enolase. The fact that human enolase isoforms are distant in terms of their sequence similarity (average identity approx. 50%) places *Mtb* enolase in the category of safe and prospective drug targets for human use.

This study, in general, will provide structural insights into the binding mechanism of enolase to the host plasminogen, which helps pathogen to thrive in the host body. Specifically, this structural information of interacting residues, their molecular interactions, and binding interface regions can help in designing better compounds which can disrupt enolase-plasminogen interactions i.e., a novel and alternative drug for tuberculosis.



## CHAPTER 6

# **Monoclonal antibody (MAbs) generation against *Mtb* enolase**

## RESULTS:

**6.1. Cloning, expression and purification:** Different segments of the ORF corresponding to *Mtb* enolase (KEGG ID: Rv1023) were simultaneously cloned in pET28a vector using BamHI and HindIII sites (Table 1). The clone containing 405 bp long N-terminal fragment of the gene was named as “pETH37RvN-termEnolase” and the one with the 894 bp fragment of the gene’s C-terminal was called as “pETH37RvC-termEnolase”. The truncated C-terminal recombinant protein was found to be expressed at approximately 35 KDa while no expression could be obtained in *E.coli* BL-21 cells for the pETH37RvN-termEnolase. For cross-reactivity assays, human alpha enolase was also cloned in pET28a using NcoI and XhoI sites as well as in pGEMT vector. The integrity of the protein was confirmed by anti-His immunostaining of the *E. coli* BL21 expression cell-lysates post induction with IPTG as mentioned before in the section 3.2.13 of materials and methods.

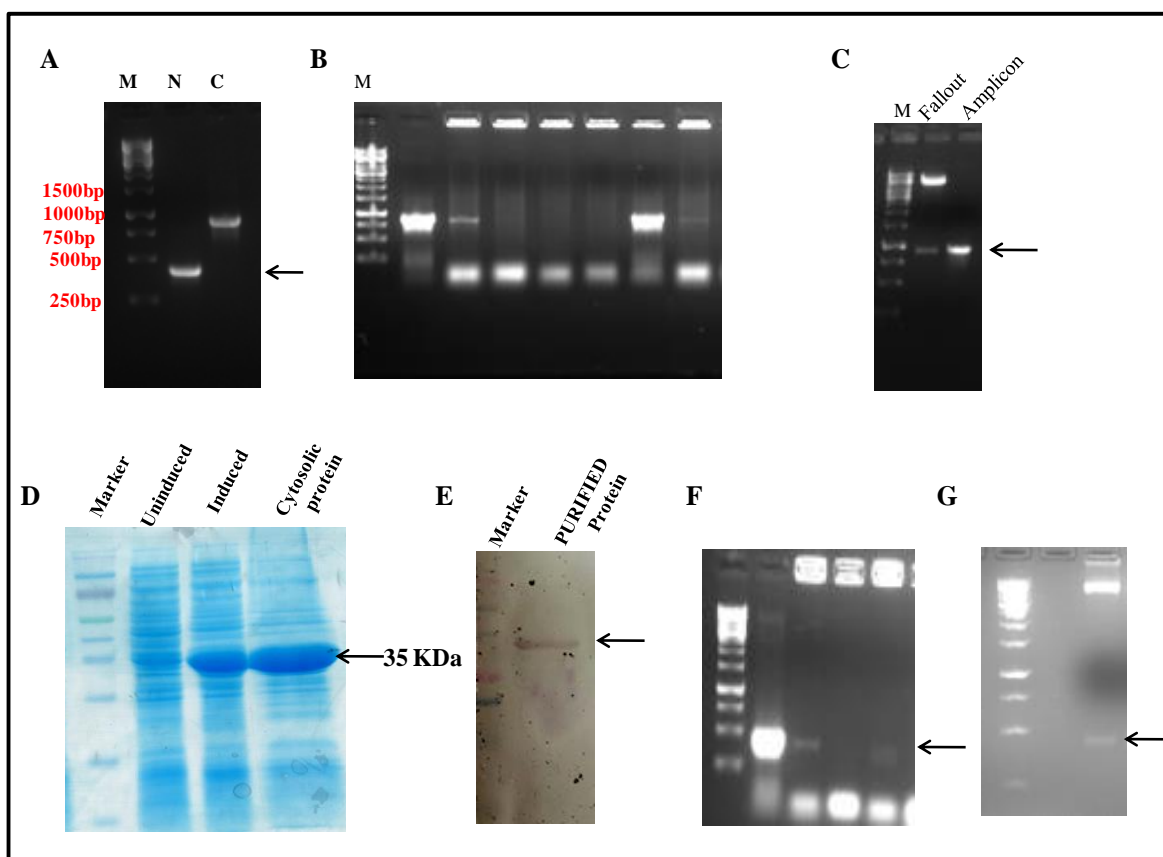


**Fig. 1. Cloning and expression of C- and N-terminal enolase.** **A.** PCR amplification of C- & N- terminal fragments, where N & C denote the N and C terminal fragments respectively **B.** Colony PCR of C-terminal clones of Enolase, **C.** Restriction digestion of C-terminal, **D.** IPTG Induction, **E.** Anti-His immuno-staining of C-terminal rEnolase clone, **F.** Colony PCR, **G.** Restriction digestion of the N-terminal rEnolase

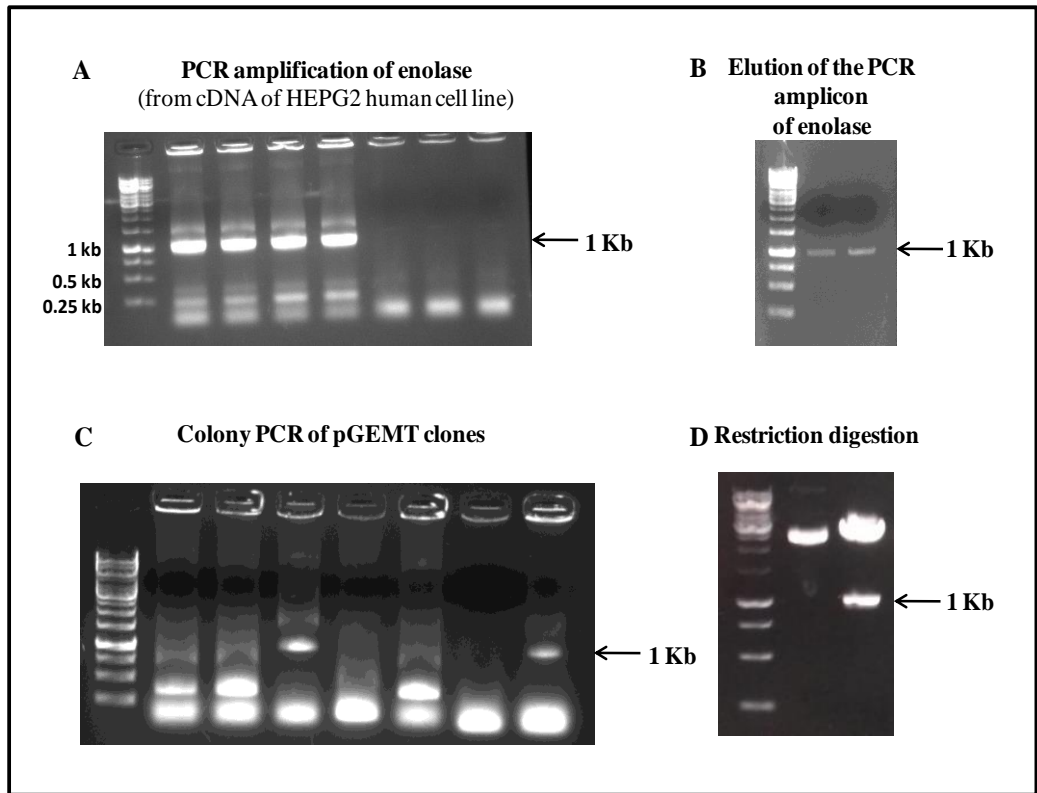


**Fig. 2. Cloning of  $\alpha$ -human enolase in pGEMT vector.** A. PCR amplification of  $\alpha$ -human enolase using c-DNA of HEPG2 cell lines, B. Gel elution of the PCR amplicons of enolase C. Colony PCR, D. Restriction digestion

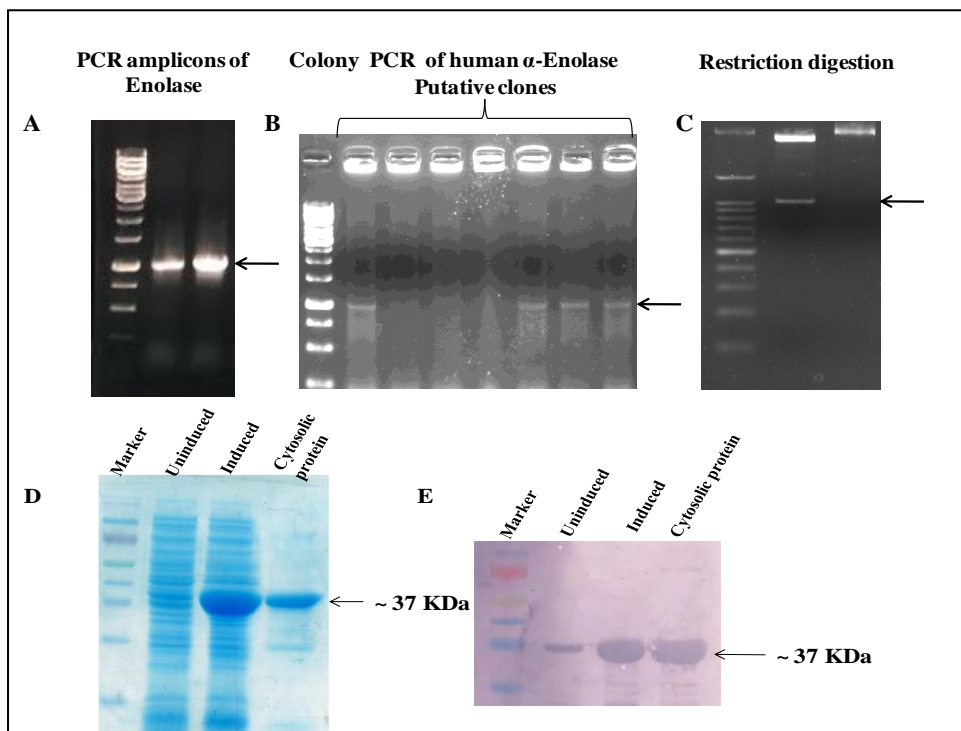


**Fig. 3. Cloning and expression of  $\alpha$ -human enolase in pET28a vector.** A. PCR amplification, B. Colony PCR, C. Restriction digestion, D. IPTG Induction, E. Anti-His immuno-staining of recombinant  $\alpha$ -human enolase

**6.2. Generation and screening of murine hybridomas:** Forty murine hybridoma clones could be screened after a conventional cell fusion experiment using the splenocytes of mice hyper-immunized with *Mtb* rEnolase,SP2/0Ag14 myeloma cells.

**Screening of the positive clones secreting anti-enolase MAbs**

S.No.	Clone No.	S/M	Recognition by Hexa-Histidine tag of a non specific protein	Recognition by full length <i>Mtb</i> r-enolase	Recognition by C-terminal fragment of <i>Mtb</i> r-enolase
1	7	S	W-/ELISA -	W+/ELISA +	W+/ELISA +
2	11	S	-do-	W+/ELISA +	W+/ELISA +
3	13	S	-do-	W+/	
4	18	M	-do-	W+/	
5	20	S	-do-	W+/ELISA+	
6	21	M	-do-		
7	24	S	-do-	W+/ELISA +	W+/ELISA +
8	27	M	-do-		
9	30	S	-do-		
10	31	M	-do-		
11	33	S	-do-	W+/ELISA +	W+/ELISA +
12	34	M	-do-		
13	35	S	-do-		
14	36	M	-do-		
15	38	S	W+/ELISA+		
16	39	S	W-/ELISA -	W+/ELISA +	W+/ELISA +
17	41	S	W-/ELISA -	W+/ELISA +	W+/ELISA +
18	42	S	W-/ELISA -		
19	43	M	W-/ELISA -		
20	44	M	W+/ELISA+		
21	45	M	W-/ELISA -	W+/ELISA +	
22	47	S			
23	48	M			
24	50	M	W+/ELISA +		
25	51	S			
26	53	S			
27	54	<b>M</b>		W+/ELISA +	W+/ELISA +
28	55				
29	56		W+/ELISA +		
30	57	S			
31	59	S		W+/ELISA +	W+/ELISA +
32	62		W+/ELISA +		
33	63	S	W+/ELISA +		
34	68				
35	69	<b>M</b>		W+/ELISA +	W+/ELISA +
36	71	S			
37	72	S		W+/ELISA +	W+/ELISA +
38	73	S			
39	74		W+/ELISA +		
40	75	S		W+/ELISA +	

**Note:** M denotes a multi cell hybridoma; S denotes a single cell hybridoma clone.

Using indirect ELISA, only twenty of such clones were found to be single cell hybridomas secreting monoclonal antibody molecules specific for a single epitope of enolase while the rest were multi-cell hybridomas. The single cell hybridomas were further selected and sub-culture to collect immunoglobulin molecules for further characterization. Amongst these, eight positive clones were found to selectively recognize the truncated C-terminal fragment of *Mtb* enolase while the rest of the twelve clones did not show any binding to it and were therefore inferred to be specific for the N-terminal region of the *Mtb* protein. The MAbs specific for hexa-histidines were also filtered by using another Hexa-His tagged protein other than enolase as an internal negative control in the immunostaining experiment i.e. only those MAbs which could bind enolase and not to another His tagged protein was identified as being anti-enolase MAb while the MAbs which recognised both the proteins i.e. enolase as well as the other his tag protein were rendered as His tag specific MAbs. The B cell clones which secreted MAbs with an exclusive specificity for the *Mtb* enolase without having any cross-reactivity with the human enolase were further distinguished and the same was concluded by Western blotting and ELISA using goat anti mouse whole IgG-AP conjugated (**Table 2**).

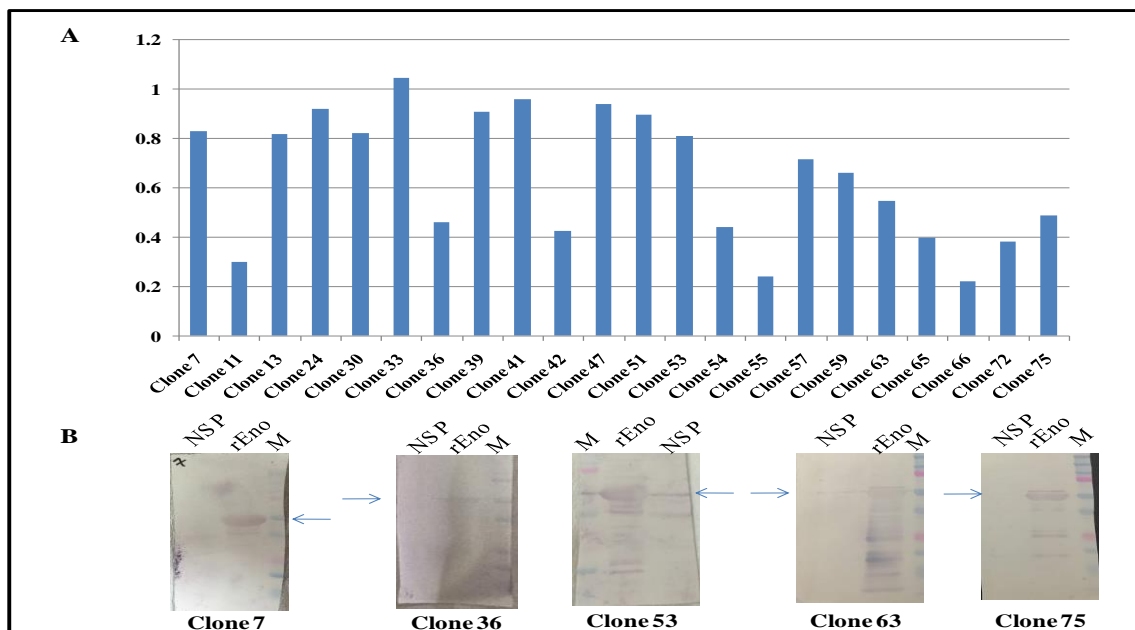


**Fig. 4. Clones secreting MAbs specific for *Mtb* rEnolase (50KDa) . A shows the ELISA using different anti enolase MAbs, B shows the western blots of the selected MAbs with the rEnolase of *Mtb* (full length)**

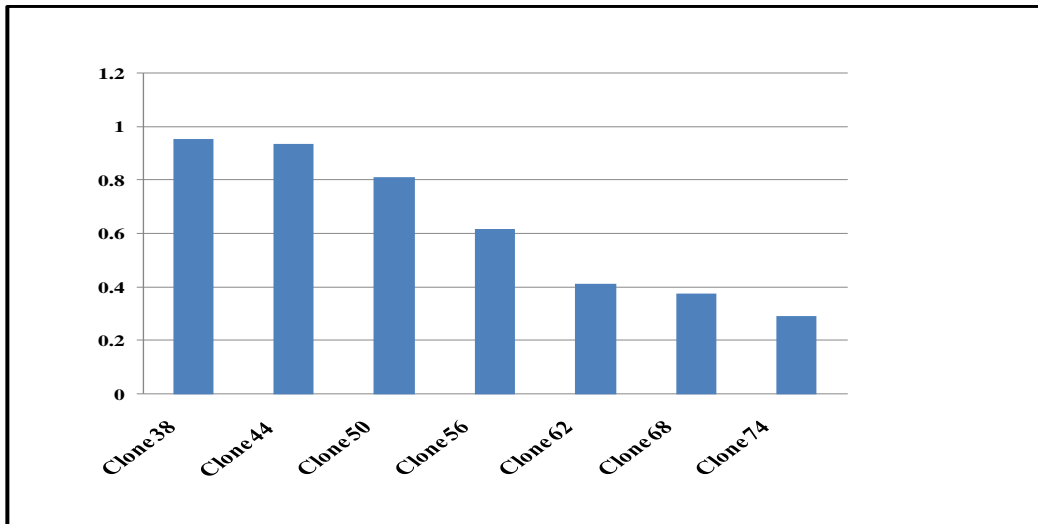


**Fig. 5. Clones secreting Mabs specific for Hexa Histidine tag.** A shows the result of ELISA with the Mabs to confirm their specificity for Hexa histidine tag and not any other epitope inside the enolase

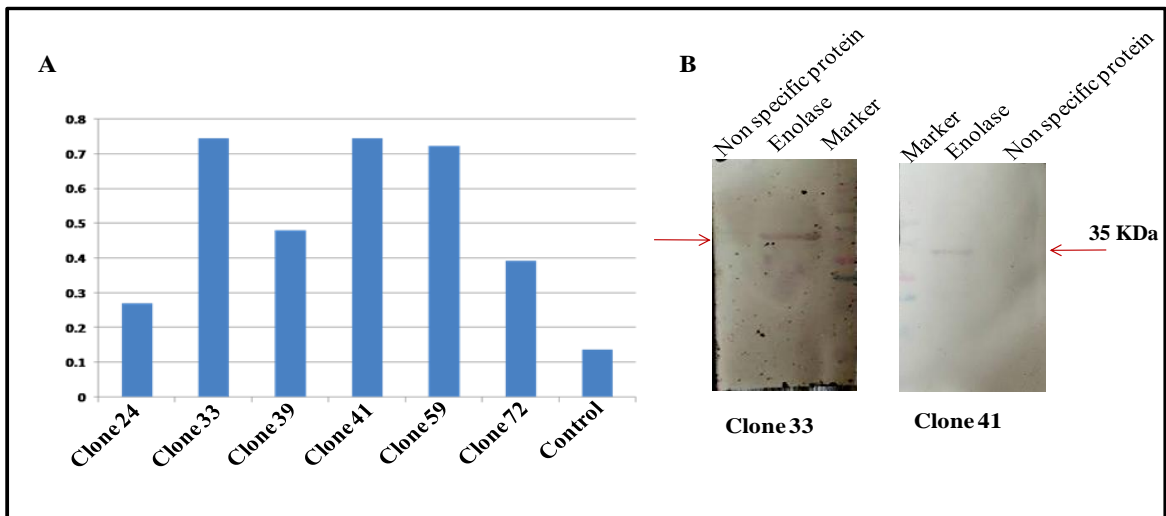


**Fig. 6. Clones secreting Mabs specific for C-terminal *Mtb*-Enolase (35 KDa).** A shows the result of ELISA using Mabs and the rEnolase (C-terminal fragment), B. Western blot using the same

**Table 2. Screening of C-terminal specific Mabs clones of *Mtb* Enolase from human enolase**

Clone No.	Recognition by C-terminal fragment of <i>Mtb</i> r-enolase	Recognition by human $\alpha$ -enolase
24	W+/ELISA +	W-/ELISA -
33	W+/ELISA +	W-/ELISA -
39	W+/ELISA +	W-/ELISA -
41	W+/ELISA +	W-/ELISA -
59	W+/ELISA +	W-/ELISA -
72	W+/ELISA +	<b>W+/ELISA +</b>

**6.3. IgG subclass determination of the monoclonal Antibodies:** To decide the further use of the MAbs, it is important to determine the IgG subclass for each of the selected monoclonal antibodies. Notably, the clone 33 and 41 were predominantly found to secrete IgG1 subclass of monoclonal antibody molecules.

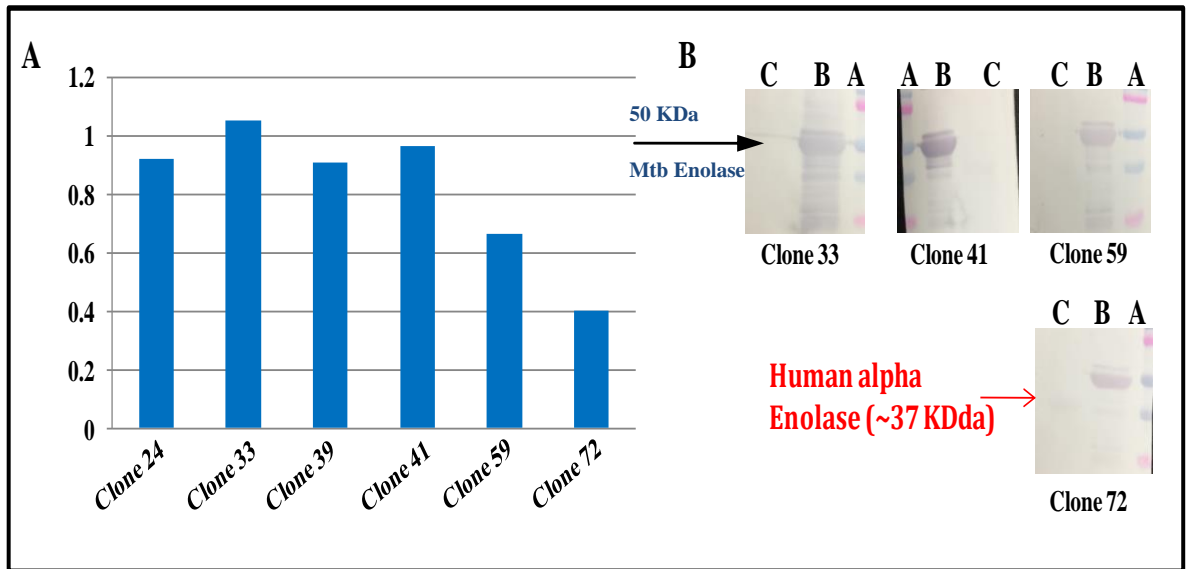


**Fig. 7. Experimental differentiation of C-terminal specific MAbs clones of *Mtb* enolase from human enolase. A. ELISA of the MAbs, B. Western Blotting with MAbs**

**6.4. Immunofluorescence and FACs analysis:** Monoclonal antibodies belonging to the screened hybridoma clone numbers: 33, 41 and 59 were found to show a specific interaction with the surface exposed enolase molecules of *Mtb* as observed via confocal microscopy and Flow cytometry (Fig 6A, 6B). A significant shift was observed in the FACs plot as compared to the *Mtb* whole cells.

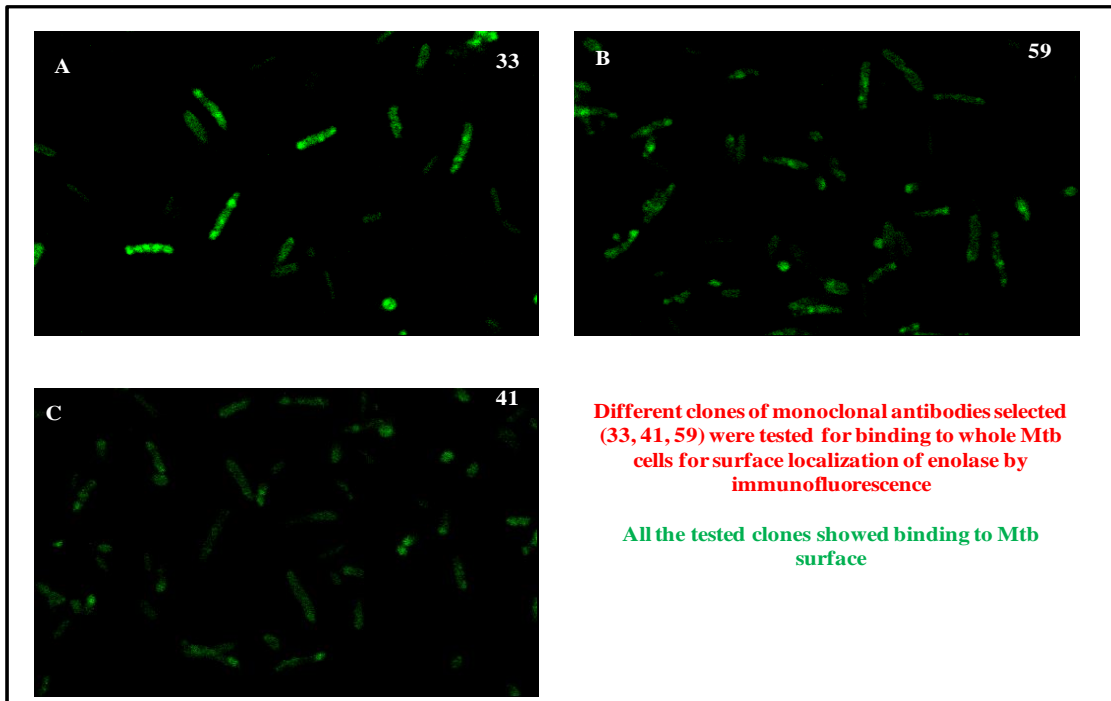


**Fig. 8. Mab Characterization- Confocal Microscopy.** A, B,C S show the confocal micrographs of the Mtb cells stained with the Mabs belonging to the different hybridoma clones

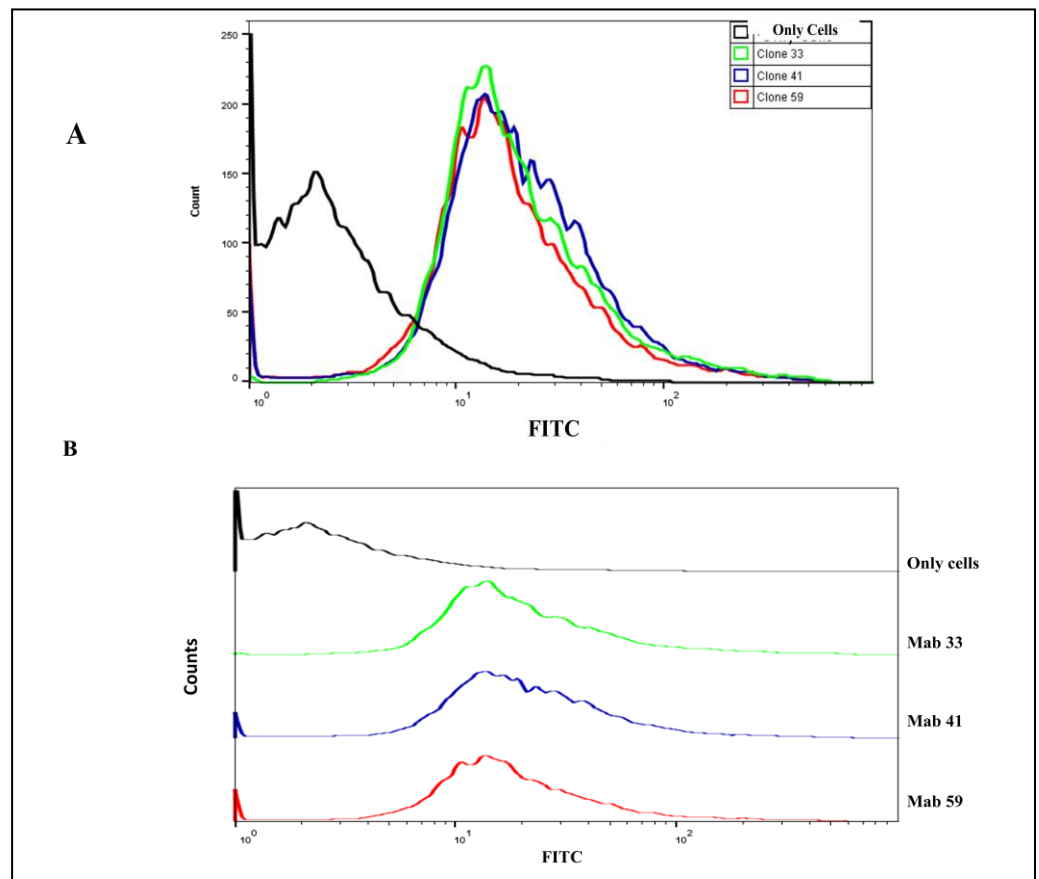


**Fig. 6. Flow cytometric histograms of MABs obtained from different murine hybridoma clones secreting anti-enolase antibody (clone 33, 41 and 59).**



## Discussion

The current situation of TB as global epidemic is swayed by an intimidating increase in the number of multi-drug resistant strains of *Mtb* [8]. The apprehended drug resistance has discouraged the frequency of newer drugs entering the market. Therefore, the time is right not only to generate but to test suitable therapeutic alternatives which can be effectively used against TB. Moreover, BCG has clearly been a failure making the prophylaxis of TB really difficult for us [91]. Use of MAbs for treating intracellular pathogens like *Salmonella*, *yersinia*, *brucella*, *coxiella*, *neisseria*, *Chlamydia*, *listeria*, *toxoplasma* etc has been already established though the same is not true completely in case of *Mtb* where the role of CMI is supposed to be superior to that of antibodies [92]. This however is strongly challenged by findings which indicate that humoral immunity helps in potentially blocking the pathogenic bacilli with the help of opsonizing antibodies. Opsono-pagocytosis is a known facilitator of macrophage mediated killing of *Mtb* and other intracellular pathogens and is corroborated by the fact that the opsonizing antibodies from healthy donors were found to impede the growth of *Mtb* H37Rv *in vitro* [8, 93]. Besides, after a natural infection of TB, the individuals have been found to vary in their anti-TB humoral content [94]. This indicates that the functions of antibody mediated anti-bacterial actions remain elusive till date in most of the pathogens including *Mtb* however their role cannot be understated [95].

Development of MAbs is becoming a fast paced therapeutics industry in this age of drug resistance. They are fascinating as tools to tag the crucial surface molecules present on the pathogen. In *Mtb*, for example an MAb (9d8) recognizing the surface arabinomannan was found to confer partial protection in mice model after respiratory challenge while the control mice succumbed to infection [96]. Therapeutic MAbs have been tested against several pathogens especially those associated with secretory toxin entities as they require an immediate neutralization and clearance. Along with this, we need to understand that a combination and no single MAb can be of absolute help to effect a substantial protection against an infection like TB.

Moreover, specific diagnosis being a prelude to the success against all the diseases, MAbs find their utility owing to their specificity of detection. Being stable, antibodies can be easily used for the design of LFAs (Lateral Flow Assays). A bispecific MAb

targeted for LAM (Lipoarabinomannan) antigen of *Mtb* has been demonstrated to be handy as point of care diagnostic in fulfilling the need of timely and accurate detection [97]. Therefore the development of antibody based POC (point of care) diagnostics as complementary treatment strategies is a need of the hour.

Several studies have been conducted for generation of monoclonal antibodies against antigens which are conserved between the human host and their pathogens. In this context, it is indispensable to check and estimate cross-reactivity of the Mabs generated post administration in human recipients. Despite being a highly conserved protein, *Mtb* Enolase is a vital anti-mycobacterial target. We have therefore tried to generate murine hybridoma clones producing monoclonal antibodies and screened them further on the basis of their binding affinity for *Mtb* enolase and human enolase.

The amino acid sequence identity between *Mtb* and human enolases is 51% with alpha-enolase, 52% identity with beta-enolase and 54% identity with gamma-enolase. The homology between the human enolases is more than 80%. Since, the human alpha isoform of enolase is the predominant form of enolase, it was cloned and purified, as a N-terminal his-tagged protein as outlined in the methods section, for specificity studies of the MAbs. Full length human-Enolase did not show protein expression under the tested conditions. Hence, an N-terminally truncated form of the protein was used for the studies. Besides their binding specificity for *Mtb* enolase, we have also checked the extent of their interaction with the human alpha-enolase. The clones expressing MAb molecules that produced self reactivity with the human alpha-enolase was excluded from further use. Conversely the clones secreting monoclonal antibodies specific for *Mtb* epitope were selected and utilized further for binding analysis. Next, we intend at using these highly *Mtb*-specific MAbs as a prospective intervention for tool TB prophylaxis/ therapy. Additionally, it is suitable for use in development of rapid TB detection kits. Prospects are also high for developing MAbs as future therapy that could replace the drugs or atleast support them as a parallel practice.

# Key points

- Enolase is a key glycolytic enzyme ubiquitously present in all the kingdoms of life.
- In *Mtb*, it is detected as a ~47.2 KDa protein (429 amino acids) expressed at the cell surface of *Mycobacterium tuberculosis* along with being a crucial component of its cell's cytosol.
- Enolase also exists as a dimer *in vitro*.
- Surface localization of the protein is enigmatic due to the absence of a signal peptide in the coding sequence of Enolase in *Mtb*.
- It is one of the plg (plasminogen) binding proteins of *Mtb* while the others include GAPDH etc.
- The key residues found to be associated with the plg binding ability of *Mtb* Enolase mainly include the C-terminal Lysine (K429) apart from the other residues e.g. Lysine 193, Lysine 194.
- The residues were predicted by employing a structure based computational approach and were further validated by Site directed mutagenesis (SDM) *in vitro*.
- Few residues of enolase failed to claim any role in plg binding as no evident decrease was observed in the binding of the protein with plg upon mutating the Serine 190 and Threonine 199 residues of the recombinant Enolase.
- Plasminogen binding by the *Mtb* enolase facilitates the activation of the former (plg) to plasmin protease in the presence of plg activators e.g. t-PA/ u-PA inside the host. This enables the pathogen to cause a full-fledged proteolytic degradation of the host tissue matrices.
- Competitive inhibition of the plg binding was observed in the presence of 0.1 M Lysine which is concordant with the previous reports illustrating a lysine dependence of the plg binding by several well known plasminogen binding proteins.
- Enolase has been found to be promising as a vaccine candidate against TB infections.
- A high titer of IgG antibodies has been detected in the sera of Human patients infected with TB, especially active TB patients.
- It has been able to induce sufficient humoral response upon immunization as exhibited by the stimulation of the B-cells
- A subsequent reduction in the bacterial load of *Mtb* H37 Rv was observed in the mice groups immunized with recombinant Enolase following a prime with two booster regimens.
- Histopathologic findings reinforce our observations of the prophylactic efficiency of recombinant Enolase which is well indicated by a decrease in the granuloma formation in the mice immunized with the rEnolase.
- Being one of the key glycolytic enzymes, we have tested the enzyme properties of the molecule and determined its Km and V<sup>max</sup> which were: 416 μM & 323 μmoles/min/mg respectively.
- Being a surface exposed effector molecule in the pathogen, it suits the portfolio of an ideal drug/ vaccine target.

- TB is a dreadful disease and yet intimidating is the fact that it is associated with a rapid emergence of drug resistance against the TB drugs.
- To address this issue Monoclonal antibodies find an apt application as the anti-TB therapeutics.
- We have generated and screened Monoclonal antibodies against *Mtb* enolase and screened them by ELISA and western blotting.
- As a primary step in the screening, all the clones secreting the MAbs were first of all, checked for their ability to bind the C-terminal truncated enolase protein or a full length antigen.
- MAbs generated against the hexa Histidine moieties were all filtered before the screening event using a his tagged non-specific negative control.
- The major clones have also been confirmed by performing Confocal microscopy and FACs analysis with the whole cells of *Mtb*.
- The monoclonal antibodies has been further filtered on the basis of their cross reactivity with the human  $\alpha$ -enolase.
- Three isoforms of enolase exist in human cells – $\alpha$ ,  $\beta$ ,  $\gamma$ .
- $\alpha$ -enolase is the most commonly located enolase isoform while  $\beta$  and  $\gamma$  isoforms are mainly localized in the muscle and neuronal cells.
- *Mtb* enolase shares approx. 49-51% amino acid sequence similarity with the human enolase isoforms.
- Therefore, inspite of being conserved between the pathogen and the host, it is possible to design drugs/ inhibitors/ monoclonal antibody based therapeutics against the amino acid stretches of the protein uniquely present in the pathogen.

# REFERENCES

1. World Health Organization releases 2015 global report on tuberculosis. *Breathe*, 2015. **11**(4): p. 244-244.
2. Rahi, A., et al., *Enolase of Mycobacterium tuberculosis is a surface exposed plasminogen binding protein*. *Biochimica Et Biophysica Acta-General Subjects*, 2017. **1861**(1): p. 3355-3364.
3. Da Silva, P.E.A. and J.C. Palomino, *Molecular basis and mechanisms of drug resistance in Mycobacterium tuberculosis: classical and new drugs*. *Journal of Antimicrobial Chemotherapy*, 2011. **66**(7): p. 1417-1430.
4. Nicas, M., W.W. Nazaroff, and A. Hubbard, *Toward understanding the risk of secondary airborne infection: Emission of respirable pathogens*. *Journal of Occupational and Environmental Hygiene*, 2005. **2**(3): p. 143-154.
5. Diaz-Ramos, A., et al., *alpha-Enolase, a Multifunctional Protein: Its Role on Pathophysiological Situations*. *Journal of Biomedicine and Biotechnology*, 2012.
6. Saylor, C., E. Dadachova, and A. Casadevall, *Monoclonal antibody-based therapies for microbial diseases*. *Vaccine*, 2009. **27**: p. G38-G46.
7. Hansel, T.T., et al., *The safety and side effects of monoclonal antibodies*. *Nature Reviews Drug Discovery*, 2010. **9**(4): p. 325-338.
8. Jacobs, A.J., et al., *Antibodies and tuberculosis*. *Tuberculosis*, 2016. **101**: p. 102-113.
9. Garhyan, J., et al., *Preclinical and Clinical Evidence of Mycobacterium tuberculosis Persistence in the Hypoxic Niche of Bone Marrow Mesenchymal Stem Cells after Therapy*. *American Journal of Pathology*, 2015. **185**(7): p. 1924-1934.
10. Golden, M.P. and H.R. Vikram, *Extrapulmonary tuberculosis: An overview*. *American Family Physician*, 2005. **72**(9): p. 1761-1768.
11. Lee, R.D., et al., *A Case of Miliary TB Presenting with Massive Upper GI Bleeding*. *American Journal of Gastroenterology*, 2009. **104**: p. S270-S271.
12. Cambau, E. and M. Drancourt, *Steps towards the discovery of Mycobacterium tuberculosis by Robert Koch, 1882*. *Clinical Microbiology and Infection*, 2014. **20**(3): p. 196-201.
13. Brennan, P.J., *Structure, function, and biogenesis of the cell wall of Mycobacterium tuberculosis*. *Tuberculosis*, 2003. **83**(1-3): p. 91-97.
14. *Tuberculosis testing: Which patients, which test? (vol 64, pg 553, 2015)*. *Journal of Family Practice*, 2015. **64**(12): p. 762-762.
15. Flynn, J.L. and J. Chan, *Tuberculosis: Latency and reactivation*. *Infection and Immunity*, 2001. **69**(7): p. 4195-4201.
16. Hauck, F.R., et al., *Identification and Management of Latent Tuberculosis Infection*. *American Family Physician*, 2009. **79**(10): p. 879-886.
17. Ganguly, N., I. Siddiqui, and P. Sharma, *Role of M-tuberculosis RD-1 region encoded secretory proteins in protective response and virulence*. *Tuberculosis*, 2008. **88**(6): p. 510-517.
18. Brulle, J.K., et al., *Cloning, expression and characterization of Mycobacterium tuberculosis lipoprotein LprF*. *Biochemical and Biophysical Research Communications*, 2010. **391**(1): p. 679-684.
19. Bermudez, L.E. and J. Goodman, *Mycobacterium tuberculosis invades and replicates within type II alveolar cells*. *Infection and Immunity*, 1996. **64**(4): p. 1400-1406.
20. Tascon, R.E., et al., *Mycobacterium tuberculosis-activated dendritic cells induce protective immunity in mice*. *Immunology*, 2000. **99**(3): p. 473-80.
21. Gengenbacher, M. and S.H.E. Kaufmann, *Mycobacterium tuberculosis: success through dormancy*. *Fems Microbiology Reviews*, 2012. **36**(3): p. 514-532.
22. Rustad, T.R., et al., *Hypoxia: a window into Mycobacterium tuberculosis latency*. *Cellular Microbiology*, 2009. **11**(8): p. 1151-1159.

23. Zignol, M., et al., *Surveillance of anti-tuberculosis drug resistance in the world: an updated analysis, 2007-2010*. Bulletin of the World Health Organization, 2012. **90**(2): p. 111-119.
24. Zumla, A., et al., *WHO's 2013 global report on tuberculosis: successes, threats, and opportunities*. Lancet, 2013. **382**(9907): p. 1765-1767.
25. Frantz, C., K.M. Stewart, and V.M. Weaver, *The extracellular matrix at a glance*. Journal of Cell Science, 2010. **123**(24): p. 4195-4200.
26. Singh, B., et al., *Human pathogens utilize host extracellular matrix proteins laminin and collagen for adhesion and invasion of the host*. Fems Microbiology Reviews, 2012. **36**(6): p. 1122-1180.
27. Wijnberg, M.J., L.G.M. Huisman, and J.H. Verheijen, *Differences in invasion between human smooth muscle cells from umbilical vein, saphenous vein and internal mammary artery: relation to the expression of the plasminogen activation system*. Fibrinolysis & Proteolysis, 2000. **14**(6): p. 358-365.
28. Mouw, J.K., G.Q. Ou, and V.M. Weaver, *Extracellular matrix assembly: a multiscale deconstruction*. Nature Reviews Molecular Cell Biology, 2014. **15**(12): p. 771-785.
29. Lahteenmaki, K., P. Kuusela, and T.K. Korhonen, *Bacterial plasminogen activators and receptors*. Fems Microbiology Reviews, 2001. **25**(5): p. 531-552.
30. Whiting, G.C., et al., *Purification of native alpha-enolase from Streptococcus pneumoniae that binds plasminogen and is immunogenic*. Journal of Medical Microbiology, 2002. **51**(10): p. 837-843.
31. Singh, B., et al., *Moraxella catarrhalis Binds Plasminogen To Evade Host Innate Immunity*. Infection and Immunity, 2015. **83**(9): p. 3458-3469.
32. Agarwal, V., et al., *Streptococcus pneumoniae Endopeptidase O (PepO) Is a Multifunctional Plasminogen- and Fibronectin-binding Protein, Facilitating Evasion of Innate Immunity and Invasion of Host Cells*. Journal of Biological Chemistry, 2013. **288**(10): p. 6849-6863.
33. Ghosh, A.K. and M. Jacobs-Lorena, *Surface-expressed enolases of Plasmodium and other pathogens*. Memorias Do Instituto Oswaldo Cruz, 2011. **106**: p. 85-90.
34. Agarwal, V., et al., *A Novel Interaction between Complement Inhibitor C4b-binding Protein and Plasminogen That Enhances Plasminogen Activation*. Journal of Biological Chemistry, 2015. **290**(30): p. 18333-18342.
35. Chaves, E.G.A., et al., *Analysis of Paracoccidioides secreted proteins reveals fructose 1,6-bisphosphate aldolase as a plasminogen-binding protein*. BMC Microbiology, 2015. **15**.
36. Koenigs, A., et al., *BBA70 of Borrelia burgdorferi Is a Novel Plasminogen-binding Protein*. Journal of Biological Chemistry, 2013. **288**(35): p. 25229-25243.
37. Oliveira, R., et al., *Characterization of Novel OmpA-Like Protein of Leptospira interrogans That Binds Extracellular Matrix Molecules and Plasminogen*. Plos One, 2011. **6**(7).
38. Avilan, L., et al., *Interaction of Leishmania mexicana promastigotes with the plasminogen-plasmin system*. Molecular and Biochemical Parasitology, 2000. **110**(2): p. 183-193.
39. Han, X.G., et al., *Enzymatic and biological characteristics of enolase in Brucella abortus A19*. Molecular Biology Reports, 2012. **39**(3): p. 2705-2711.
40. Lu, Q., et al., *An octamer of enolase from Streptococcus suis*. Protein & Cell, 2012. **3**(10): p. 769-780.
41. Hannaert, V., et al., *Enolase from Trypanosoma brucei, from the amitochondriate protist Mastigamoeba balamuthi, and from the chloroplast and cytosol of Euglena gracilis: Pieces in the evolutionary puzzle of the eukaryotic glycolytic pathway*. Molecular Biology and Evolution, 2000. **17**(7): p. 989-1000.



42. Reed, G.H., et al., *Structural and mechanistic studies of enolase*. Current Opinion in Structural Biology, 1996. **6**(6): p. 736-743.
43. Lebioda, L. and B. Stec, *Mechanism of Enolase - the Crystal-Structure of Enolase-Mg<sup>2+</sup>-2-Phosphoglycerate Phosphoenolpyruvate Complex at 2.2-Å Resolution*. Biochemistry, 1991. **30**(11): p. 2817-2822.
44. Pancholi, V. and V.A. Fischetti, *A novel plasminogen/plasmin binding protein on the surface, of group A streptococci*. Streptococci and the Host, 1997. **418**: p. 597-599.
45. Sha, J., et al., *Surface-Expressed Enolase Contributes to the Pathogenesis of Clinical Isolate SSU of Aeromonas hydrophila*. Journal of Bacteriology, 2009. **191**(9): p. 3095-3107.
46. Kolberg, J., et al., *Streptococcus pneumoniae enolase is important for plasminogen binding despite low abundance of enolase protein on the bacterial cell surface*. Microbiology-Sgm, 2006. **152**: p. 1307-1317.
47. Mason, A.B., H.R. Buckley, and J.A. Gorman, *Molecular-Cloning and Characterization of the Candida-Albicans Enolase Gene*. Journal of Bacteriology, 1993. **175**(9): p. 2632-2639.
48. Angiolella, L., et al., *Identification of a glucan-associated enolase as a main cell wall protein of Candida albicans and an indirect target of lipopeptide antimycotics*. Journal of Infectious Diseases, 1996. **173**(3): p. 684-690.
49. Nogueira, S.V., et al., *Paracoccidioides brasiliensis Enolase Is a Surface Protein That Binds Plasminogen and Mediates Interaction of Yeast Forms with Host Cells*. Infection and Immunity, 2010. **78**(9): p. 4040-4050.
50. Pal-Bhowmick, I., et al., *Protective properties and surface localization of Plasmodium falciparum enolase*. Infection and Immunity, 2007. **75**(11): p. 5500-5508.
51. Vega-Rodriguez, J., et al., *Multiple pathways for Plasmodium ookinete invasion of the mosquito midgut*. Proceedings of the National Academy of Sciences of the United States of America, 2014. **111**(4): p. E492-E500.
52. Maldonado, J., et al., *A study of cutaneous lesions caused by Leishmania mexicana in plasminogen-deficient mice*. Experimental and Molecular Pathology, 2006. **80**(3): p. 289-294.
53. Sali, A. and T.L. Blundell, *Comparative Protein Modeling by Satisfaction of Spatial Restraints*. Journal of Molecular Biology, 1993. **234**(3): p. 779-815.
54. Laskowski, R.A., et al., *Procheck - a Program to Check the Stereochemical Quality of Protein Structures*. Journal of Applied Crystallography, 1993. **26**: p. 283-291.
55. Duhovny, D., R. Nussinov, and H.J. Wolfson, *Efficient unbound docking of rigid molecules*. Algorithms in Bioinformatics, Proceedings, 2002. **2452**: p. 185-200.
56. Schneidman-Duhovny, D., et al., *PatchDock and SymmDock: servers for rigid and symmetric docking*. Nucleic Acids Research, 2005. **33**: p. W363-W367.
57. Laskowski, R.A. and M.B. Swindells, *LigPlot+: Multiple Ligand-Protein Interaction Diagrams for Drug Discovery*. Journal of Chemical Information and Modeling, 2011. **51**(10): p. 2778-2786.
58. Wallace, A.C., R.A. Laskowski, and J.M. Thornton, *Ligplot - a Program to Generate Schematic Diagrams of Protein Ligand Interactions*. Protein Engineering, 1995. **8**(2): p. 127-134.
59. Ghosh, K.S., et al., *A Spectroscopic Investigation into the Interactions of 3'-O-Carboxy Esters of Thymidine with Bovine Serum Albumin*. Biopolymers, 2009. **91**(9): p. 737-744.
60. Edgar, R.C., *MUSCLE: multiple sequence alignment with high accuracy and high throughput*. Nucleic Acids Research, 2004. **32**(5): p. 1792-1797.
61. Clamp, M., et al., *The Jalview Java alignment editor*. Bioinformatics, 2004. **20**(3): p. 426-427.

62. Waterhouse, A.M., et al., *Jalview Version 2-a multiple sequence alignment editor and analysis workbench*. Bioinformatics, 2009. **25**(9): p. 1189-1191.
63. Fulde, M., M. Steinert, and S. Bergmann, *Interaction of streptococcal plasminogen binding proteins with the host fibrinolytic system*. Frontiers in Cellular and Infection Microbiology, 2013. **3**.
64. Bergmann, S., et al., *alpha-Enolase of Streptococcus pneumoniae is a plasmin(ogen)-binding protein displayed on the bacterial cell surface*. Molecular Microbiology, 2001. **40**(6): p. 1273-1287.
65. Jones, M.N. and R.G. Holt, *Cloning and characterization of an alpha-enolase of the oral pathogen Streptococcus mutans that binds human plasminogen*. Biochemical and Biophysical Research Communications, 2007. **364**(4): p. 924-929.
66. Pancholi, V. and V.A. Fischetti, *alpha-enolase, a novel strong plasmin(ogen) binding protein on the surface of pathogenic streptococci*. Journal of Biological Chemistry, 1998. **273**(23): p. 14503-14515.
67. Adrian, P.V., et al., *Development of antibodies against pneumococcal proteins alpha-enolase, immunoglobulin A1 protease, streptococcal lipoprotein rotamase A, and putative proteinase maturation protein A in relation to pneumococcal carriage and Otitis Media*. Vaccine, 2004. **22**(21-22): p. 2737-2742.
68. Barbour, A.G., et al., *A genome-wide proteome array reveals a limited set of immunogens in natural infections of humans and white-footed mice with Borrelia burgdorferi*. Infection and Immunity, 2008. **76**(8): p. 3374-3389.
69. Haiko, J., et al., *The Omptins of Yersinia pestis and Salmonella enterica Cleave the Reactive Center Loop of Plasminogen Activator Inhibitor 1*. Journal of Bacteriology, 2010. **192**(18): p. 4553-4561.
70. Fulde, M., et al., *Pneumococcal phosphoglycerate kinase interacts with plasminogen and its tissue activator*. Thrombosis and Haemostasis, 2014. **111**(3): p. 401-416.
71. Winram, S.B. and R. Lottenberg, *The plasmin-binding protein Plr of group A streptococci is identified as glyceraldehyde-3-phosphate dehydrogenase*. Microbiology-Sgm, 1996. **142**: p. 2311-2320.
72. Bendtsen, J.D., et al., *Non-classical protein secretion in bacteria*. BMC Microbiology, 2005. **5**.
73. Monroy, V., et al., *Binding and activation of human plasminogen by Mycobacterium tuberculosis*. Infection and Immunity, 2000. **68**(7): p. 4327-4330.
74. Xolalpa, W., et al., *Identification of novel bacterial plasminogen-binding proteins in the human pathogen Mycobacterium tuberculosis*. Proteomics, 2007. **7**(18): p. 3332-3341.
75. Sinha, S., et al., *Immunogenic membrane-associated proteins of Mycobacterium tuberculosis revealed by proteomics*. Microbiology-Sgm, 2005. **151**: p. 2411-2419.
76. Kerns, P.W., et al., *Mycobacterium tuberculosis pellicles express unique proteins recognized by the host humoral response*. Pathogens and Disease, 2014. **70**(3): p. 347-358.
77. Horwitz, M.A., et al., *Protective Immunity against Tuberculosis Induced by Vaccination with Major Extracellular Proteins of Mycobacterium-Tuberculosis*. Proceedings of the National Academy of Sciences of the United States of America, 1995. **92**(5): p. 1530-1534.
78. Santangelo, M.D., et al., *Glycolytic and Non-glycolytic Functions of Mycobacterium tuberculosis Fructose-1,6-bisphosphate Aldolase, an Essential Enzyme Produced by Replicating and Non-replicating Bacilli*. Journal of Biological Chemistry, 2011. **286**(46): p. 40219-40231.
79. Pancholi, V., *Multifunctional alpha-enolase: its role in diseases*. Cellular and Molecular Life Sciences, 2001. **58**(7): p. 902-920.

80. Derbise, A., et al., *Role of the C-terminal lysine residues of streptococcal surface enolase in Glu- and Lys-plasminogen-binding activities of group A streptococci*. Infection and Immunity, 2004. **72**(1): p. 94-105.
81. Bergmann, S., et al., *Identification of a novel plasmin(ogen)-binding motif in surface displayed alpha-enolase of Streptococcus pneumoniae*. Molecular Microbiology, 2003. **49**(2): p. 411-423.
82. Fulde, M., et al., *Cooperative Plasminogen Recruitment to the Surface of Streptococcus canis via M Protein and Enolase Enhances Bacterial Survival*. Mbio, 2013. **4**(2).
83. Bergmann, S., H. Schoenen, and S. Hammerschmidt, *The interaction between bacterial enolase and plasminogen promotes adherence of Streptococcus pneumoniae to epithelial and endothelial cells*. International Journal of Medical Microbiology, 2013. **303**(8): p. 452-462.
84. Lahteenmaki, K., et al., *Bacterial Plasminogen Receptors - in-Vitro Evidence for a Role in Degradation of the Mammalian Extracellular-Matrix*. Infection and Immunity, 1995. **63**(9): p. 3659-3664.
85. Bergmann, S., et al., *The nine residue plasminogen-binding motif of the pneumococcal enolase is the major cofactor of plasmin-mediated degradation of extracellular matrix, dissolution of fibrin and transmigration*. Thrombosis and Haemostasis, 2005. **94**(2): p. 304-311.
86. Cork, A.J., et al., *Defining the Structural Basis of Human Plasminogen Binding by Streptococcal Surface Enolase*. Journal of Biological Chemistry, 2009. **284**(25): p. 17129-17137.
87. Taylor, J.L., et al., *Role for matrix metalloproteinase 9 in granuloma formation during pulmonary Mycobacterium tuberculosis infection*. Infection and Immunity, 2006. **74**(11): p. 6135-6144.
88. Salgame, P., *MMPs in tuberculosis: granuloma creators and tissue destroyers*. Journal of Clinical Investigation, 2011. **121**(5): p. 1686-1688.
89. Brandt, L., et al., *ESAT-6 subunit vaccination against Mycobacterium tuberculosis*. Infection and Immunity, 2000. **68**(2): p. 791-795.
90. de Valliere, S., et al., *Enhancement of innate and cell-mediated immunity by antimycobacterial antibodies*. Infection and Immunity, 2005. **73**(10): p. 6711-6720.
91. Achkar, J.M. and A. Casadevall, *Antibody-Mediated Immunity against Tuberculosis: Implications for Vaccine Development*. Cell Host & Microbe, 2013. **13**(3): p. 250-262.
92. Winslow, G.M., et al., *Antibody-mediated elimination of the obligate intracellular bacterial pathogen Ehrlichia chaffeensis during active infection (vol 68, pg 2187, 2000)*. Infection and Immunity, 2000. **68**(9): p. 5469-5469.
93. Kumar, S.K., P. Singh, and S. Sinha, *Naturally produced opsonizing antibodies restrict the survival of Mycobacterium tuberculosis in human macrophages by augmenting phagosome maturation*. Open Biology, 2015. **5**(12).
94. Nunes-Alves, C., et al., *In search of a new paradigm for protective immunity to TB*. Nature Reviews Microbiology, 2014. **12**(4): p. 289-299.
95. Achkar, J.M., J. Chan, and A. Casadevall, *B cells and antibodies in the defense against Mycobacterium tuberculosis infection*. Immunological Reviews, 2015. **264**(1): p. 167-181.
96. Teitelbaum, R., et al., *A mAb recognizing a surface antigen of Mycobacterium tuberculosis enhances host survival*. Proceedings of the National Academy of Sciences of the United States of America, 1998. **95**(26): p. 15688-15693.
97. Sarkar, S., et al., *A Bispecific Antibody Based Assay Shows Potential for Detecting Tuberculosis in Resource Constrained Laboratory Settings*. Plos One, 2012. **7**(2).

# APPENDIX

# Appendix

## Stock Solutions of Commonly used Reagents

### **1 M Tris**

Dissolve 121.1 g of Tris base in 800 ml of MILLIQ and adjust to the desired pH (6.8, 7.5, 8.0, 8.8) with HCl. Make up the final volume to 1 l and autoclave.

### **0.5 M EDTA**

Add 186.1 g of disodium EDTA.2H<sub>2</sub>O in 800 ml of MILLIQ. Stir vigorously on a stirrer, adjust the pH to 8.0 with NaOH (about 20 g of NaOH pellets), make up the final volume to 1 l and autoclave.

### **3 M Sodium Acetate**

Dissolve 204.5 g of C<sub>2</sub>H<sub>3</sub>O<sub>2</sub>Na.3H<sub>2</sub>O in 400 ml of MILLIQ. Adjust the pH to 5.3 with glacial acetic acid. Make up the final volume to 500 ml and autoclave.

### **10 mg/ml Ethidium Bromide**

Dissolve 10 mg of Ethidium Bromide in 1 ml MILLIQ. Store in a dark bottle.

### **30% Acrylamide Stock**

Dissolve 29 g of acrylamide and 1 g of bis-acrylamide in 50 ml of MILLIQ. Make the final volume to 100 ml, filter the solution through Whatman no. 1 paper and store in a dark bottle.

### **8 M Urea**

Dissolve 48 gm of urea in 600 ml MQ and heat to 37°C on to dissolve urea completely. Autoclave for sterilization.

### **1 M MgCl<sub>2</sub>**

Dissolve 203.3 gm of MgCl<sub>2</sub> in 800 ml of MQ. Adjust the volume to 1 L with MQ and sterilize by autoclaving.

### **0.1 M Calcium Chloride**

Dissolve 147 g of CaCl<sub>2</sub>.2H<sub>2</sub>O in 100 ml of MILLIQ and sterilize by autoclaving.

## Antibiotic Solutions

### **Ampicillin**

Prepare 100 mg/ml stock in a/c MILLIQ and store by freezing at -20°C.

## **Kanamycin**

Prepare 50 mg/ml stock solution in a/c MILLIQ and store by freezing at -20°C.

## **Streptomycin**

Prepare 10 mg/ml stock solution in a/c MILLIQ and store by freezing at -20°C.

## **Buffers**

### **50 X TAE Buffer (Tris acetate, EDTA)**

Dissolve 242 g of Tris base in 700 ml of MILLIQ, add 57.1 ml of glacial acetic acid and 100 ml of 0.5 M EDTA (pH 8.0). Make up the final volume to 1 l.

### **5 X TBE Buffers (Tris borate, EDTA)**

Dissolve 54 g of Tris base, 27.5 g of boric acid and 20 ml of 0.5 M EDTA (pH 8.0) in 700 ml MILLIQ. Make up the final volume to 1 liter.

### **10 X Phosphate Buffered Saline (PBS)**

Dissolve 80 g of NaCl, 2 g of KCl, 14.4 g of Na<sub>2</sub>HPO<sub>4</sub> and 2 g of KH<sub>2</sub>PO<sub>4</sub> in 800 ml of MILLIQ. Adjust the pH to 7.4 with HCl. Make up the final volume to 1 l and sterilize by autoclaving at 121°C, 15 lbs for 20 min and store at room temperature.

### **1 X SDS-PAGE Electrophoresis Buffer**

Dissolve 3 g of Tris base, 14.4 g of glycine and 1 g of SDS in 1 liter of MilliQ.

### **1 X Electrode Transfer Buffer**

Dissolve 5.8 gm of Tris base, 2.9 gm of glycin and 0.33 gm of SDS in 0.5 liter of MilliQ. Add 200 ml methanol and make up the final volume to 1 liter.

### **1 X SDS-PAGE Electrophoresis Buffer**

Dissolve 3 g of Tris base, 14.4 g of glycine and 1 g of SDS in 1 L MILLIQ.

### **2 X SDS-PAGE Sample Buffer**

100 mM	Tris-Cl (pH 6.8)
4%	SDS
0.2%	Bromophenol blue
20%	Glycerol
10%	β-mercaptoethanol

### **6 X DNA Loading Dye**

Dissolve 0.2 g of bromophenol blue, 0.2 g of xylene cyanol and 30 ml of glycerol and make up the volume to 100 by a/c MILLIQ.

**2X RNA Loading Dye**

95% (v/v) deionized formamide

0.05% (w/v) bromophenol blue

0.05% (w/v) xylene cyanol FF

10 mM EDTA (pH 8)

0.05% SDS

**Composition of 12% Resolving Gel (10 ml)**

4.0 ml	30% acrylamide solution
2.5 ml	1.5 M Tris-Cl, pH 8.8
3.3 ml	MILLIQ
100 µl	10% SDS
100 µl	10% APS
5 µl	TEMED

**Composition of 10% Resolving Gel (10 ml)**

3.3 ml	30% acrylamide solution
2.6 ml	1.5 M Tris-Cl, pH 8.8
4.0 ml	MILLIQ
100 µl	10% SDS
100 µl	10% APS
5 µl	TEMED

**Composition of 5% Stacking gel (5.0 ml)**

0.83 ml	30% acrylamide solution
0.63 ml	1.5 M Tris-Cl, pH 8.8
3.4 ml	MILLIQ
100 µl	10% SDS
100 µl	10% APS
5 µl	TEMED

### **Coomassie Blue Staining Solution**

Dissolve 1 g of coomassie blue in 450 ml of methanol. Add 100 ml of glacial acetic acid and make up the volume to 1 l with MILLIQ. Filter through Whatman no. 1 paper and store at room temperature.

### **Destaining Solution**

Mix methanol : water : acetic acid in the ratio 4 : 5 : 1. Store at room temperature.

### **Preparation of Bacterial Culture Media**

#### **LB medium (Luria Broth)**

Dissolve 25 g of LB powder (Difco) in 1 l of MILLIQ. Sterilize the media by autoclaving for 20 min at 121°C, 15 lbs.

#### **LB Agar**

Dissolve 40 g of LB agar powder (Difco) in 1 l of MILLIQ. Sterilize the media by autoclaving for 20 min at 121°C, 15 lbs.

For plates, allow LB agar to cool and pour in 90 mm disposable petri-plates (Tarsons)

#### **Middlebrook 7H9 Broth**

Dissolve 4.7 g of the powder (Middlebrook, Difco) in 900 mL of MILLIQ (containing 2 mL glycerol and 0.5 mL tween 80). Autoclave at 121°C for 10 min, 15 lbs. Aseptically, add 100 mL of Middlebrook ADC Enrichment to the medium when cooled to 45°C.

#### **Middlebrook 7H10 Agar**

Dissolve 19 gm of the powder (Middlebrook, Difco) in 900 mL of MilliQ water and mix in 5 ml glycerol. Autoclave at 121°C for 10 min, 15 lbs. Aseptically, add 100 mL of Middlebrook OADC supplement to the medium when cooled to 45°C. Add PANTA or 5 antibiotics for avoiding fungal and other bacterial contamination.

#### **Middlebrook 7H11 Agar**

Dissolve 21 g of the powder (Middlebrook, Difco) in 900 mL of MILLIQ and mix in 5 mL glycerol. Autoclave at 121°C for 10 min, 15 lbs. Aseptically, add 100 mL of Middlebrook OADC supplement to the medium when cooled to 45°C. Add PANTA or 5 antibiotics for avoiding fungal and other bacterial contamination.





## Enolase of *Mycobacterium tuberculosis* is a surface exposed plasminogen binding protein



Amit Rahi<sup>1</sup>, Sumit Kumar Matta<sup>1</sup>, Alisha Dhiman<sup>1</sup>, Jaishree Garhyan<sup>2</sup>, Monisha Gopalani<sup>2</sup>, Subhash Chandra<sup>3</sup>, Rakesh Bhatnagar<sup>\*</sup>

Laboratory of Molecular Biology and Genetic Engineering, School of Biotechnology, Jawaharlal Nehru University, New Delhi, India

### ARTICLE INFO

#### Article history:

Received 18 April 2016

Received in revised form 12 August 2016

Accepted 24 August 2016

Available online 26 August 2016

#### Keywords:

*Mycobacterium tuberculosis*

enolase

plasminogen

plasmin

surface localization

extracellular matrix (ECM)

### ABSTRACT

**Background:** Enolase, a glycolytic enzyme, has long been studied as an anchorless protein present on the surface of many pathogenic bacteria that aids in tissue remodeling and invasion by binding to host plasminogen.

**Methods:** Anti-*Mtb* enolase antibodies in human sera were detected using ELISA. Immunoelectron microscopy, immunofluorescence microscopy and flow cytometry were used to show surface localization of *Mtb* enolase. SPR was used to determine the affinity of enolase-plasminogen interaction. Plasmin formation upon plasminogen binding to enolase and *Mtb* surface was measured by ELISA. Mice challenge and histopathological studies were undertaken to determine the protective efficacy of enolase immunization.

**Results:** Enolase of *Mtb* is present on its surface and binds human plasminogen with high affinity. There was an average of 2-fold increase in antibody mediated recognition of *Mtb* enolase in human sera from TB patients with an active disease over control individuals. Substitution of C-terminal lysine to alanine in rEno decreased its binding affinity with human plasminogen by >2-folds. Enolase bound plasminogen showed urokinase mediated conversion into plasmin. Binding of plasminogen to the surface of *Mtb* and its conversion into fibrinolytic plasmin was significantly reduced in the presence of anti-rEno antibodies. Immunization with rEno also led to a significant decrease in lung CFU counts of mice upon infection with *Mtb* H37Rv.

**Conclusions:** *Mtb* enolase is a surface exposed plasminogen binding protein which upon immunization confers significant protection against *Mtb* challenge.

**General significance:** Plasminogen binding has been recognized for *Mtb*, however, proteins involved have not been characterized. We show here that *Mtb* enolase is a moonlighting plasminogen binding protein.

© 2016 Elsevier B.V. All rights reserved.

### 1. Introduction

Tuberculosis (TB) is a global disease caused by *Mycobacterium tuberculosis* (*Mtb*), resulting in serious disease burden and death of human population in millions. This alarming scenario is the case when approximately one third of infections in humans remain asymptomatic or latent [1]. *Mtb* is a facultative intracellular human pathogen which has the ability to grow extracellularly, invade host tissues and spread systemically leading to a debilitating disease. Upon reactivation of latent infection, due to factors such as aging or immunosuppression,

the bacilli can induce an active spread of the disease dependent on host matrix metalloproteinases (MMPs) leading to tissue degeneration [2]. MMPs are endopeptidases capable of degrading components of the extracellular matrix (ECM) like collagen [3].

Emergence of antibiotic resistant strains of *Mtb* alongwith the inefficacy of widely used Bacillus Calmette-Guerin (BCG) vaccine in adults are major challenges in the treatment and prevention of TB. Elucidation and characterization of new vaccine and drug candidates are therefore required in order to design a multi-pronged strategy to prevent and treat this disease. *Mtb* produces a variety of virulence factors that aid in its extracellular and intracellular survival within the macrophages. A formidable and unusually lipid-rich cell wall is by far its most effective virulence factor, contributing to its intrinsic resistance to a number of therapeutic agents [4]. With respect to the secretion system, virulent phenotype in *Mtb* is associated with its ESX-1 secretion system that exports ESAT-6 and CFP-10 in the extracellular environment, which in turn are majorly responsible for regulating many of the anti-bacterial responses of the host and cell to cell spread of *Mtb* infection [5].

Recruitment of plasminogen on to the bacterial surface has long been acknowledged as a mechanism involved in bacterial attachment

Abbreviations: *Mtb*, *Mycobacterium tuberculosis*; TB, Tuberculosis; rEno, recombinant enolase; MMP, Matrix Metalloproteinases; ECM, Extracellular Matrix.

\* Corresponding author at: Laboratory of Molecular Biology and Genetic Engineering, School of Biotechnology, Jawaharlal Nehru University, New Delhi 110067, India.

E-mail addresses: amitrah184@gmail.com (A. Rahi), sumitmatta@yahoo.co.in (S.K. Matta), alisha.dhiman1986@gmail.com (A. Dhiman), jgarhyan@gmail.com (J. Garhyan), monishasb@gmail.com (M. Gopalani), scjnu@yahoo.co.in (S. Chandra), rakeshbhatnagar@jnu.ac.in (R. Bhatnagar).

<sup>1</sup> Equal contribution as first authors.

<sup>2</sup> Equal contribution as second authors.

<sup>3</sup> Current address: Kumaon University, SSJ Campus, Almora, Uttarakhand, India



Contents lists available at ScienceDirect

International Journal of Biological Macromolecules

journal homepage: [www.elsevier.com/locate/ijbiomac](http://www.elsevier.com/locate/ijbiomac)

## Role of the recognition helix of response regulator WalR from *Bacillus anthracis* in DNA binding and specificity



Alisha Dhiman<sup>a</sup>, Amit Rahi<sup>a</sup>, Monisha Gopalani<sup>a</sup>, Sailesh Bajpai<sup>b</sup>, Sonika Bhatnagar<sup>c,\*</sup>, Rakesh Bhatnagar<sup>a,\*</sup>

<sup>a</sup> Laboratory of Molecular Biology and Genetic Engineering, School of Biotechnology, Jawaharlal Nehru University, New Delhi, India

<sup>b</sup> GE Healthcare Life Sciences, Gurgaon, Haryana, India

<sup>c</sup> Computational and Structural Biology Lab., Division of Biotechnology, Netaji Subhas Institute of Technology, Dwarka, New Delhi, India

### ARTICLE INFO

#### Article history:

Received 28 June 2016

Received in revised form 7 December 2016

Accepted 8 December 2016

Available online 14 December 2016

#### Keywords:

Two component system

WalR

Recognition helix

### ABSTRACT

WalRK two-component system of *Bacillus anthracis* potentially regulates multiple genes spanning diverse cellular functions. Its constituent response regulator (RR), WalR belongs to the OmpR/PhoB family which possesses a winged helix-turn-helix motif for DNA binding. An *in silico* knowledge based model of WalR C-terminal DNA binding domain in complex with its *ftsE* promoter region binding motif was used to identify specific residues of the recognition helix important for DNA binding. The model was validated by mutagenesis in conjunction with *in vitro* DNA binding analysis. The *ftsE* promoter region DNA binding motif was also varied. Optimal binding of WalR to DNA required the presence of both half-sites in its binding motif. Substitution of invariant bases of WalR DNA binding motif abrogated the binding whereas changes at variable motif positions governed affinity. D199 was not in direct contact with the DNA but its substitution modified the WalR-DNA specificity indicating the importance of contact avoidance by this residue for DNA specificity. This represents the first in-depth study of RR-DNA interaction from *B. anthracis*.

© 2016 Elsevier B.V. All rights reserved.

### 1. Introduction

Bacteria and certain eukaryotes like yeast, fungi, and plants use signal transduction modules called Two Component Systems (TCSs) to sense and respond to various environmental stimuli. Such stimuli can include osmolarity, pH, ionic concentrations and nutrient levels among others. The downstream processes governed range from fundamental physiological phenomena like osmoregulation, ion uptake, chemotaxis to specialized pathogenic attributes like host-pathogen interactions and virulence factors regulation [1–5]. The central role of TCSs in virulence, survival and host-pathogen interactions, their ubiquitous abundance in bacteria, combined with complete absence in humans points to their potential as antimicrobial targets [6,7].

An archetypal TCS consists of a membrane bound Histidine Kinase (HK) and its cognate Response Regulator (RR). RRs have a conserved N-terminal receiver domain and a variable C-terminal effector domain which is responsible for manifesting the response,

mostly through DNA binding and changes in gene expression [1]. The receiver domain of any RR can exist in two conformations—inactive or unphosphorylated and active or phosphorylated. Phosphorylation of the receiver domain enhances the DNA binding affinity through percolative conformational changes in its associated effector domain. However, structural studies have proven that unphosphorylated receiver domains can continuously switch between both inactive and active conformations, where phosphorylation shifts the equilibrium towards the active conformation [2].

*Bacillus anthracis*, the causative agent of anthrax, can cause fatal infections in animals and humans [8]. The threat posed by *B. anthracis* as a biological weapon is heightened by occurrence of strains that may be antibiotic resistant. Consequently, we need to identify crucial pathways in *B. anthracis* that could be targeted for the development of antimicrobials. TCS inhibitors could present a new class of antibiotics, active even against drug-resistant bacteria [6,7,9]. Although the development of TCS inhibitors has largely focused on HKs, RRs offer advantages since RR inhibition can directly affect the gene expression and also, overcome shortcomings of targeting the HKs. *B. anthracis* is predicted to code for 41 pairs of TCSs in its genome [10]. One such TCS, WalRK, has homologs that regulate virulence in several Gram positive pathogens and are essential for survival [11–13]. In *B. anthracis*, WalRK forms a

\* Corresponding authors.

E-mail addresses: [ecc999@gmail.com](mailto:ecc999@gmail.com) (S. Bhatnagar), [rakeshbhatnagar@jnu.ac.in](mailto:rakeshbhatnagar@jnu.ac.in) (R. Bhatnagar).

<http://dx.doi.org/10.1016/j.ijbiomac.2016.12.037>

0141-8130/© 2016 Elsevier B.V. All rights reserved.

RESEARCH ARTICLE

# Identification, Functional Characterization and Regulon Prediction of a Novel Two Component System Comprising BAS0540-BAS0541 of *Bacillus anthracis*


Monisha Gopalani, Alisha Dhiman<sup>‡</sup>, Amit Rahi<sup>‡</sup>, Divya Kandari, Rakesh Bhatnagar\*

Laboratory of Molecular Biology and Genetic Engineering, School of Biotechnology, Jawaharlal Nehru University, New Delhi-110067, India

<sup>‡</sup> These authors contributed equally to this work.

\* [rakeshbhatnagar@jnu.ac.in](mailto:rakeshbhatnagar@jnu.ac.in)



 OPEN ACCESS

**Citation:** Gopalani M, Dhiman A, Rahi A, Kandari D, Bhatnagar R (2016) Identification, Functional Characterization and Regulon Prediction of a Novel Two Component System Comprising BAS0540-BAS0541 of *Bacillus anthracis*. PLoS ONE 11(7): e0158895. doi:10.1371/journal.pone.0158895

**Editor:** Esteban Chaves-Clarke, Universidad de Costa Rica, COSTA RICA

**Received:** December 24, 2015

**Accepted:** June 23, 2016

**Published:** July 8, 2016

**Copyright:** © 2016 Gopalani et al. This is an open access article distributed under the terms of the [Creative Commons Attribution License](https://creativecommons.org/licenses/by/4.0/), which permits unrestricted use, distribution, and reproduction in any medium, provided the original author and source are credited.

**Data Availability Statement:** All relevant data are within the paper and its Supporting Information files.

**Funding:** This study was funded in part by Department of Science and Technology, Govt. of India. MG and AD acknowledge fellowships by Council of Scientific and Industrial Research-India. The funders had no role in study design, data collection and analysis, decision to publish, or preparation of the manuscript.

**Competing Interests:** The authors have declared that no competing interests exist.

## Abstract

Two component systems (TCSs) can be envisaged as complex molecular devices that help the bacteria to sense its environment and respond aptly. 41 TCSs are predicted in *Bacillus anthracis*, a potential bioterrorism agent, of which only four have been studied so far. Thus, the intricate signaling network contributed by TCSs remains largely unmapped in *B. anthracis* and needs comprehensive exploration. In this study, we functionally characterized one such system composed of BAS0540 (Response regulator) and BAS0541 (Histidine kinase). BAS0540-BAS0541, the closest homolog of CiaRH of *Streptococcus* in *B. anthracis*, forms a functional TCS with BAS0541 displaying autophosphorylation and subsequent phosphotransfer to BAS0540. BAS0540 was also found to accept phosphate from physiologically relevant small molecule phosphodonors like acetyl phosphate and carbamoyl phosphate. Results of qRT-PCR and immunoblotting demonstrated that BAS0540 exhibits a constitutive expression throughout the growth of *B. anthracis*. Regulon prediction for BAS0540 in *B. anthracis* was done *in silico* using the consensus DNA binding sequence of CiaR of *Streptococcus*. The predicted regulon of BAS0540 comprised of 23 genes, which could be classified into 8 functionally diverse categories. None of the proven virulence factors were a part of the predicted regulon, an observation contrasting with the regulon of CiaRH in *Streptococci*. Electrophoretic mobility shift assay was used to show direct binding of purified BAS0540 to the upstream regions of 5 putative regulon candidates- BAS0540 gene itself; a gene predicted to encode cell division protein FtsA; a self-immunity gene; a RND family transporter gene and a gene encoding stress (heat) responsive protein. A significant enhancement in the DNA binding ability of BAS0540 was observed upon phosphorylation. Overexpression of response regulator BAS0540 in *B. anthracis* led to a prodigious increase of ~6 folds in the cell length, thereby conferring it a filamentous phenotype. Furthermore, the sporulation titer of the pathogen also decreased markedly by ~16 folds. Thus, this study characterizes a novel TCS of *B. anthracis* and elucidates its role in two of the most important physiological processes of the pathogen: cell division and sporulation.





## Overexpression of the pleiotropic regulator CodY decreases sporulation, attachment and pellicle formation in *Bacillus anthracis*



Monisha Gopalani<sup>1</sup>, Alisha Dhiman<sup>1</sup>, Amit Rahi<sup>1</sup>, Rakesh Bhatnagar<sup>\*</sup>

Laboratory of Molecular Biology and Genetic Engineering, School of Biotechnology, Jawaharlal Nehru University, New Delhi, 110067, India

### ARTICLE INFO

#### Article history:

Received 20 November 2015

Accepted 5 December 2015

Available online 11 December 2015

#### Keywords:

CodY

*Bacillus anthracis*

Sporulation

Pellicle

### ABSTRACT

CodY, a global transcriptional regulator, primarily functions as a nutrient and energy sensor. It is activated by metabolic effectors like BCAA and GTP. In low G + C Gram positive bacteria, it facilitates coupling of changes in the cellular metabolite pool with those required in the transcriptome of the cell. This pleiotropic regulator controls the expression of a vast number of genes as the cell transits from exponential to the stationary phase. Earlier studies have shown that CodY is required for the virulence of *Bacillus anthracis*. We sought to investigate the effect of its overexpression on the physiology of *B. anthracis*. In our study, we found that cellular CodY levels were unchanged during this phase-transition. Expression of endogenous CodY remained the same in different nutrient limiting conditions. Immunoblotting studies revealed CodY presence in the whole spore lysate of *B. anthracis* indicating it to be a component of the spore proteome. We could also detect CodY in the secretome of *B. anthracis*. Further, CodY was overexpressed in *B. anthracis* Sterne strain and this led to a 100-fold decrease in the sporulation titer and a 2.5-fold decrease in the *in vitro* attachment ability of the bacteria. We also observed a decrease in the pellicle formation by CodY overexpressed strain when compared to wildtype bacilli. The CodY overexpressed strain showed chaining phenotype during growth in liquid media and pellicle.

© 2015 Elsevier Inc. All rights reserved.

### 1. Introduction

Nutrient availability and gene regulation are tightly linked in bacteria. There is no need for well-fed bacterium to express the genes required for adaptation to nutrient stress. Similarly, a starved bacterium need not express the genes for cell division. For sensing nutrient availability and responding to it in an apt fashion, bacteria have developed precocious adaptation circuits. CodY is a pleiotropic transcriptional regulator present in almost all low G + C Gram positive bacteria. It senses the nutrient and energy status of the cell by binding to BCAA and GTP, respectively and regulates gene expression accordingly [1]. Previous studies from *Bacillus subtilis* have shown that CodY represses expression of stationary phase genes, like those involved in catabolism, sporulation,

biosynthesis of some amino acids and transport systems, during the exponential phase [2]. BCAA and GTP pools in an exponentially growing cell are abundant and interact with CodY, thereby enhancing its DNA binding ability, to keep its regulon repressed. When bacteria enter stationary phase, the levels of intracellular BCAA and GTP decrease, thus they can no longer interact with CodY reducing its DNA binding affinity and leading to derepression of the genes in its regulon [1]. GTP pool also decreases during stringent response by two mechanisms: firstly, the alarmones ppGPP and pppGPP are produced by enzymatic phosphorylation of GTP and GDP resulting in a decrease in the cellular GTP pool and secondly, by the inhibition of inosine monophosphate dehydrogenase [1]. Hence, nutrient limiting conditions, low cellular energy status and stringent response can lead to expression of CodY regulon.

In addition to its role in metabolic regulation, CodY is also implicated in survival strategies like sporulation, biofilm and pellicle formation, motility etc. in *B. subtilis*, *Bacillus cereus*, *Streptococcus mutans* and *Staphylococcus aureus* [2–7]. Multicellular aggregations associated with a surface and enclosed by a self-secreted extracellular matrix are known as biofilms [8]. Biofilm structure varies with environmental conditions. Pellicle is regarded

Abbreviations: BCAA, branched chain amino acid.

\* Corresponding author.

E-mail addresses: [monishasbt@gmail.com](mailto:monishasbt@gmail.com) (M. Gopalani), [alisha.dhiman1986@gmail.com](mailto:alisha.dhiman1986@gmail.com) (A. Dhiman), [amitrahi84@gmail.com](mailto:amitrahi84@gmail.com) (A. Rahi), [rakeshbhatnagar@jnu.ac.in](mailto:rakeshbhatnagar@jnu.ac.in) (R. Bhatnagar).

<sup>1</sup> Equal contribution.

<http://dx.doi.org/10.1016/j.bbrc.2015.12.019>

0006-291X/© 2015 Elsevier Inc. All rights reserved.



## Generation of protective immune response against anthrax by oral immunization with protective antigen plant-based vaccine



Jyotsna Gorantala<sup>a</sup>, Sonam Grover<sup>b</sup>, Amit Rahi<sup>a</sup>, Prerna Chaudhary<sup>c</sup>, Ravi Rajwanshi<sup>c</sup>, Neera Bhalla Sarin<sup>c</sup>, Rakesh Bhatnagar<sup>a,\*</sup>

<sup>a</sup> Laboratory of Molecular Biology and Genetic Engineering, School of Biotechnology, Jawaharlal Nehru University, New Delhi, India

<sup>b</sup> Molecular Technology Laboratory, School of Biotechnology, Jawaharlal Nehru University, New Delhi, India

<sup>c</sup> School of Life Sciences, Jawaharlal Nehru University, New Delhi 110067, India

### ARTICLE INFO

#### Article history:

Received 26 September 2013

Received in revised form

30 December 2013

Accepted 29 January 2014

Available online 15 February 2014

#### Keywords:

Anthrax vaccine

Protective antigen

Lethal toxin

Toxin challenge

### ABSTRACT

In concern with frequent recurrence of anthrax in endemic areas and inadvertent use of its spores as biological weapon, the development of an effective anthrax vaccine suitable for both human and veterinary needs is highly desirable. A simple oral delivery through expression in plant system could offer promising alternative to the current methods that rely on injectable vaccines extracted from bacterial sources. In the present study, we have expressed protective antigen (PA) gene in Indian mustard by *Agrobacterium*-mediated transformation and in tobacco by plastid transformation. Putative transgenic lines were verified for the presence of transgene and its expression by molecular analysis. PA expressed in transgenic lines was biologically active as evidenced by macrophage lysis assay. Intraperitoneal (i.p.) and oral immunization with plant PA in murine model indicated high serum PA specific IgG and IgA antibody titers. PA specific mucosal immune response was noted in orally immunized groups. Further, antibodies indicated lethal toxin neutralizing potential *in-vitro* and conferred protection against *in-vivo* toxin challenge. Oral immunization experiments demonstrated generation of immunoprotective response in mice. Thus, our study examines the feasibility of oral PA vaccine expressed in an edible plant system against anthrax.

© 2014 Elsevier B.V. All rights reserved.

### 1. Introduction

Anthrax, a disease caused by *Bacillus anthracis* has gained prominence in the recent times due its potential implication as bio-warfare agent. Apart from the bioterrorist attacks, natural outbreaks continue to occur in many parts of the world especially in Central Asia, South America and Africa. The disease in nature affects animals but humans also contract the disease from animals or animal products. Recently, incidences of anthrax in wildlife from various national parks have also come in to light (Fasanella et al., 2010;

Hudson et al., 2008). The situation demands a pragmatic vaccination approach suitable for both human and veterinary purposes under natural circumstances or during iniquitous bioterror events.

The present human and veterinary anthrax vaccines rely on rather old-fashioned methods. The veterinary anthrax vaccine developed in 1930's by Sterne is essentially an attenuated, non-encapsulated, toxigenic strain of *B. anthracis*, while the licensed human vaccine predominantly contains 'protective antigen', the main immunogenic component of the tripartite anthrax toxin. Both the vaccines have potential side effects. The ancient veterinary anthrax vaccine waned in its potency and showed discrepancies in virulence leading to occasional death of animals (Brossier et al., 1999; Shakya et al., 2007). In both these vaccines, the presence of residual virulence lead to local and systemic reactions in the subjects (Wang and Roehrl, 2005). These vaccines being injectable make vaccine delivery process tougher for medical professionals particularly in cases of affected livestock and wild animals and contribute to systemic immunity alone. Oral vaccines may provide significant respite in such circumstances by simplifying the vaccine delivery and activating both mucosal as well as systemic immunity.

Several heterologous expression systems such as bacterial, viral or plant systems have been employed for oral delivery of vaccines (Aloni-Grinstein et al., 2005; Baillie et al., 2008; Bielinska et al., 2007; Brey, 2005). Plant-based vaccines due to their

**Abbreviations:** BAP, benzyl amino purine; BC, before challenge titers; CFU, colony forming units; CT, cholera toxin; DMEM, Dulbecco's modified eagle medium; ELISA, enzyme linked immunosorbent assay; HRP, horseradish peroxidase; IBA, indole-3-butyric acid; i.p., intraperitoneal; LeTx, lethal toxin; LF, lethal factor; MTT, 3-(4,5-dimethylthiazol-2-yl)-5-diphenyltetrazolium bromide; MS media, Murashige and Skoog media; MWCO, molecular weight cut-off; NAA,  $\alpha$ -naphthalene acetic acid; NBT, nitroblue tetrazolium; PAGE, poly acrylamide gel electrophoresis; PBS, phosphate buffered saline; PMSF, phenyl methyl sulfonyl fluoride; PA, protective antigen; SDS, sodium dodecyl sulphate; SM, selection medium; TSP, total soluble protein; TMB, tetramethylbenzidine; RM, regeneration medium; UTR, untranslated region; WT, wild type.

\* Corresponding author. Tel.: +91 1126704079/+91 1126742040;

fax: +91 112674158.

E-mail address: [rakeshbhatnagar@mail.jnu.ac.in](mailto:rakeshbhatnagar@mail.jnu.ac.in) (R. Bhatnagar).

0168-1656/\$ – see front matter © 2014 Elsevier B.V. All rights reserved.

<http://dx.doi.org/10.1016/j.jbiotec.2014.01.033>

# A Single-Dose PLGA Encapsulated Protective Antigen Domain 4 Nanoformulation Protects Mice against *Bacillus anthracis* Spore Challenge

Manish Manish<sup>2</sup>, Amit Rahi<sup>2</sup>, Manpreet Kaur<sup>2</sup>, Rakesh Bhatnagar<sup>2</sup>, Samer Singh<sup>1\*</sup>

<sup>1</sup> Special Centre for Nano Sciences, Jawaharlal Nehru University, New Delhi, India, <sup>2</sup> Laboratory of Molecular Biology and Genetic Engineering, School of Biotechnology, Jawaharlal Nehru University, New Delhi, India

## Abstract

*Bacillus anthracis*, the etiological agent of anthrax, is a major bioterror agent. Vaccination is the most effective prophylactic measure available against anthrax. Currently available anthrax vaccines have issues of the multiple booster dose requirement, adjuvant-associated side effects and stability. Use of biocompatible and biodegradable nanoparticles to deliver the antigens to immune cells could solve the issues associated with anthrax vaccines. We hypothesized that the delivery of a stable immunogenic domain 4 of protective antigen (PAD4) of *Bacillus anthracis* encapsulated in a poly (lactide-co-glycolide) (PLGA) - an FDA approved biocompatible and biodegradable material, may alleviate the problems of booster dose, adjuvant toxicity and stability associated with anthrax vaccines. We made a PLGA based protective antigen domain 4 nanoparticle (PAD4-NP) formulation using water/oil/water solvent evaporation method. Nanoparticles were characterized for antigen content, morphology, size, polydispersity and zeta potential. The immune correlates and protective efficacy of the nanoparticle formulation was evaluated in Swiss Webster outbred mice. Mice were immunized with single dose of PAD4-NP or recombinant PAD4. The PAD4-NP elicited a robust IgG response with mixed IgG1 and IgG2a subtypes, whereas the control PAD4 immunized mice elicited low IgG response with predominant IgG1 subtype. The PAD4-NP generated mixed Th1/Th2 response, whereas PAD4 elicited predominantly Th2 response. When we compared the efficacy of this single-dose vaccine nanoformulation PAD4-NP with that of the recombinant PAD4 in providing protective immunity against a lethal challenge with *Bacillus anthracis* spores, the median survival of PAD4-NP immunized mice was 6 days as compared to 1 day for PAD4 immunized mice ( $p < 0.001$ ). Thus, we demonstrate, for the first time, the possibility of the development of a single-dose and adjuvant-free protective antigen based anthrax vaccine in the form of PAD4-NP. Further work in this direction may produce a better and safer candidate anthrax vaccine.

**Citation:** Manish M, Rahi A, Kaur M, Bhatnagar R, Singh S (2013) A Single-Dose PLGA Encapsulated Protective Antigen Domain 4 Nanoformulation Protects Mice against *Bacillus anthracis* Spore Challenge. PLoS ONE 8(4): e61885. doi:10.1371/journal.pone.0061885

**Editor:** Gourapura J. Renukaradhya, The Ohio State University, United States of America

**Received:** November 13, 2012; **Accepted:** March 14, 2013; **Published:** April 29, 2013

**Copyright:** © 2013 Manish et al. This is an open-access article distributed under the terms of the Creative Commons Attribution License, which permits unrestricted use, distribution, and reproduction in any medium, provided the original author and source are credited.

**Funding:** The study was supported in part by funding from the Department of Biotechnology (DBT) and Department of Science and Technology (DST), India. SS is a Ramalingaswami Fellow supported by DBT, India. MM is the recipient of Utrecht University Short Stay Fellowship, Fulbright fellowship and SBRI-India GID fellowship (NIH Research Grant number D43 TW000924 funded by the Fogarty International Center). The funders had no role in study design, data collection and analysis, decision to publish, or preparation of the manuscript.

**Competing Interests:** The current work is related to a patent application number 3469/DEL/2012 titled "Novel anthrax vaccine formulation" which deals with making of PA containing PLGA nanoparticles. This association does not alter the authors' adherence to all the PLOS ONE policies on sharing data and materials, as detailed online.

\* E-mail: samersingh@gmail.com

## Introduction

Anthrax is primarily a disease of herbivores with occasional accidental human infection. It is caused by *Bacillus anthracis* - a Gram positive and spore forming bacterium. The ease of weaponization of *Bacillus anthracis* spores combined with the rapid course of the disease and the similarity of initial symptoms to common cold, make it a major biowarfare agent or bioterror threat. The mortality rate in inhalational anthrax is 45–90% even when the anthrax gets diagnosed early and followed by an aggressive antimicrobial schedule [1]. Furthermore, *Bacillus anthracis* spores can persist in the lung for 58 days; hence a prolonged antibiotic treatment is needed to prevent the disease relapse [2]. This scenario often makes the chemotherapy an ineffective measure for anthrax containment in case of a massive anthrax attack when supply of antibiotics could be limiting or when toxemia has already developed. Though there had been only

limited casualties as a result of any anthrax outbreak in recent past, the anthrax spore attacks through postal mail in USA, 2001 [3] had exposed the limitations of the available vaccines in any emergency situation and prompted the research towards development of a more effective, safer and easily administrable vaccine [4–6]. Furthermore, the speculation that terrorist groups may have access to anthrax spores [7] or different rogue governments may use it as a biowarfare agent had kept the momentum of anthrax prevention research going.

The pathogenesis of *Bacillus anthracis* mainly depends on tripartite exotoxin protein complex and an anti-phagocytic poly- $\gamma$ -d-glutamic acid capsule. Tripartite exotoxin is composed of protective antigen (PA), lethal factor (LF) and edema factor (EF). Protective antigen is the cell-binding moiety that acts as a carrier to translocate lethal factor and edema factor into the cytosol. Commensurate with the central role of PA in anthrax exotoxin activity, it is the major immunogen of all anthrax vaccines





Contents lists available at ScienceDirect

Biochemical and Biophysical Research Communications

journal homepage: [www.elsevier.com/locate/ybbrc](http://www.elsevier.com/locate/ybbrc)

## Enzymatic characterization of Catalase from *Bacillus anthracis* and prediction of critical residues using information theoretic measure of Relative Entropy

Amit Rahi<sup>a,1</sup>, Mohd Rehan<sup>b,1</sup>, Rajni Garg<sup>a</sup>, Deeksha Tripathi<sup>a</sup>, Andrew M. Lynn<sup>b,\*</sup>, Rakesh Bhatnagar<sup>a,\*</sup>

<sup>a</sup> Laboratory of Molecular Biology and Genetic Engineering, School of Biotechnology, Jawaharlal Nehru University, New Delhi 110067, India

<sup>b</sup> School of Computational and Integrative Sciences, Jawaharlal Nehru University, New Delhi 110067, India

### ARTICLE INFO

Article history:  
Received 8 June 2011  
Available online 24 June 2011

#### Keywords:

Catalase  
*Bacillus anthracis*  
Sequence analysis  
Relative Entropy  
ROS  
Activity  
Mutagenesis

### ABSTRACT

In order to cope up with the reactive oxygen species (ROS) generated by host innate immune response, most of the intracellular organisms express Catalase for the enzymatic destruction/detoxification of hydrogen peroxide, to combat its deleterious effects. Catalase thus, scavenges ROS thereby playing a pivotal role in facilitating the survival of the pathogen within the host, and thus contributes to its pathogenesis. *Bacillus anthracis* harbors five isoforms of Catalase, but none of them has been studied so far. Thus, this study is the first attempt to delineate the biochemical and functional characteristics of one of the isoforms of Catalase (Cat1.4) of *B. anthracis*, followed by identification of residues critical for catalysis. The general strategy used, so far for mutational analysis in Catalases is structure based, i.e. the residues in the vicinity of heme were mutated to decipher the enzymatic mechanism. However, in the present study, protein sequence analysis was used for the prediction of catalytically important residues of Catalase. Essential measures were adopted to ensure the accuracy of predictions like after retrieval of well-annotated sequences from the database with EC 1.11.1.6, preprocessing was done to remove irrelevant sequences. The method used for multiple alignment of sequences, was guided by structural alignment and thereafter, an information theoretic measure, Relative Entropy was used for the critical residue prediction. By exploiting this strategy, we identified two previously known essential residues, H55 and Y338 in the active site which were demonstrated to be crucial for the activity. We also identified six novel crucial residues (Q332, Y117, H215, W257, N376 and H146) located distantly from the active site. Thus, the present study highlights the significance of this methodology to identify not only those crucial residues which lie in the active site of Catalase, but also the residues located distantly.

© 2011 Elsevier Inc. All rights reserved.

### 1. Introduction

*Bacillus anthracis*, a Gram-positive, non-motile, spore-forming organism is the etiological agent of anthrax. Owing to the emergence of multidrug resistance and ineffective vaccinations against anthrax, the inhalation of anthrax spores can prove fatal. Although, the major anti-anthrax drugs/vaccines primarily remain focused on the tripartite exotoxin complex (PA, EF and LF); the other factors underlying the anthrax pathogenesis remain poorly understood. To successfully thrive and confront the hostile microenvironment within the host, most of the pathogens including *B. anthracis*, exploit oxidative stress defense mechanism to subvert and evade the host innate immune system. It has been demonstrated that *katB* or *Catalases* are up-regulated during the growth

of *B. anthracis* within the macrophages [1]. The pathogens are endowed with protective mechanisms against reactive oxygen species (ROSs) generated within the host, such as ones generated by professional phagocytic cells [2]. Antioxidant enzymes, like Catalases and superoxide dismutases (SODs) play a pivotal role in facilitating the survival of pathogen within the host and thus, indirectly contribute to the pathogenesis of bacterium. The study of the effect of different organic solvents on the conformation and activity of Catalase could provide clue to understand the mechanism of enzyme action [3]. Catalase, a ubiquitous metalloenzyme guards aerobic organisms, as an intracellular H<sub>2</sub>O<sub>2</sub>-scavenger. The pathogen-encoded nitric oxide synthase has been shown to activate Catalase and subsequently, suppress the Fenton reaction [4]. Four SODs (including two on the exosporium) provide redundant and combinatorial protection to the bacterium from oxidative stress in the macrophages [5]. The ability of anthrax spores to effectively scavenge free radicals, further indicates that these enzymes are functionally active on the exosporium. On the contrary, the significance of Catalases in combating oxidative stress has not been

\* Corresponding authors. Fax: +91 11 26742040 26 (R. Bhatnagar).

E-mail addresses: [andrew@mail.jnu.ac.in](mailto:andrew@mail.jnu.ac.in) (A.M. Lynn), [rakeshbhatnagar@mail.jnu.ac.in](mailto:rakeshbhatnagar@mail.jnu.ac.in) (R. Bhatnagar).

<sup>1</sup> These authors contributed equally to this work.



## A plant based protective antigen [PA(dIV)] vaccine expressed in chloroplasts demonstrates protective immunity in mice against anthrax<sup>☆</sup>

Jyotsna Gorantala<sup>a</sup>, Sonam Grover<sup>b,1</sup>, Divya Goel<sup>a,1</sup>, Amit Rahi<sup>a</sup>, Sri Krishna Jayadev Magani<sup>a</sup>, Subhash Chandra<sup>a,2</sup>, Rakesh Bhatnagar<sup>a,\*</sup>

<sup>a</sup> Laboratory of Molecular Biology and Genetic Engineering, School of Biotechnology, Jawaharlal Nehru University, New Delhi, India

<sup>b</sup> Molecular Technology Laboratory, School of Biotechnology, Jawaharlal Nehru University, New Delhi, India

### ARTICLE INFO

#### Article history:

Received 2 September 2010

Received in revised form 11 March 2011

Accepted 22 March 2011

Available online 17 April 2011

#### Keywords:

Protective antigen

Domain IV

Anthrax

Transplastomic plants

Lethal toxin

Protection

### ABSTRACT

The currently available anthrax vaccines are limited by being incompletely characterized, potentially reactogenic and have an expanded dosage schedule. Plant based vaccines offer safe alternative for vaccine production. In the present study, we expressed domain IV of *Bacillus anthracis* protective antigen gene [PA(dIV)] in *planta* (by nuclear agrobacterium and chloroplast transformation) and *E. coli* [rPA(dIV)]. The presence of transgene and the expression of PA(dIV) in *planta* was confirmed by molecular analysis. Expression levels up to 5.3% of total soluble protein (TSP) were obtained with AT rich (71.8% AT content) PA(dIV) gene in transplastomic plants while 0.8% of TSP was obtained in nuclear transformants. Further, we investigated the protective response of plant and *E. coli* derived PA(dIV) in mice by intraperitoneal (i.p.) and oral immunizations with or without adjuvant. Antibody titers of  $>10^4$  were induced upon i.p. and oral immunizations with plant derived PA(dIV) and oral immunization with *E. coli* derived PA(dIV). Intraperitoneal injections with adjuvanted *E. coli* derived PA(dIV), generated highest antibody titers of  $>10^5$ . All the immunized groups demonstrated predominant IgG1 titers over IgG2a indicating a polarized Th2 type response. We also evaluated the mucosal antibody response in orally immunized groups. When fecal extracts were analyzed, low sIgA titer was demonstrated in adjuvanted plant and *E. coli* derived PA(dIV) groups. Further, PA(dIV) antisera enhanced *B. anthracis* spore uptake by macrophages *in vitro* and also demonstrated an anti-germinating effect suggesting a potent role at mucosal surfaces. The antibodies from various groups were efficient in neutralizing the lethal toxin *in vitro*. When mice were challenged with *B. anthracis*, mice immunized with adjuvanted plant PA(dIV) imparted 60% and 40% protection while *E. coli* derived PA(dIV) conferred 100% and 80% protection upon i.p. and oral immunizations. Thus, our study is the first attempt in highlighting the efficacy of plant expressed PA(dIV) by oral immunization in murine model.

© 2011 Elsevier Ltd. All rights reserved.

**Abbreviations:** AP, alkaline phosphatase; AVA, anthrax vaccine adsorbed; BAP, benzyl amino purine; BC, before challenge titers; cfu, colony forming units; CTAB, cetyltrimethyl ammonium bromide; CT, cholera toxin; DMEM, Dulbecco's modified eagle medium; EF, edema factor; ELISA, enzyme linked immunosorbent assay; HRP, horseradish peroxidase; HEPES, *N*-(2-hydroxyethyl) piperazine-*N'*-(2-ethanesulfonic acid); i.p., intraperitoneal; IPTG, isopropyl  $\beta$ -D-1-thiogalactopyranoside; LeTx, lethal toxin; LF, lethal factor; MAP kinase, mitogen activated protein kinase; MTT, 3-(4,5-dimethylthiazol-2-yl)-5-diphenyltetrazolium bromide; MTD, mean time death; MWCO, molecular weight cut-off; NAA,  $\alpha$ -naphthalene acetic acid; NBT, nitroblue tetrazolium; (NTdIV Nu), domain 4 from nuclear transformed plants; PA(dIV), domain IV of protective antigen *B. anthracis*; PAGE, poly acrylamide gel electrophoresis; PBS, phosphate buffered saline; PGA, poly-D-glutamic acid; PMSF, phenyl methyl sulfonyl fluoride; PA, protective antigen; SDS, sodium dodecyl sulphate; SM, selection medium; TSP, total soluble protein; TMB, tetramethylbenzidine; RM, regeneration medium; UTR, untranslated region; WT, wild type.

<sup>☆</sup> Gen Bank accession numbers of data deposited; pET-28a-PA(dIV): HQ130722, pCAM1303PA(dIV): HQ130723, pCHV-RKB: HQ130724, pCHV-RKB-PA(dIV): HQ130725.

\* Corresponding author at: School of Biotechnology, Jawaharlal Nehru University, New Delhi 110067, India, Tel.: +91 11 26704079; fax: +91 11 26717040.

E-mail addresses: [rakbhat01@yahoo.com](mailto:rakbhat01@yahoo.com), [rakeshbhatnagar@mail.jnu.ac.in](mailto:rakeshbhatnagar@mail.jnu.ac.in) (R. Bhatnagar).

<sup>1</sup> Both the authors have contributed equally.

<sup>2</sup> Present address: Dept. of Pop. Med. and Sciences, Veterinary Medical Centre, Cornell University, Ithaca, NY, USA.

0264-410X/\$ – see front matter © 2011 Elsevier Ltd. All rights reserved.  
doi:10.1016/j.vaccine.2011.03.082



**Title:** Exploring the interaction between *Mycobacterium tuberculosis* Enolase and human plasminogen using computational methods and experimental techniques.

### Abstract

Surface localized microbial enolase's binding with human plasminogen has been increasingly proven to have an important role in initial infection cycle of several human pathogens. Similarly, surface localized *Mycobacterium tuberculosis* (*Mtb*) enolase also binds to human plasminogen, and this interaction may entail crucial consequences for granuloma stability. The current study is the first attempt to explore the plasminogen interacting residues of enolase from *Mtb*. Beginning with the structure modeling of *Mtb* enolase, the binding pose of *Mtb* enolase and human plasminogen was also predicted using protein-protein docking simulations. The binding pose revealed the interface region with interacting residues and molecular interactions. Next, the interacting residues were emphasized and ranked by using various criteria. Finally, the selected interacting residues were tested for their involvement in plasminogen binding. The two consecutive lysine residues, Lys-193 and Lys-194, turned out to be active residues for plasminogen binding. These residues when substituted for alanine along with Lys-429, the most active residue i.e., the triple mutant (K193A+K194A+K429A), showed nearly 50 % reduction in plasminogen binding. Interestingly, *Mtb* enolase lost nearly half of the plasminogen binding activity with only three simultaneous substitutions, without significant secondary structure perturbation. Further, the sequence comparison between *Mtb* and human enolases suggests the possibility of selective targeting of the *Mtb* enolase to obstruct binding of human plasminogen. .

### INTRODUCTION

Enolase is a highly conserved metalloprotein and an empirical glycolytic enzyme found in both prokaryotes as well as eukaryotes [1]. Converting 2-phosphoglycerate (2-PGA) to phosphoenolpyruvate (PEP) in a reversible reaction of the glycolysis pathway, enolase plays a crucial role in regulating cell's energy metabolism. However, unlike other housekeeping glycolytic genes, the expression of enolase and its sub-cellular localization has been found to vary during various pathophysiological conditions [2]. This most likely corroborates with the non-glycolytic cellular functions which enolase is frequently associated with. It has been reported that during apoptosis as well as during the incidence of several bacterial and fungal infections, enolase can be found on cell-surface despite lacking a signal peptide [2-3]. In this context, the role of enolase from *Mycobacterium tuberculosis* has recently been elaborated by us as a surface exposed plasminogen binding protein [4].

Plasminogen is a glycoprotein ubiquitously expressed in the body fluids and a vital component of the ECM (extracellular matrix) homeostasis [5-8]. Synthesized in the liver, it is released into the blood circulation as a zymogen. Plasmin, the active form of this pro-enzyme, is a broad specificity serine protease. Upon activation, it initiates a cascade of events including the conversion of pro-collagenase to collagenase. This attribute of plasmin activation is often exploited by pathogens to breach the host-tissue framework and degrade the major components of the surrounding ECM facilitating invasion. The ECM comprises of a chief component of the acellular proteinaceous extracellular architecture holding the cells and tissues in place and is stringently regulated by the plasminogen/plasmin system [8]. Plasmin is capable of degrading a variety of ECM proteins like fibronectin, laminin, and thrombospondin [9]. Apart from this, plasmin also stimulates certain complement mediators and thereby, can engender local inflammation [10]. Additionally, plasmin has also been shown to induce several transcription factors like AP-1 and NfκB in the host cells, thereby resulting in essential cellular responses in the form of cytokine/chemokine production [11-13].

The structure of human plasminogen consists of five kringle domains at its N-terminus and an activator binding domain towards the C-terminus, where kringle domain acts as a receptor to several pathogen associated proteins which can affect plasminogen activation [14-15]. Till date, numerous plasminogen receptor cum activator proteins have been identified [14]. Enolase is part of a big repertoire of such multifunctional proteins. It has been found on the surface of several pathogens, where it interacts with human plasminogen thereby promoting its activation by plasminogen activators like tissue-type plasminogen activator (t-PA) and urokinase-type plasminogen activator (u-PA) to form plasmin which confers a proteolytic phenotype to bacterial cell surface [16].

Plasminogen binding plays an important, if not, indispensable role in the infection cycle of several human pathogens [14, 17]. Enolase has been reported to be essential for *in vivo* virulence and incurrence of a fulminant infection during Leishmaniasis. Inhibition of enolase expressed on the pathogen's cell surface leads to an overall reduction in the invasion efficiency of *Leishmania sp.* and several other bacteria like *S. pneumoniae* [14]. A study of cutaneous lesions caused by *Leishmania mexicana* in plasminogen-deficient mice clearly indicated that the plasminogen interaction is crucial indeed for a successful invasion by the parasite inside the host tissues reciprocating the existence of plasminogen binders on pathogen's surface proteome [18]. This also points

## RESEARCH ARTICLE

# Biochemical characterization of the GTP-sensing protein, CodY of *Bacillus anthracis*

Shikha Joon<sup>1,2,†</sup>, Monisha Gopalani<sup>1,†</sup>, Amit Rahi<sup>1,†</sup>, Parul Kulshreshtha<sup>3,‡</sup>, Himanshu Gogoi<sup>1,‡</sup>, Sonika Bhatnagar<sup>2,\*\*</sup> and Rakesh Bhatnagar<sup>1,\*</sup>

<sup>1</sup>Laboratory of Molecular Biology and Genetic Engineering, School of Biotechnology, Jawaharlal Nehru University, Munirka, New Delhi 110067, India, <sup>2</sup>Structural and Computational Biology Laboratory, Department of Biotechnology, Netaji Subhas Institute of Technology, New Delhi 110078, India and <sup>3</sup>Shivaji College, University of Delhi, New Delhi 110027, India

\*Corresponding author: Laboratory of Molecular Biology and Genetic Engineering, School of Biotechnology, Jawaharlal Nehru University, Munirka, New Delhi-110067, India. Tel: +91-11-26704079; Fax: +91-11-26717040; E-mail: [rakeshbhatnagar@jnu.ac.in](mailto:rakeshbhatnagar@jnu.ac.in)

\*\*Co-corresponding author: Structural and Computational Biology Laboratory, Department of Biotechnology, Netaji Subhas Institute of Technology, Dwarka, New Delhi 110078, India.

†These authors have contributed equally.

‡These authors have contributed equally.

**One sentence summary:** CodY of *Bacillus anthracis* binds to and hydrolyze GTP and autophosphorylates itself at a conserved serine residue.

**Editor:** Ake Forsberg

## ABSTRACT

The pleiotropism of the GTP-sensing transcriptional regulator CodY is evident by the gamut of processes that it regulates in almost all low G+C Gram-positive bacteria, including general metabolism, biosynthesis of some amino acids and transport systems, nitrogen uptake, sporulation, biofilm formation, motility and virulence. The role of CodY in virulence has been established in *Bacillus anthracis*, the top rated bioterrorism agent. In this study, we investigated the biochemical attributes of this global regulator. Homology modeling and sequence/structure analysis revealed putative GTP-binding residues in CodY of *B. anthracis*. CodY exhibited an interaction with the GTP as tested by ultraviolet cross-linking experiments. It could autophosphorylate itself at a conserved Ser<sup>215</sup> residue. This was further corroborated by the impairment of autophosphorylation activity in the CodYS215A mutant. Autophosphorylation may be speculated as an additional mechanism regulating CodY activity in the cell. The protein could also hydrolyze GTP, albeit weakly, as indicated by thin-layer chromatography and spectrophotometric quantification of its kinetic parameters. Altogether, these observations provide us an insight into the mechanism of action of this global regulator and a better understanding of its functional regulation.

**Keywords:** *Bacillus anthracis*; CodY; homology modeling; GTP-binding; autophosphorylation; thin-layer chromatography

## ABBREVIATIONS

CD: Circular dichroism

UV: Ultraviolet

Pi: Inorganic phosphate

Ser: Serine

Ala: Alanine

## INTRODUCTION

*Bacillus anthracis*, a Gram-positive, spore-forming, non-motile, aerobic bacterium, is the causative agent of anthrax, a disease that mainly affects ruminants, with humans being accidental victims (Mock and Fouet 2001; Hudson et al. 2008). The fact that its spores can persist for decades in the environment and that they can be easily weaponized and disseminated as aerosols to large populations make this pathogen the top-rated agent of biological warfare and bioterrorism (Hudson et al. 2008). The major virulence factors of this bacterium include a poly- $\gamma$ -D-glutamic acid capsule and a tripartite toxin, encoded by the plasmids pXO2 and pXO1, respectively, that abets the pathogen in evasion from the host immune system, in the initiation of the infection and in causing lethality during the last stages of the disease (Collier and Young 2003). However, regulation of virulence in *B. anthracis* involves a convoluted network comprising of several factors, Anthrax Toxin Activator (AtxA) located on the plasmid pXO1 being one of them, which plays a cardinal role in regulating the expression of virulence determinants (Dai and Koehler 1997).

CodY is a pleiotropic transcriptional regulator that actuates adaptation in response to the nutritional and energetic status of the cell in many low G+C Gram-positive bacteria. CodY regulates a prodigious array of processes, including catabolism, biosynthesis of some amino acids and transport systems, chemotaxis, motility, genetic competence, biofilm and pellicle formation, and virulence (Ratnayake-Lecamwasam et al. 2001; Tu Quoc et al. 2007; Hsueh, Somers and Wong 2008; Lemos et al. 2008; Majerczyk et al. 2008; Lindback et al. 2012; Gopalani et al. 2016b). CodY senses the intracellular GTP and branched-chain amino acids (BCAAs) levels and brings about appropriate changes in the transcriptome of the cell, thereby regulating a vast number of genes, constituting its regulon. During the exponential phase, both the GTP and BCAAs being plenteous in the cell interact with CodY to enhance its DNA-binding capability, thereby keeping the genes of its regulon repressed. As the cell transits from the exponential to the stationary phase, the level of the effectors goes down, thereby resulting in the abolition of the DNA-binding ability of CodY. Consequently, the genes of its regulon are derepressed (Ratnayake-Lecamwasam et al. 2001; Stenz et al. 2011).

While the binding of CodY to BCAAs is well documented, its binding to GTP is poorly understood. BCAAs binds to the GAF domain within the metabolite-binding domain (MBD) harbored at the N-terminal of the protein. The well-conserved G1, G3 and G4 motifs common to the small GTPases are present in CodY and are speculated to be involved in GTP binding (Ratnayake-Lecamwasam et al. 2001; Handke, Shivers and Sonenshein 2008). However, Han et al. recently reported that in CodY of *Staphylococcus aureus*, the residues critical for GTP binding were located in the MBD and the long helical linker (LHL) connecting the MBD and the DNA-binding domain (DBD) and excluded the GAF domain within the MBD. Therefore, in the structure described by them, GTP was bound to CodY at a site completely different from the above-defined three motifs. (Han et al. 2016). Contradictorily, CodY of *Lactococcus lactis* and *Streptococcus pneumoniae* does not follow the paradigm of binding and responding to GTP (Petranovic et al. 2004; Hendriksen et al. 2008).

CodY regulates about 500 genes either directly or indirectly in *B. anthracis* (Chateau et al. 2013). Its role in the survival strategies of the pathogen like sporulation and pellicle formation has been demonstrated (Gopalani et al. 2016b). Moreover, its disruption in *B. anthracis* leads to complete abolishment of its virulence.

It is anticipated that CodY regulates virulence of the pathogen by promoting the post-translational agglomeration of AtxA, which is required for the expression of toxin components (van Schaik et al. 2009). However, biochemical aspects of CodY of *B. anthracis* such as GTP binding, phosphorylation etc. are yet unmapped and need to be reconnoitered, which this study aims at.

In this study, we carried out the homology modeling of *baCodY* (*B. anthracis* CodY) using *saCodY* (*S. aureus* CodY) as a template. The residues involved in GTP binding in *saCodY* were well conserved in *baCodY*. Mapping of the putative GTP-binding residues and the G1, G3 and G4 motifs on the *baCodY* homology model depicted that these motifs were located spatially far away from the GTP-binding residues that were inferred from *saCodY*. Next, we investigated the biochemical attributes of this physiologically important protein of the pathogen. We demonstrate that CodY of *B. anthracis* can bind to GTP and hydrolyze it. CodY exhibits autophosphorylation activity. Ser<sup>215</sup> was identified as the critical residue undergoing phosphorylation. Thus, this is the first study that provides insights into the biochemical attributes of CodY in *B. anthracis*.

## MATERIALS AND METHODS

### Bacterial strains and chemicals

*Escherichia coli* DH5 $\alpha$  and BL21 ( $\lambda$ DE3) strains were used as the cloning and expression hosts, respectively. The strains were cultured in Luria-Bertani (LB) medium, supplemented with appropriate antibiotics wherever needed (Kanamycin (50 mg/ml)). The genomic DNA was isolated from an avirulent *Bacillus anthracis* Sterne 34F2 strain (pXO1<sup>+</sup> pXO2<sup>-</sup>). Expression vector pET29a+ from Novagen (Madison, WI, USA) was used for heterologous gene expression. The routine biochemical reagents were purchased from Sigma-Aldrich (St. Louis, MO, USA) and Merck (Darmstadt, Germany). Ni<sup>2+</sup>-NTA agarose resin was purchased from Qiagen (Hilden, Germany). The restriction enzymes and DNA polymerases were from New England Biolabs Inc. (Ipswich, MA, USA). All the antibodies and oligonucleotides used in this study were procured from Sigma-Aldrich (St. Louis). [ $\gamma$ -<sup>32</sup>P]-GTP and [ $\alpha$ -<sup>32</sup>P]-GTP were purchased from BRIT (Hyderabad, India).

### Sequence analysis of *cody* from *Bacillus anthracis*

*cody* gene was identified in the *B. anthracis* genome using the KEGG database (Kanehisa et al. 2014). The corresponding protein sequence was used to identify homologs in other species by BLASTP. ClustalW was used to align CodY of *B. anthracis* with its homologs from other low G+C Gram-positive bacteria (Larkin et al. 2007). The domain information was mapped using the CDD search at NCBI (Marchler-Bauer and Bryant 2004). While the G1 motif was identified from the literature (Ratnayake-Lecamwasam et al. 2001), the G3 and G4 motifs were deduced by manual inspection of the alignment (Bourne, Sanders and McCormick 1991). A suitable template for homology modeling was identified using BLASTP search of PDB with the *baCodY* (*B. anthracis* CodY) sequence as query. Homology model of *baCodY* was built using Swiss-Model (<http://swissmodel.expasy.org>) with available *saCodY* (*Staphylococcus aureus* CodY) structure (5EY1.pdb) as a template. GTP was modeled by the superposition of GTP-bound CodY structure from *S. aureus*. The final model was validated by Swiss-Model validation suite (Biasini et al. 2014).

## Cloning of *cody* in pET29a + vector and site-directed mutagenesis

The ORF corresponding to *cody* gene was PCR amplified using gene specific primers (Table S1, Supporting Information) from the genomic DNA of *B. anthracis* Sterne strain followed by double digestion and ligation into *KpnI* and *Sall* sites of pET29a+ vector to obtain pET29-*cody* construct. Using pET29-*cody* as the template and specific primers, PCR-based site-directed mutagenesis was carried out to generate *CodYS215A* mutant (Ser<sup>215</sup>-Ala<sup>215</sup>). The resulting base substitution was confirmed by automated dideoxy DNA sequencing.

## Expression and purification of *CodY* and *CodYS215A* mutant

Both the recombinant proteins were expressed and purified as N-terminal 6x-His-tagged proteins. Both the constructs were transformed into *E. coli* BL21 ( $\lambda$ DE3) cells, grown up to mid-exponential phase (OD ~ 0.6), induced with 1 mM IPTG at 37°C and harvested 6 h after induction. The proteins were purified to near homogeneity from the soluble fraction using Ni<sup>2+</sup>-NTA affinity chromatography (Qiagen). The identity of both the proteins was confirmed by immunoblotting using anti-histidine monoclonal antibody. While the concentration of the proteins was estimated by Bradford reagent (Bio-Rad), the purity of the proteins was confirmed by silver staining of the SDS-PAGE (Chevallet, Luche and Rabilloud 2006). Native-PAGE followed by immunoblotting using anti-*CodY* antisera raised in Swiss-albino mice was used to check the oligomeric status of the protein (Laemmli 1970).

## Ethics statement

All mice experiments were carried out as approved by Institutional Animal Ethics Committee, Jawaharlal Nehru University, New Delhi. Mice were maintained and housed in individually ventilated animal caging system in the animal house facility of Jawaharlal Nehru University, Delhi, India.

## Circular dichroism spectroscopy

In order to nullify the presence of any structural differences induced by site-directed mutagenesis, circular dichroism (CD) spectrum of His<sub>6</sub>-*CodYS215A* was recorded and compared with the wild-type protein i.e. His<sub>6</sub>-*CodY*. The spectra were measured between 200 and 260 nm on a J-815 CD spectrophotometer (Jasco Corp.) at 25°C under nitrogen flow with a bandwidth of 1nm, scan step 0.5 nm at a scanning speed of 50 nm per min. The optical path length of the quartz cell was 1 mm. The CD spectrum was expressed in terms of the mean residual ellipticity (Fort and Spray 2009).

## Ultraviolet-mediated GTP cross-linking assay

Cross-linking of GTP to His<sub>6</sub>-*CodY* was assessed as described previously (Ratnayake-Lecamwasam et al. 2001). Briefly, 1  $\mu$ g of His<sub>6</sub>-*CodY* was incubated with 15 nM [ $\alpha$ -<sup>32</sup>P]-GTP in 25  $\mu$ l of reaction buffer (50 mM Tris-HCl, pH 8.0 and 400 mM KCl). The samples were incubated for 30 min on ice followed by ultraviolet (UV) irradiation for different time periods. The reaction was terminated by the addition of 5  $\mu$ l of 2 X SDS-loading dye. The reaction mixtures were electrophoresed on a 12% SDS-PAGE followed by

drying the gels under vacuum at 70°C for 60–90 min and visualization and analysis of the radiolabeled bands on a Typhoon FLA 9500 phosphorimager. Unlabeled nucleotides were also included as competitors in an independent assay to check the specificity of cross-linking of GTP with *CodY*. BAS0540, a response regulator (RR) of *B. anthracis* incubated with [ $\alpha$ -<sup>32</sup>P]-GTP under conditions similar to that for *CodY* served as the negative control. *CodY* incubated with [ $\alpha$ -<sup>32</sup>P]-GTP but not subjected to UV exposure was also used.

## Autophosphorylation of *CodY* and *CodYS215A*

Autophosphorylation of *CodY* was analyzed by incubating 1  $\mu$ g of His<sub>6</sub>-*CodY* or His<sub>6</sub>-*CodYS215A* with 15 nM of [ $\gamma$ -<sup>32</sup>P]-GTP (3500 Ci/mmol) in 20  $\mu$ l of phosphorylation buffer [75 nM cold GTP; 50 mM Tris-HCl, pH 8.0 and 5 mM MgCl<sub>2</sub>] at 37°C for 0, 15, 30 and 60 min. The reactions were quenched by the addition of 10 mM EDTA and 5  $\mu$ l of 2X SDS-loading dye followed by subjecting the samples to a 12% SDS-PAGE and visualization by autoradiography. We also tested the autophosphorylation of His<sub>6</sub>-*CodY* in the presence of [ $\gamma$ -<sup>32</sup>P]-ATP under reaction conditions as described above.

## Chemical stability assay of the phosphor linkage

In an independent assay, *CodY* was phosphorylated as described above. The gel was then sliced into three parts such that each slice contained one radioactive *CodY* band. One slice was kept as a control; the second slice was incubated at 65°C for 2 h in 6 M HCl and the third was incubated at 65°C for 2 h in 1 M NaOH prior to visualization on a phosphorimager screen (Klumpp and Kriegstein 2002).

## GTPase assay

The GTP hydrolyzing activity of *CodY* was tested by thin-layer chromatography as described by Hwang and Inouye (2001) with some modifications. Briefly, 1  $\mu$ g of purified *CodY* was incubated with 15 nM of [ $\gamma$ -<sup>32</sup>P]-GTP in 50  $\mu$ l of buffer (Tris-HCl, pH 8.0; 400 mM KCl; 5 mM MgCl<sub>2</sub>; 1 mM DTT) at 37°C for 0, 10, 20, 30, 45 and 60 min. The reaction was terminated by the addition of 10  $\mu$ l of ice-cold 0.5 M EDTA. Two microliters of each reaction was then spotted immediately on to a PEI-cellulose TLC plate (Merck, Darmstadt, Germany) followed by separation using 0.75 mM KH<sub>2</sub>PO<sub>4</sub>, pH 3.65 as resolving buffer. In order to enhance the stringency of the assay, BSA, only buffer and protein fraction obtained from a mock *CodY* purification, i.e. from cells that do not express *CodY* were used as negative controls and incubated with [ $\gamma$ -<sup>32</sup>P]-GTP under conditions similar to that for *CodY*. For the mock protein/only vector control (only vector and mock protein can be used synonymously), a soluble extract from *E. coli* BL21 ( $\lambda$  DE3) cells harboring pET29a+ vector was prepared which was chromatographed in parallel with the soluble extract of cells harboring pET29-*cody* construct. The spots corresponding to the released inorganic phosphate were identified using phosphorimager.

## Determination of enzyme kinetic parameters for *CodY* by coupled-enzymatic assay

The kinetic parameters of His<sub>6</sub>-*CodY* were measured by coupling its reaction to pyruvate kinase (PYK) and lactate dehydrogenase (LDH) and monitoring the decrease in absorbance



at 340 nm due to conversion of NADH (extinction coefficient  $\epsilon = 6222 \text{ M}^{-1} \text{ cm}^{-1}$ ) to NAD in a spectrophotometric assay on Cecil CE 7500. The assay was performed at 25°C in a total reaction volume of 1 ml. The reaction mixture contained 2  $\mu\text{g}$  of His<sub>6</sub>-CodY, 20 mM Tris-HCl (pH 8.0), 5 mM MgCl<sub>2</sub>, 100 mM KCl, 8 mM DTT, 2 mM PEP, 0.2 mM NADH, 1 U/ml PYK and 1.4 U/ml LDH and a varying concentration of the substrate i.e. GTP ranging from 10 to 200  $\mu\text{M}$ . The Michaelis constant and other kinetic parameters were calculated from the Michaelis-Menten plot. All experimental data resulted from at least three independent estimations.

## RESULTS AND DISCUSSION

### Multiple sequence alignment and homology modeling of *Bacillus anthracis* CodY

Homology comparison of *ba*CodY with that of other Gram-positive bacteria revealed the presence of conserved GTP-binding motifs namely G1, G3 and G4, respectively, common to small GTPases (Fig. 1A). While the G1 motif lies in the N-terminal GAF (cGMP-specific phosphodiesterases, Adenylyl cyclases and FhlA) domain, the G3 and G4 motifs are positioned within the C-terminal helix-turn-helix (HTH) DBD of the protein

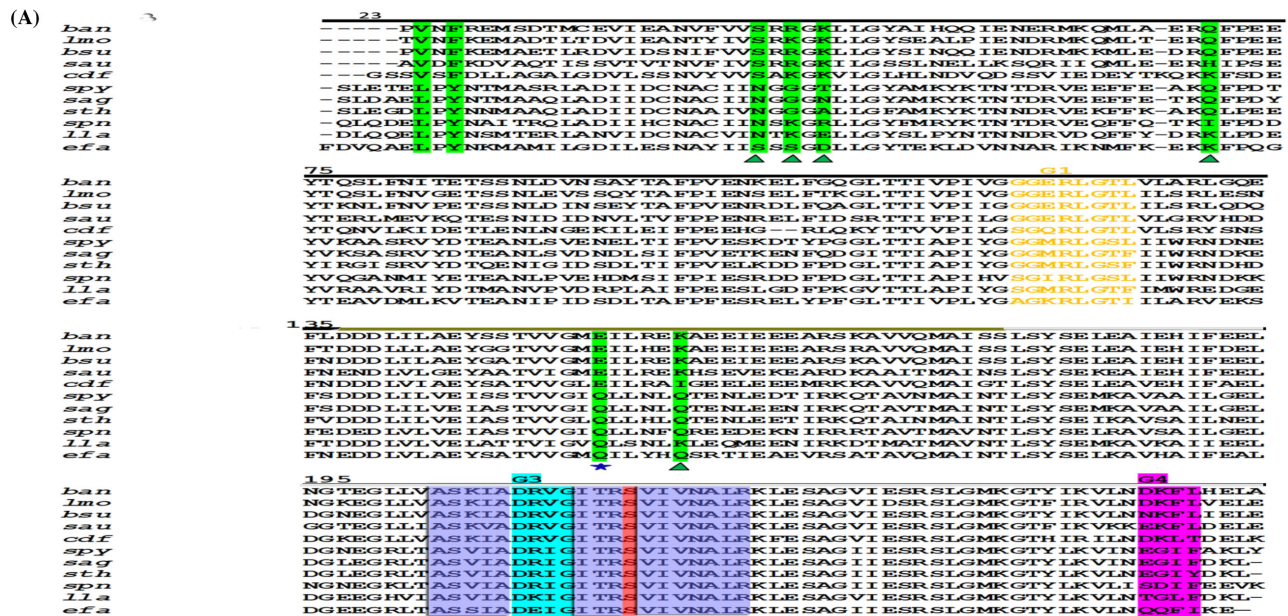


**Figure 1.** Sequence/structure analysis of *B. anthracis* CodY. (A) Sequence features mapped onto a multiple sequence alignment of *ba*CodY with its homologs from other Gram-positive bacteria. The metabolite-binding domain (MBD; 1–136), long helical linker (LHL; 137–178) and DNA-binding domain (DBD; 179–255) are spanned by black, olive and gray lines, respectively. The well-conserved G1, G3 and G4 motifs are shown in orange (G1), cyan (G3) and magenta (G4), respectively. The putative residues that are involved in GTP binding (inferred from homology modeling) are highlighted in green. The residues marked with green triangles and a blue star represents those involved in forming the P-pocket and G-pocket, respectively (defined in the citation). The residues highlighted in violet correspond to the HTH motif. The HTH region spans the G3 motif (cyan highlighted residues) and harbors the Ser<sup>215</sup> (red highlighted) residue. Organisms with NCBI-protein IDs in the bracket are as follows: *Ban*: *Bacillus anthracis* (YP\_02\_9930); *Lmo*: *Listeria monocytogenes* (NP\_464\_805); *Bsu*: *Bacillus subtilis* (NP\_389\_499); *Sau*: *Staphylococcus aureus* (EEOV03904); *Cdf*: *Clostridium difficile* (YP\_010\_87769); *Spy*: *Streptococcus pyogenes* (NP\_269\_792); *Sag*: *Streptococcus agalactiae* (NP\_688\_666); *Sth*: *Streptococcus thermophilus* (KEGG ID-T303.0\_9005); *Spn*: *Streptococcus pneumoniae* (AAK75670); *Lla*: *Lactococcus lactis* (NP\_266\_317); *Efa*: *Enterococcus faecalis* (NP\_815\_353). (B) Cartoon rendering of the homology model of *ba*CodY. *sa*CodY was used as the template. The G1 motif in MBD is shown in orange, while the G3 and G4 motifs in the DBD are shown in cyan and magenta, respectively. The GTP-binding pocket residues are shown as green sticks in the MBD and a single residue (E153) residing in the LHL as blue ribbon. The bound GTP is shown as light pink spheres. The HTH motif in the DBD (violet) encompasses the G3 motif and Ser<sup>215</sup> (red). The figure was prepared using Pymol (Delano Scientific).

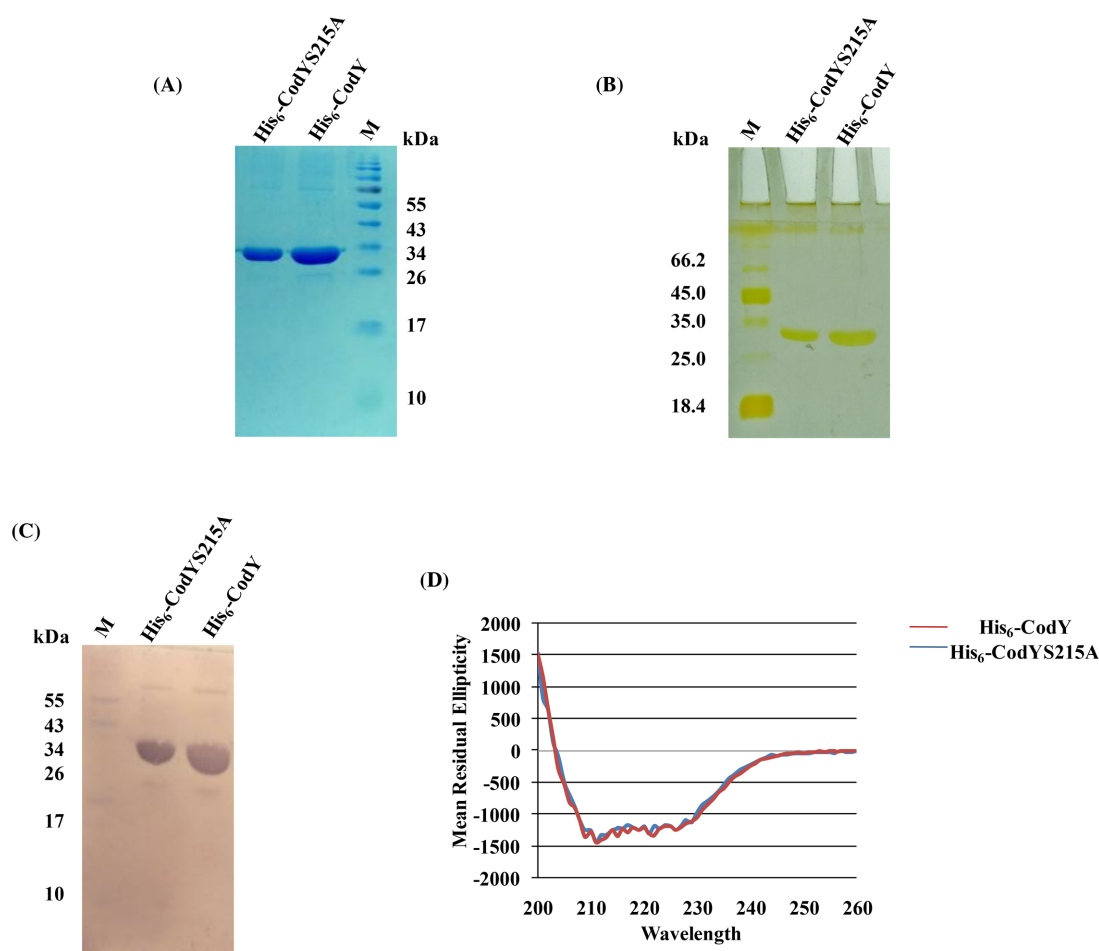


**Figure 2.** Expression and purification of CodY and CodYS215A and CD spectroscopy. (A) SDS-PAGE of purified His<sub>6</sub>-CodY and His<sub>6</sub>-CodYS215A. (B) Silver staining of SDS-PAGE depicting purified His<sub>6</sub>-CodY and His<sub>6</sub>-CodYS215A proteins. The proteins were >97% pure. (C) Immunoblotting of the purified proteins using anti-histidine antibody. (D) Superimposition of the CD spectrum of His<sub>6</sub>-CodY and His<sub>6</sub>-CodYS215A. While the X-axis indicates wavelength (nm), the Y-axis is mean residual ellipticity. M, molecular weight markers in kDa.

(Ratnayake-Lecamwasam et al. 2001). Although it has for long been speculated that these motifs are implicated in GTP binding, a recent study on CodY of *Staphylococcus aureus* described CodY in its GTP-bound state wherein the GTP was found to be positioned in an entirely different site which certainly does not overlap with the above-defined motifs (Han et al. 2016).

Homology modeling of *baCodY* was done using *saCodY* as a template in order to get an insight into the putative GTP-binding residues of *baCodY*. The BLASTP search of PDB revealed a high similarity of 80% between *baCodY* and *saCodY*. The query coverage and E-value of the alignment were 99% and  $7e^{-115}$ , respectively. The *baCodY* model so generated had a Q-mean score of 0.76. 96.6% of the residues were in the core region, 3.4% were in the allowed and none were in the disallowed region (Fig. 1B). The superimposition of the *baCodY* model with *saCodY* template structure had a root-mean-square deviation of 0.27Å over 238 C $\alpha$  atoms (Fig. S1, Supporting Information) and did not have any bad contacts. Altogether there were eight residues in the *saCodY* crystal structure that were involved in interaction with GTP. Six out of these eight residues (namely V22, F24 S43, R45, K47 and Q70) were present in the MBD, whereas two residues E153 and K158 were harbored in the LHL. While the residues S43, R45, K47, Q70 and K158 form the P-pocket (phosphate-binding site), the residue E153 forms the G-pocket (guanine base binding site) of

the GTP-binding site (Han et al. 2016). As evident from our homology modeling results, all the above-mentioned residues are well conserved in *baCodY* as well. Moreover, just like in *saCodY*, the G1, G3 and the G4 motifs were found to be located far from the GTP-binding pocket in *baCodY* also. However, these *in silico* predictions are just preliminary leads and in order to validate them and point out the critical residues precisely a comprehensive *in vitro* analysis is required. Figure 1A and B shows the alignment and the *baCodY* model, respectively, with the G1, G3 and G4 motifs and the structurally equivalent residues from the GTP-binding pocket of *saCodY* mapped onto them.

### Cloning, expression and purification of CodY and CodYS215A mutant

The ORF corresponding to *cody* was cloned in the expression vector pET29a+ such that a 6x His-tag was added to the N-terminus of the recombinant protein. Both the CodY and CodYS215A were readily expressed in BL21 ( $\lambda$ DE3) cells and purified from the soluble fraction. The proteins were analyzed on a 12% SDS-PAGE and migrated at their expected molecular weight of ~31 kDa (Fig. 2A). Their identity was confirmed by immunoblotting using anti-histidine monoclonal antibody (Fig. 2C). Proteins

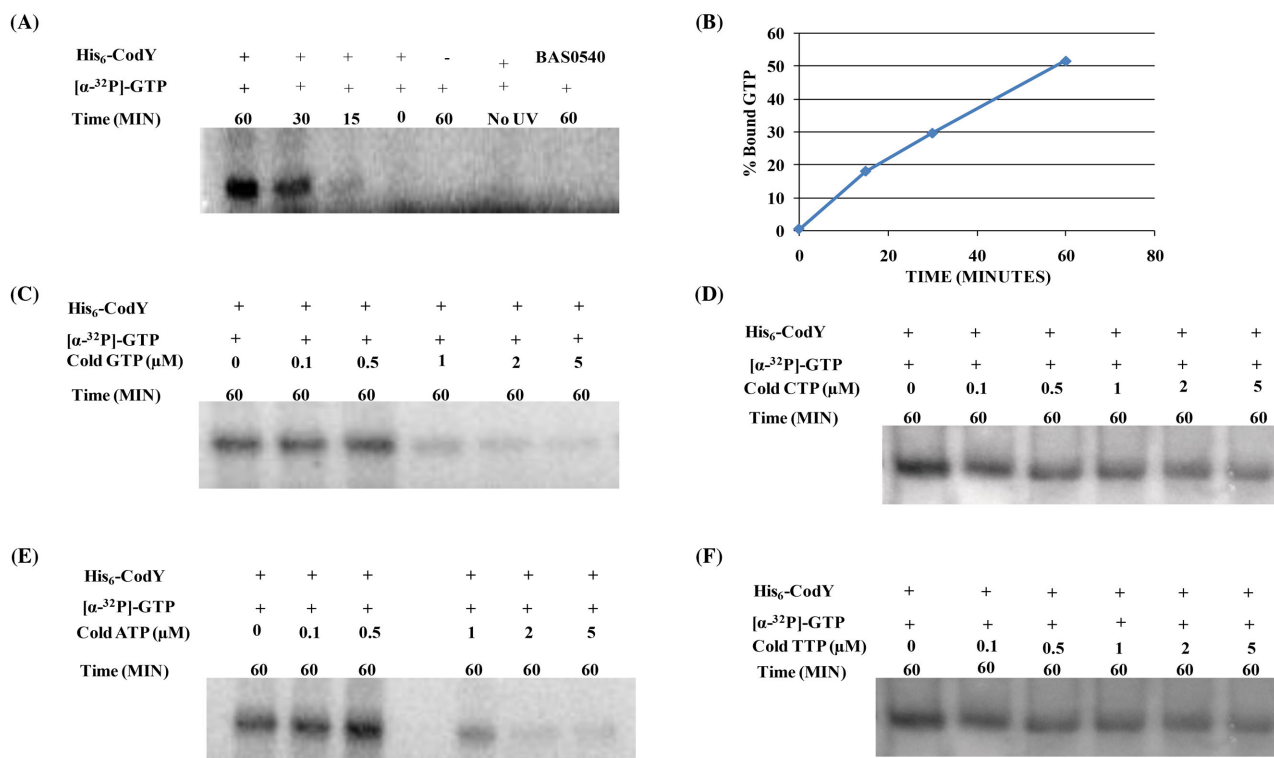


**Figure 3.** UV cross-linking assay for His<sub>6</sub>-CodY. (A) Purified CodY was incubated with [ $\alpha$ -<sup>32</sup>P]-GTP followed by UV-mediated cross-linking. BAS0540, an RR of *B. anthracis*, was used as a negative control. It did not show any cross-linking to GTP even on a UV exposure of 60 min. CodY incubated with [ $\alpha$ -<sup>32</sup>P]-GTP but not exposed to UV also served as a negative control. (B) ImageJ 1.45S software was used for the intensity analysis. Intensity units (% bound GTP) are plotted against time in minutes. (C-F) Competition in the presence of unlabeled nucleotides namely GTP, CTP, ATP and TTP. Only protein and no protein controls were used wherever needed. The reaction samples were resolved on a 12% SDS-PAGE and visualized by autoradiography.

were more than 97% pure as indicated by the silver staining (Chevallet, Luche and Rabilloud 2006) (Fig. 2B). Recombinant protein existed in the form of both monomeric and dimeric species as indicated by native-PAGE and immunoblotting (Fig. S2A and B, Supporting Information).

### CD spectroscopy of the recombinant proteins

CD spectroscopy was used to investigate the occurrence of, if any, differences in the secondary structure of wild-type His<sub>6</sub>-CodY and its mutant His<sub>6</sub>-CodYS215A. The CD spectrum of His<sub>6</sub>-CodY exhibits the typical characteristics of a well-folded protein, i.e. the maximum at 200 nm and a minimum at 208 nm (Greenfield 2006). In particular, the spectrum indicates the existence of a high  $\alpha$ -helix content, as marked by the two negative peaks at  $\sim$ 208 nm and  $\sim$ 222 nm, and a positive peak at  $\sim$ 200 nm (Fort and Spray 2009). The superimposition of the spectra obtained for His<sub>6</sub>-CodY and His<sub>6</sub>-CodYS215A demonstrates that there exists no gross alteration between the secondary structures of the two proteins (Fig. 2D).

### CodY of *Bacillus anthracis* binds to and hydrolyzes GTP

The GTP-binding capability of CodY was assayed using [ $\alpha$ -<sup>32</sup>P]-GTP and UV cross-linking. The radiolabeled GTP was cross-linked to the purified His<sub>6</sub>-CodY in the presence of UV radiation as indicated by the radiolabeled protein bands observed after autoradiography of the gel. Binding of GTP to His<sub>6</sub>-CodY could be observed as early as 5 min post UV irradiation, which further increased, reaching a maximum at 60 min (Fig. 3A). Furthermore,

the binding was inhibited by the addition of unlabeled GTP but not with CTP and TTP (Fig. 3C, D and F). Moreover, ATP also exhibited an inhibitory effect on the GTP binding of CodY, albeit to a very less extent (Fig. 3E). Thus, CodY displays specificity for purine nucleotides, an observation that corroborates with that for the CodY of *B. subtilis* (Joseph, Ratnayake-Lecamwasam and Sonenshein 2005). BAS0540 served as the negative control in our cross-linking assay. BAS0540 is a quintessential RR of *B. anthracis* that can accept phosphate from its cognate histidine kinase, BAS0541 and high energy small molecule phosphoryl donors (Gopalani et al. 2016a). RRs do not bind to ATP/GTP. The same is evident from our UV cross-linking assay since the negative control (BAS0540) did not cross-link to GTP even on a UV exposure of 60 min (Fig. 3A, lane 7). No cross-linking was observed in the samples that contained CodY and [ $\alpha$ -<sup>32</sup>P]-GTP but were not subjected to UV exposure (Fig. 3A, lane 6).

It was in our interest to test if CodY can also hydrolyze GTP for which His<sub>6</sub>-CodY was incubated with [ $\gamma$ -<sup>32</sup>P]-GTP and the <sup>32</sup>Pi (inorganic phosphate) release was monitored at different time points. CodY could hydrolyze GTP and the <sup>32</sup>Pi release increased between 0 and 60 min (Fig. 4A, left panel). Mg<sup>2+</sup> ions were found to be essential for this hydrolysis (Fig. 4A, lane 7). Moreover, <sup>32</sup>Pi release was inhibited by the addition of unlabeled GTP indicative of a competition between the labeled and the unlabeled GTP and specificity of the hydrolysis reaction (data not shown). The negative controls, i.e. BSA, mock protein and only buffer, did not show any significant <sup>32</sup>Pi release. It can thus be inferred that the low GTPase activity observed was indeed due to CodY (Fig. 4A, right panel). Since the <sup>32</sup>Pi release due to CodY-mediated GTP hydrolysis was not very high and because of the fact that the



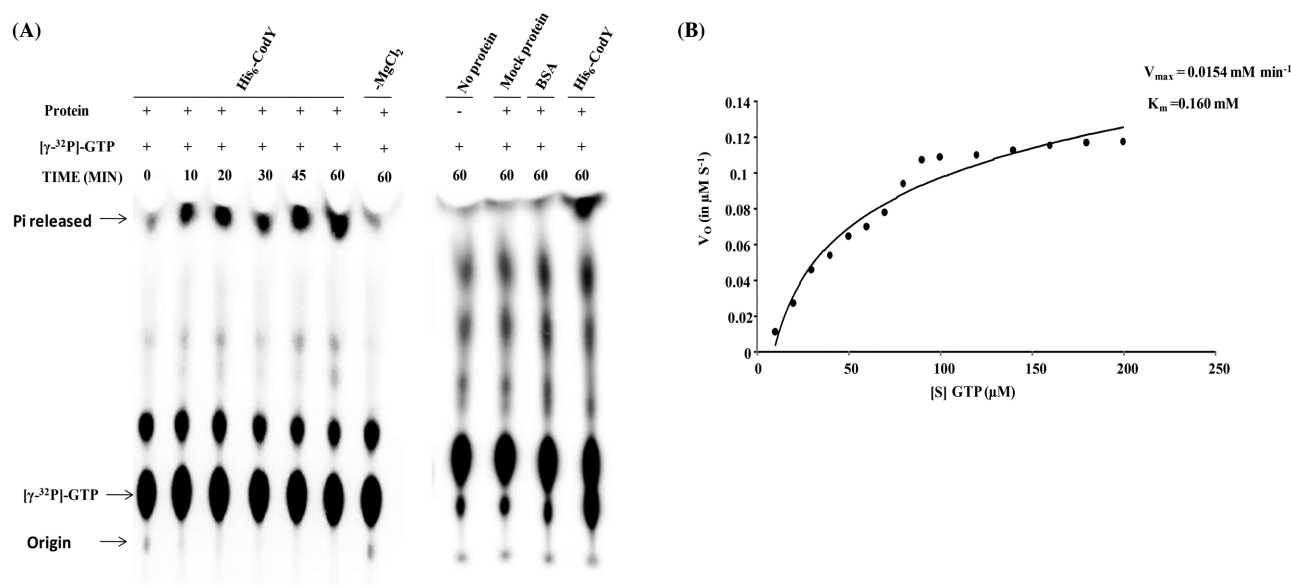


**Figure 4.** GTPase activity of His<sub>6</sub>-CodY. **(A)** Purified CodY was incubated with [γ-<sup>32</sup>P]-GTP for different time periods (left panel). BSA, only buffer and protein fraction obtained from a mock CodY purification, i.e. from cells that do not express CodY (mock protein/only vector control) were used as negative controls (right panel). **(B)** Spectrophotometric quantification of the GTPase activity of His<sub>6</sub>-CodY. Michaelis-Menten plot. The points represent mean ± SD from three independent experiments performed in triplicates.

TLC plates are generally overloaded with the radioactive sample ([γ-<sup>32</sup>P]-GTP being in its first half-life), the decrease in the GTP does not correspond with the increase in the <sup>32</sup>Pi release (Fig. 4A) (Sekiguchi et al. 2001; Mattoo et al. 2008; Pungaliya et al. 2010; Sengottaiyan et al. 2012).

Next, we also measured the kinetic parameters for this hydrolysis reaction.  $K_m$  and  $V_{max}$  were calculated from the Michaelis-Menten plot which was 0.16 mM and 0.0154 mM min<sup>-1</sup>, respectively (Fig. 4B). As mentioned earlier, the binding of GTP to CodY is still poorly understood and the G1, G3 and G4 motifs have been for long conjectured to effectuate this binding. The G1 motif was previously reported in the CodY of *B. anthracis*, the other two motifs were identified in this study by sequence alignment (Fig. 1A). The homology modeling of *ba*CodY done using *sa*CodY as a template revealed that the residues involved in GTP binding in *sa*CodY were well conserved in *ba*CodY and that they were spatially far away from the three motifs (Fig. 1B). However, the GTP-binding site in the crystal structure of *sa*CodY was not associated with hydrolysis (Han et al. 2016), an observation different from the one drawn by us for *ba*CodY, which could hydrolyze GTP, albeit weakly. Therefore, though the residues of *sa*CodY involved in GTP binding are well conserved in *ba*CodY, we speculate that the site for GTP hydrolysis might be different. Thus, we conclude that CodY of *B. anthracis* follows the paradigm of GTP-sensing, binding, and responding, howbeit, our *in silico* predictions based on homology modeling assuredly needs an *in vitro* validation in order to point out the critical residues with high precision.

### CodY autophosphorylates at a conserved serine residue

GTP-binding proteins often manifest autophosphorylation activity. In our attempts to study the GTP-binding ability of CodY, we observed that it could use the γ phosphoryl group of GTP to phosphorylate itself. Phosphorylation was assayed by incubating purified 31 kDa His<sub>6</sub>-CodY with radioactive [γ-<sup>32</sup>P]-GTP and could be detected as early as 5 min post radiolabeled GTP ad-

dition which further increased reaching a maximum at 60 min (Fig. 5A). Furthermore, we found that Mg<sup>+2</sup> ions were indispensable for the phosphorylation reaction. The above reaction could be essentially marked as an autophosphorylation reaction since no other protein species were present in the reaction mixture. Moreover, CodY could also use the γ phosphoryl group of ATP to phosphorylate itself however to a lesser extent as evidenced by a low-intensity band in Fig. 5E.

CodY was identified as a phosphoprotein in *B. subtilis* by Macek et al. (2007) where they identified Ser<sup>215</sup> as the residue undergoing phosphorylation. In order to decipher the nature of amino acid residue undergoing phosphorylation in our study, phosphorylated CodY was subjected to treatment with HCl and NaOH, respectively. We observed that the phosphorylated species were acid stable and base labile, a feature common to phosphoserine and phosphothreonine residues (Fig. 5C) (Klumpp and Krieglstein 2002). The Ser<sup>215</sup> residue is conserved in CodY of *B. anthracis* as well, indicated by the multiple sequence alignment of CodY sequences from Gram-positive bacteria using ClustalW (Fig. 1A). Our results indicate that the point mutation of this Ser<sup>215</sup> to alanine completely abolish the autophosphorylation activity of CodY, connoting it to be a critical residue for phosphorylation (Fig. 5D).

In an earlier study, Joseph et al. identified the critical residues in the HTH motif of CodY of *B. subtilis* which were involved in the DNA binding. They demonstrated that substituting Ser<sup>215</sup> by alanine resulted in a significant decrease in the DNA-binding activity of CodY, which was measured in terms of its repressor activity at the two promoters *dpp* and *ilvB*. This HTH motif is well conserved in the CodY homologs. Moreover, in terms of the sequence, the HTH motif of *B. anthracis* is identical to the HTH motif of *B. subtilis* (Joseph, Ratnayake-Lecamwasam and Sonenshein 2005). Therefore, it can be conjectured that Ser<sup>215</sup> might be critical for DNA binding in CodY of *B. anthracis* as well. The conventional notion of the regulation of CodY activity in the cell is via the intracellular allosteric regulators GTP and BCAAs sensing (Stenz et al. 2011). Combining our observation of autophospho-



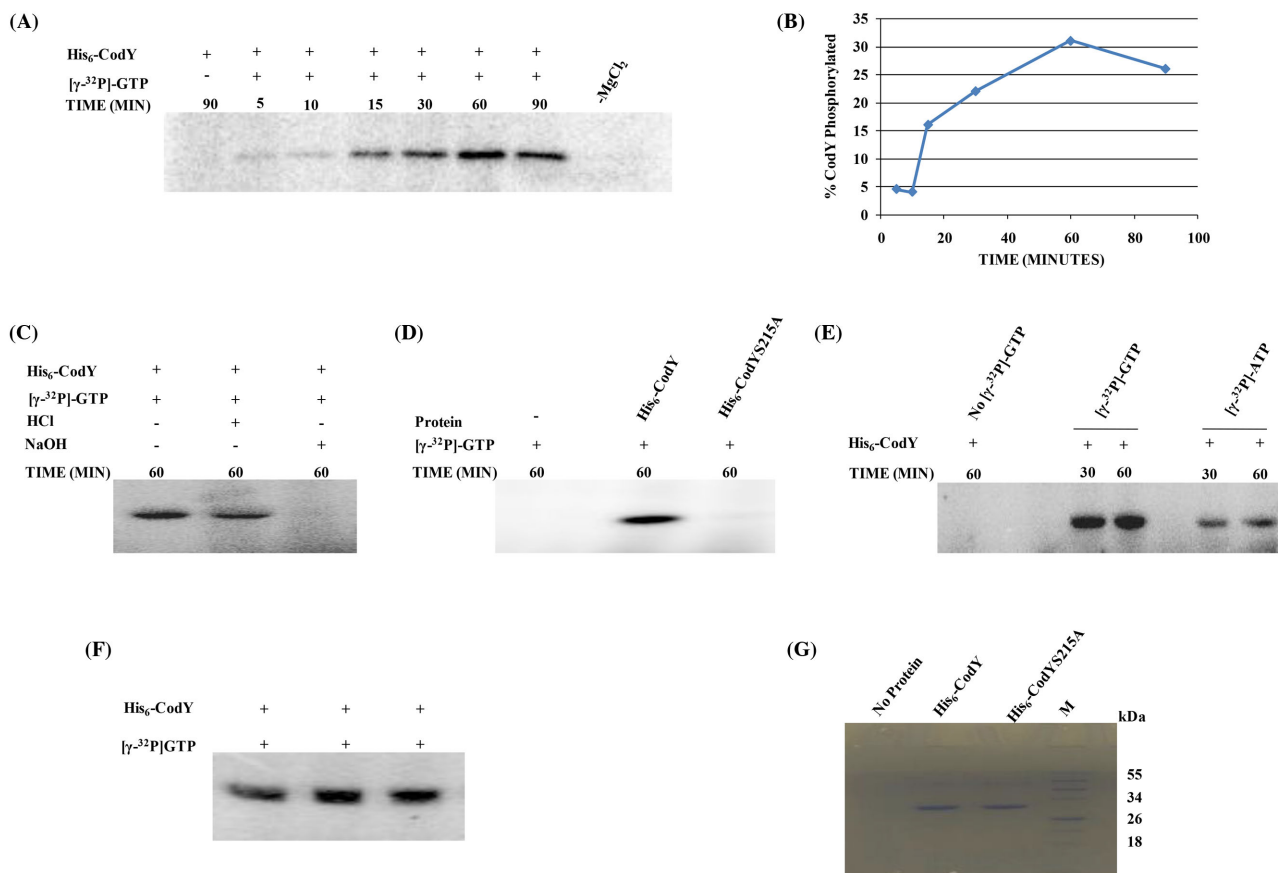


**Figure 5.** Autophosphorylation of His<sub>6</sub>-CodY and His<sub>6</sub>-CodYS215A. (A) Autophosphorylation of His<sub>6</sub>-CodY was observed in the presence of [ $\gamma$ -<sup>32</sup>P]-GTP, which exhibited a time-dependent increase. Reaction mixtures lacking [ $\gamma$ -<sup>32</sup>P]-GTP in the buffer (lane 1) and in the absence of MgCl<sub>2</sub> (lane 8) were taken as negative controls. (B) ImageJ 1.45S software was used for intensity analysis. Intensity units (% CodY phosphorylated) are plotted against time in minutes. (C) Acid-base stability of the phosphorylated His<sub>6</sub>-CodY. (D) Comparison of autophosphorylation activity of His<sub>6</sub>-CodY and His<sub>6</sub>-CodYS215A. His<sub>6</sub>-CodYS215A could not exhibit autophosphorylation. (E) Autophosphorylation of His<sub>6</sub>-CodY in the presence of [ $\gamma$ -<sup>32</sup>P]-ATP was also tested. (F) Replica phosphor image showing the equal loading of protein for testing acid-base stability. (G) Replica coomassie image showing the equal loading of proteins for comparing the autophosphorylation activity of His<sub>6</sub>-CodY and His<sub>6</sub>-CodYS215A. 12% SDS-PAGE followed by autoradiography was used to analyze and visualize the reaction samples. Only protein and only buffer controls were put wherever needed.

rylation of CodY at Ser<sup>215</sup> with that of the critical role of Ser<sup>215</sup> in DNA binding, we anticipate that autophosphorylation of Ser<sup>215</sup> residue could be yet another mode of regulation of CodY activity in the cell. However, an augmented insight into this mode of regulation of CodY activity can be gained by investigating the effect of autophosphorylation of Ser<sup>215</sup> residue on the DNA-binding capability of CodY by electrophoretic mobility shift assays which is part of our next study.

## SUPPLEMENTARY DATA

Supplementary data are available at [FEMSPD](http://FEMSPD) online.

## ACKNOWLEDGMENTS

While Shikha Joon is a recipient of Senior Research Fellowship from ICMR, Government of India, Monisha Gopalani is a recipient of Senior Research Fellowship from CSIR, Government of India. AIRF, JNU is acknowledged for the technical help in conducting CD-spectroscopy experiments.

## FUNDING

While Ms Shikha Joon is a recipient of Senior Research Fellowship from Indian Council of Medical Research (ICMR), Government of India, Ms Monisha Gopalani is a recipient of Senior Research Fellowship from Council of Scientific and Industrial Research (CSIR), Government of India. The funding agency has no role in study design or data analysis and interpretation.

**Conflict of interest.** None declared.

## REFERENCES

- Biasini M, Bienert S, Waterhouse A et al. SWISS-MODEL: modelling protein tertiary and quaternary structure using evolutionary information. *Nucleic Acids Res* 2014;**42**:W252–8.
- Bourne HR, Sanders DA, McCormick F. The GTPase superfamily: conserved structure and molecular mechanism. *Nature* 1991;**349**:117–27.
- Chateau A, van Schaik W, Joseph P et al. Identification of CodY targets in *Bacillus anthracis* by genome-wide in vitro binding analysis. *J Bacteriol* 2013;**195**:1204–13.

- Chevallet M, Luche S, Rabilloud T. Silver staining of proteins in polyacrylamide gels. *Nat Protoc* 2006;1:1852–8.
- Collier RJ, Young JA. Anthrax toxin. *Annu Rev Cell Dev Bi* 2003;19:45–70.
- Dai Z, Koehler TM. Regulation of anthrax toxin activator gene (*atxA*) expression in *Bacillus anthracis*: temperature, not CO<sub>2</sub>/bicarbonate, affects *AtxA* synthesis. *Infect Immun* 1997;65:2576–82.
- Fort AG, Spray DC. Trifluoroethanol reveals helical propensity at analogous positions in cytoplasmic domains of three connexins. *Biopolymers* 2009;92:173–82.
- Gopalani M, Dhiman A, Rahi A et al. Identification, functional characterization and regulon prediction of a novel two component system comprising BAS0540-BAS0541 of *Bacillus anthracis*. *PLoS One* 2016a;11:e0158895.
- Gopalani M, Dhiman A, Rahi A et al. Overexpression of the pleiotropic regulator *CodY* decreases sporulation, attachment and pellicle formation in *Bacillus anthracis*. *Biochem Bioph Res Co* 2016b;469:672–8.
- Greenfield NJ. Using circular dichroism spectra to estimate protein secondary structure. *Nat Protoc* 2006;1:2876–90.
- Han AR, Kang HR, Son J et al. The structure of the pleiotropic transcription regulator *CodY* provides insight into its GTP-sensing mechanism. *Nucleic Acids Res* 2016;44:9483–93.
- Handke LD, Shivers RP, Sonenshein AL. Interaction of *Bacillus subtilis* *CodY* with GTP. *J Bacteriol* 2008;190:798–806.
- Hendriksen WT, Bootsma HJ, Esteveo S et al. *CodY* of *Streptococcus pneumoniae*: link between nutritional gene regulation and colonization. *J Bacteriol* 2008;190:590–601.
- Hsueh YH, Somers EB, Wong AC. Characterization of the *codY* gene and its influence on biofilm formation in *Bacillus cereus*. *Arch Microbiol* 2008;189:557–68.
- Hudson MJ, Beyer W, Bohm R et al. *Bacillus anthracis*: balancing innocent research with dual-use potential. *Int J Med Microbiol* 2008;298:345–64.
- Hwang J, Inouye M. An essential GTPase, *der*, containing double GTP-binding domains from *Escherichia coli* and *Thermotoga maritima*. *J Biol Chem* 2001;276:31415–21.
- Joseph P, Ratnayake-Lecamwasam M, Sonenshein AL. A region of *Bacillus subtilis* *CodY* protein required for interaction with DNA. *J Bacteriol* 2005;187:4127–39.
- Kanehisa M, Goto S, Sato Y et al. Data, information, knowledge and principle: back to metabolism in KEGG. *Nucleic Acids Res* 2014;42:D199–205.
- Klumpp S, Krieglstein J. Phosphorylation and dephosphorylation of histidine residues in proteins. *Eur J Biochem* 2002;269:1067–71.
- Laemmli UK. Cleavage of structural proteins during the assembly of the head of bacteriophage T4. *Nature* 1970;227:680–5.
- Larkin MA, Blackshields G, Brown NP et al. Clustal W and Clustal X version 2.0. *Bioinformatics* 2007;23:2947–8.
- Lemos JA, Nascimento MM, Lin VK et al. Global regulation by (p)ppGpp and *CodY* in *Streptococcus mutans*. *J Bacteriol* 2008;190:5291–9.
- Lindback T, Mols M, Basset C et al. *CodY*, a pleiotropic regulator, influences multicellular behaviour and efficient production of virulence factors in *Bacillus cereus*. *Environ Microbiol* 2012;14:2233–46.
- Macek B, Mijakovic I, Olsen JV et al. The serine/threonine/tyrosine phosphoproteome of the model bacterium *Bacillus subtilis*. *Mol Cell Proteomics* 2007;6:697–707.
- Majerczyk CD, Sadykov MR, Luong TT et al. *Staphylococcus aureus* *CodY* negatively regulates virulence gene expression. *J Bacteriol* 2008;190:2257–65.
- Marchler-Bauer A, Bryant SH. CD-Search: protein domain annotations on the fly. *Nucleic Acids Res* 2004;32:W327–31.
- Mattoo AR, Saif Zaman M, Dubey GP et al. *Spo0B* of *Bacillus anthracis* - a protein with pleiotropic functions. *FEBS J* 2008;275:739–52.
- Mock M, Fouet A. Anthrax. *Annu Rev Microbiol* 2001;55:647–71.
- Petranovic D, Guedon E, Sperandio B et al. Intracellular effectors regulating the activity of the *Lactococcus lactis* *CodY* pleiotropic transcription regulator. *Mol Microbiol* 2004;53:613–21.
- Pungaliya PP, Bai Y, Lipinski K et al. Identification and characterization of a leucine-rich repeat kinase 2 (LRRK2) consensus phosphorylation motif. *PLoS One* 2010;5:e13672.
- Ratnayake-Lecamwasam M, Serror P, Wong KW et al. *Bacillus subtilis* *CodY* represses early-stationary-phase genes by sensing GTP levels. *Gene Dev* 2001;15:1093–103.
- Sekiguchi T, Hirose E, Nakashima N et al. Novel G proteins, *Rag C* and *Rag D*, interact with GTP-binding proteins, *Rag A* and *Rag B*. *J Biol Chem* 2001;276:7246–57.
- Sengottaiyan P, Spetea C, Lagerstedt JO et al. The intrinsic GTPase activity of the *Gtr1* protein from *Saccharomyces cerevisiae*. *BMC Biochem* 2012;13:11.
- Stenz L, Francois P, Whiteson K et al. The *CodY* pleiotropic repressor controls virulence in gram-positive pathogens. *FEMS Immunol Med Mic* 2011;62:123–39.
- Tu Quoc PH, Genevaux P, Pajunen M et al. Isolation and characterization of biofilm formation-defective mutants of *Staphylococcus aureus*. *Infect Immun* 2007;75:1079–88.
- van Schaik W, Chateau A, Dillies MA et al. The global regulator *CodY* regulates toxin gene expression in *Bacillus anthracis* and is required for full virulence. *Infect Immun* 2009;77:4437–45.